Power Management Strategy of a Fuel Cell Hybrid Electric Vehicle with Integrated Ultra-Capacitor with Driving Pattern Recognition

by

Puneet Jethani

A Thesis Presented in Partial Fulfillment
of the Requirements for the Degree
Master of Science

Approved March 2017 by the
Graduate Supervisory Committee:

Abdel Ra'ouf Mayyas, Chair
Yi Ren
Spring Berman

ARIZONA STATE UNIVERSITY

May 2017

ABSTRACT

The greenhouse gases in the atmosphere have reached a highest level due to high number of vehicles. A Fuel Cell Hybrid Electric Vehicle (FCHEV) has zero greenhouse gas emissions compared to conventional ICE vehicles or Hybrid Electric Vehicles and hence is a better alternative. All Electric Vehicle (AEVs) have longer charging time which is unfavorable. A fully charged battery gives less range compared to a FCHEV with a full hydrogen tank. So FCHEV has an advantage of a quick fuel up and more mileage than AEVs. A Proton Electron Membrane Fuel Cell (PEMFC) is the commonly used kind of fuel cell vehicles but it possesses slow current dynamics and hence not suitable to be the sole power source in a vehicle. Therefore, improving the transient power capabilities of fuel cell to satisfy the road load demand is critical.

This research studies integration of Ultra-Capacitor (UC) to FCHEV. The objective is to analyze the effect of integrating UCs on the transient response of FCHEV powertrain. UCs has higher power density which can overcome slow dynamics of fuel cell. A power management strategy utilizing peak power shaving strategy is implemented. The goal is to decrease power load on batteries and operate fuel cell stack in it's most efficient region. Complete model to simulate the physical behavior of UC-Integrated FCHEV (UC-FCHEV) is developed using Matlab/SIMULINK. The fuel cell polarization curve is utilized to devise operating points of the fuel cell to maintain its operation at most efficient region. Results show reduction of hydrogen consumption in aggressive US06 drive cycle from 0.29 kg per drive cycle to 0.12 kg. The maximum charge/discharge battery current was reduced from 286 amperes to 110 amperes in US06 drive cycle. Results for the FUDS drive cycle show a reduction in fuel consumption from 0.18 kg to 0.05 kg in one drive

cycle. This reduction in current increases the life of the battery since its protected from overcurrent. The SOC profile of the battery also shows that the battery is not discharged to its minimum threshold which increasing the health of the battery based on number of charge/discharge cycles.

To my parents, Rita Jethani and Vasudev Jethani

ACKNOWLEDGMENTS

I would like to express my sincere gratitude to my Chair and Mentor Dr. Abdel Ra'ouf Mayyas for his guidance, support and motivation. His constant encouragement helped me overcome the challenges I faced in my thesis. This has helped me grow as an engineer and widen my portfolio of work. I am thankful to Dr. Mayyas for all the time and effort he puts in for the success of students.

I am thankful to Prof Max for his constant support and being patient all the time. You went above and beyond your duty to help me with my thesis. I would like to thank Prof. Berman for being on my thesis committee.

I would like to thank my colleagues and friends in our research group. I would like to specially thank Mohammed Alzorgan for his valuable inputs and ideas. Last but not the least. I want to thank my parents, all my friends and folks who have been a major part of my journey at ASU and who motivated me throughout my research.

TABLE OF CONTENTS

Page

LIST OF TABLES

Table Page

LIST OF FIGURES

Figure Page

Figure Page

Figure Page

ABBREVIATIONS

AEV	All Electric Vehicle
HEV	Hybrid Electric Vehicle
PHEV	Plug in Hybrid Electric Vehicle
FC	Fuel Cell
FCHEV	Fuel Cell Hybrid Electric Vehicles
PEMFC	Proton Exchange Membrane Fuel Cell
ESS	Energy Storage System
PMS	Power Management Strategies
SOC	The State of Charge
ICE	Internal Combustion Engine

1. BACKGROUND

Recently, there has been very rapid advances and development in the auto industry. The ever increasing use of electric motors and advances in the efficiency and capacity of high voltage energy storage devices has opened new frontiers. Along with these latest developments in electric powertrain components, the level of greenhouse gases has reached an alarming level. This has motivated the auto industry to do research and development in All Electric Vehicles (AEV) and Hybrid Electric Vehicle (HEV) and Plug in Hybrid Electric (PHEV) as they are seen as potential solutions to reduce greenhouse gases [1] and depleting oil reserves. But the research for alternative power source for vehicle is not limited to AEVs, HEVs and PHEVs. Alternatively, fuel cell vehicles seem to have a promising future as they have an advantage of going longer range in one complete hydrogen (~4 kg of compressed H_2) tank compared to AEVs which go lesser range with a very heavy battery pack. The time taken to refill the hydrogen gas is about 3-5 minutes as compared to AEVs which can take hours to get same amount of mileage. HEVs on the other hand still use gasoline and so have greenhouses gases coming out of exhaust pipes. In the current scenario of environmental crisis and stringent environment laws and capping of greenhouse gases, the advances in fuel cell (FC) vehicle research has made people think that FC can be a viable substitute to Internal Combustion Engine and a better alternative to AEVs if the advancement and infrastructure reaches a level that it becomes convenient to have a FCHEV.

Although a fuel cell has shown promising capabilities as a main power source in a vehicle, it has some inherent characteristics that need to be taken care of in the power management strategy. Since a Fuel cell has a slow dynamic [2] and a battery also can

handle the sudden surge in power demand only so much [3], an Ultra-Capacitor (UC) bridges the gap. In order to make FCHEVs a commercial success, some obstacles it faces needs to be discussed. This will help in understanding the need to add an additional third power source in the powertrain and the need to create a PMS for this type of configuration.

1.1. Impediments in the Commercialization of Fuel Cell Vehicles

For the fuel cell vehicles to be successfully commercialized, the infrastructure requirements like hydrogen refueling stations, affordable price of hydrogen gas and service centers are needed to be in place. Some of the most common obstacles are discussed below.

1.2. Availability of Hydrogen, Cost and Quality of Fuel

Economic viability and social acceptance of the fuel cell technology go hand in hand for the commercial success of this technology. The most important factor among all is the available of hydrogen fueling stations. A map shown below is of the locations of the hydrogen fueling stations across United States. According to data provided by Alternative Fuels Data Center, there are just 31 hydrogen gas fueling stations which are shown in the map in Figure 1. 31 out of which 28 are in California [4]. Because of the scarcity of hydrogen fueling stations, efforts are constantly being made to increase the range of FCHEVs in one gas tank.

Figure 1 Hydrogen Fueling Stations Across US [4]

1.3. Commercial Aspect of The Fuel Cell Hybrid Electric Vehicle

A lot of research and development is being done by the automotive companies as explained above to bring the cost down. According to a Depart of Energy (DOE) report the cost of fuel cell system would roughly be around $55/kW at 500,000 units produced per year [5]. The cost presented in the DOE report will only be possible with high volume production. The International Energy Agency is also considering hydrogen fuel cell vehicles as probable solution to clean transportation. A techno-economic analysis done in [6] shows that by 2030, the cost of fuel cell stacks produced would be $35-75/kW of fuel cell. According to a study done in [7] a technology learning curve in the range of 0.78-0.85 is expected. This is expected to bring down the cost by 22% to 15% which will make fuel

cell technology even more economical. A summary of capital cost predictions for 2030 is presented in [6] shows and summarized in *Table 1*.

Table 1 Powertrain Cost Summary for 2030 [6]

Powertrain Cost	Minimum	Maximum	Average
Fuel cell$/kW	$35[b]	$75[b]	$55
Battery $/kWh	$200	$300	$250
Electric drive train	$1200[a]	$2030[a]	$1615
Hydrogen storage	$900[a]	$2000[a]	$1450
Conventional (ICE)	$2400[a]	$2530[a]	$2465

[a] denotes those used from [7]
[b] denotes those adopted from [8]

Along with the capital cost, analysis of running cost is also an important factor necessary to make any technology viable. The running cost is mainly the cost of the fuel which is the cost incurred at a regularly excluding any kind of maintenance cost. *Table 2* as presented in [6] summarizes the prediction of fuel cost in 2030.

Table 2 Running Cost Predictions Based on Fuel Prices for 2030 [6]

Fuel cost	Minimum (GJ^{-1})	Maximum (GJ^{-1})	Average (GJ^{-1})	Miles (GJ^{-1})	Typical Unit
Gasoline	$19	$38	$28.5	342	54
Hydrogen	$14	$56	$35	684	97
Electric	$27	$45	$36	1367	4.9

The auto makers are pushing to make FCHEV technology reach to a level where it is considered at par with gasoline vehicles in terms of durability, safety, performance, etc. In order for that to happen the capital cost and the running cost as discussed above both should

be brought down for these vehicles to become mainstream. This will promote more production of FCHEVs which will bring down cost even further.

1.4. Motivation For Developing A Power Management Strategy With Integrated UC

With all the scarcity of hydrogen refueling stations and cost of production of fuel cell stack, increasing the mileage of the car in one full tank of hydrogen by adding a third power source will improve performance and reliability. This will increase commercial viability bringing down the cost of fuel cell stack production in future. Adding a third power source not only added more degree of freedom, but also gives the flexibility to find and operate fuel cell in its most optimum region as the other two sources can satisfy power demand at other time. This research investigates designing a transformational power management strategy that distributes requested power among all three power sources. All three power sources used in the powertrain have different characteristics. Along with satisfying the power demand while accelerating efficiently, harvesting the regenerative power efficiently with an added degree of freedom is also a challenge in designing an efficient PMS. The effect of using UC for transient and high power demands on the behavior of the battery and how it can affect the life of the battery is a part of this research. This PMS also ensures that the fuel cell operates in the ohmic loss region on its polarization curve which is the most efficient region. Apart from the prospect of efficiently managing positive power, the regenerative power can also be harvested in a much better way. Since there are two power sources that can use regenerative power, a very less amount goes waste. The UC can handle a higher in rush of current and can be used to absorb higher proportion of power compared to battery. This has an addition advantage of protecting the battery from overcurrent. Thus

by adding UC into the ESS, improvements in hydrogen consumption, reduces current from battery and FC which extend their shell life is expected.

2. FUEL CELL VEHICLE POWER TRAIN TECHNOLOGY

In the recent years, a lot of research and development is being put towards non-conventional powertrain vehicles. Companies like Tesla and cars like GM Volt have changed the automotive industries' outlook. With a lot of research Fuel cells have emerged as an alternative to the Internal Combustion Engines (ICE). Fuel cell vehicles have no or limited real environment concerns. The fuel used is hydrogen H_2 gas which undergoes a reaction along with oxygen and produces electricity, water and heat as a byproduct making it very environment friendly.

Talking about the advantages on system level, the FCHEVs have quite simple structure compared to ICE vehicles. There are no moving parts in a FCHEV since most of it is electronic solid state devices. With the absence of moving parts, there are no vibration or noise issues that come with FCHEVs. Lubrication is also not a problem. The overall maintenance cost comes down with no moving parts and no parts requiring lubrication which means no oil change and no lubrication change in transmissions and other parts.

With the environmental laws becoming more stringent than ever and FCHEVs offering all the benefits discussed above, all the major car companies are putting their resources towards the development of FCHEV. Commercially available Toyota Mirai uses a 114kW fuel cell stack with a range of 312 miles on a 1.6kWh battery. The Hyundai Tucson fuel cell EV has a 100kW fuel cell stack with a 0.95kWh battery and roughly 265 miles. These vehicles have shown that the fuel cell vehicles technology is worth researching since they provide a cleaner alternative transportation option. For this reason, a lot of car manufacturers are investing in developing fuel cell vehicles.

Along with improving the fuel cell stack efficiency and technology, the powertrain type and the ESS components used in hybridization of the FCV also play a huge role in its performance and range. So, a lot of investigation is done about different powertrain configurations. Table 3 shows the list of companies and their R&D efforts in FCHEV.

Table 3 Car Manufacturers and their FCHEV Projects [9]

Company	System Type
Daimler Chrysler	Straight fuel cell- Fuel cell–battery hybrid
Ford	Straight fuel cell
General Motors	Fuel cell-battery hybrid
Honda	Fuel cell-ultra capacitor hybrid
Mazda	Fuel cell-ultra capacitor hybrid
Nissan	Fuel cell-battery hybrid
Renault	Fuel cell-battery hybrid
Toyota	Fuel cell-battery hybrid
Volkswagen	Straight fuel cell Fuel-cell–battery hybrid
ZeTech	Fuel cell-battery hybrid

2.1. Fuel Cell System

A Fuel Cell is an electrochemical device that carries out a chemical reaction and produces electricity in the process. But it's an energy producing device and does not have the capability of storing electricity like batteries or UC. A PEMFC is made up of two electrodes with a membrane acting as an insulator between the two electrodes. The

electrodes along with the membrane form Membrane Electrode Assembly (MEA). The chemical reaction that occurs in this MEA is shown below [10]:

Anode: $H_2 \longrightarrow 2H^+ + 2e^-$ (1)

Cathode: $0.5O_2 + 2H^+ + 2e^- \longrightarrow H_2O$ (2)

Figure 2 shows the structure of a MEA assembly and the inputs and outputs of a fuel cell.

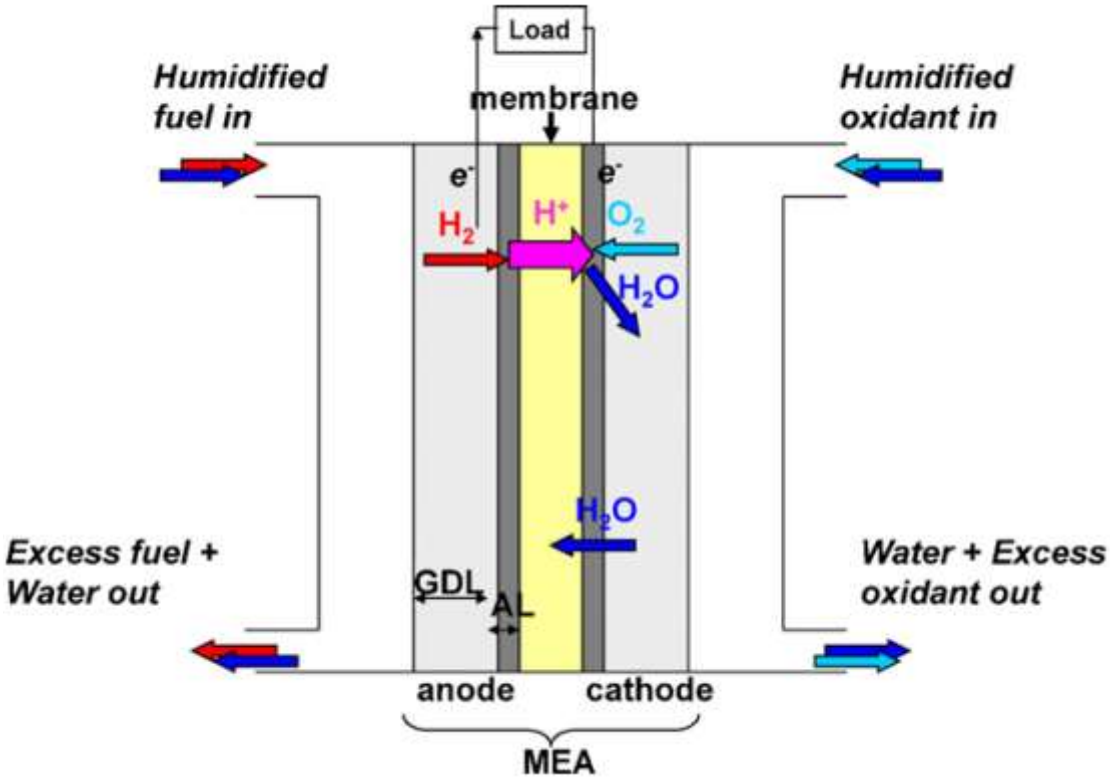

Figure 2 Membrane Electrode Assembly Working Procedure [11]

Starvation in fuel cells is another phenomenon that occurs in fuel cell stack which is the biggest concern. Apart from the cathodic reaction shown in Eq. 2, there is another reaction shown in Eq. 3 which is negligible under normal operating conditions. That reaction is:

$C + 2\,H_2O \longrightarrow CO_2 + 4H^+ + 4e^-$ (3)

This reaction becomes significant when large power is drawn from a fuel cell stack under transient conditions such as start/stop or rapid acceleration. A fuel cell on its own produces insufficient power to propel a vehicle as a stand-alone power system which makes its hybridization inevitable. The Figure 3 below shows the structure of a fuel cell stack

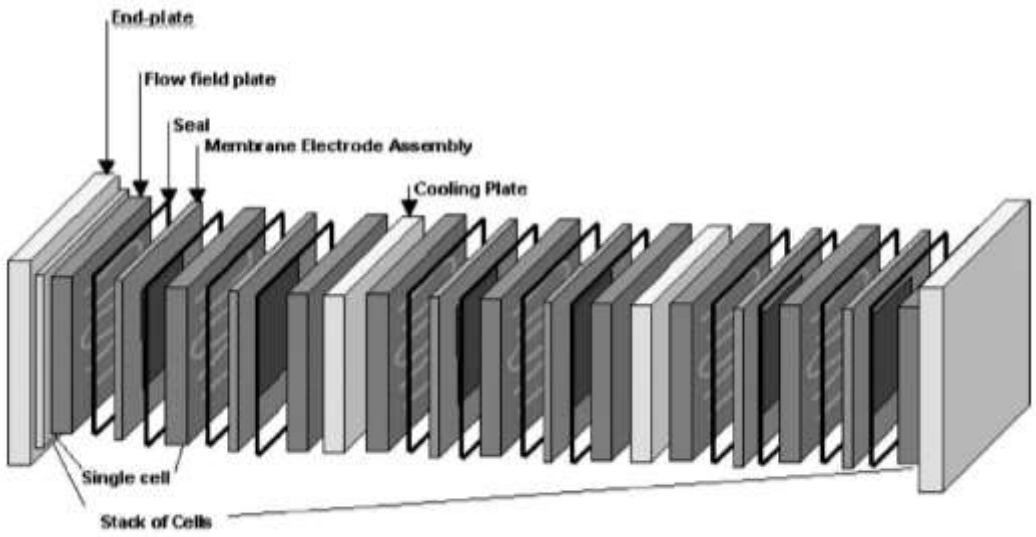

Figure 3. Structure of PEMFC Stack [12]

Temperature is one of the most important factor among all the operating conditions for a fuel cell. At appropriate operating temperature, the oxygen reduction reaction is enhanced which avoids major voltage loss of PEMFC [13]. When operated at 1 atm pressure and 100 degrees C, water exists in vapor, so transport of water along membrane, catalyst and diffusion layer is easier. Working temperatures above 100 degrees C will completely vaporize water. This will cause deficiency of water and dehydration of the membrane which reduces the proton conductivity in the membrane [9]. Compared to different types of fuel cells, PEMFCs have low temperature with their operating

temperature between 60 – 100 degrees C [8]. Due to all these characteristics of a PEMFC, they are the most preferred type of fuel cell for automotive and buses [9].

PEMFC even though a better alternative compared to other fuel cells still needs a PMS. Drawing appropriate amount of current will make sure that the temperature of PEMFC remains in the favorable scale which can be achieved through PMS. When high current is drawn from fuel cell, the CO_2 released according to Eq. 3 can cause permanent loss of carbon and reduces the durability of MEA membrane [10]. An efficient PMS will make sure to avoid reaction 3 from becoming intense which will release more carbon into the, energy storage devices are used in a powertrain in fuel cell vehicles to facilitate and supply power in cases of high power transient demand.

Starvation is another impeding factor that prevents the FC from serving as a stand-alone power source in vehicles. If a large amount of current is drawn from the FC in a vehicle while driving, there is a possibility of damaging its membrane due to starvation. So, energy storage devices are always used along with the fuel cell stack making it a FCHEV. The preferable energy storage device in the auto industry are battery packs which are widely used in HEVs, PHEVs and AEVs. In the commercial fuel cell vehicles in the market like Toyota Mirai or Hyundai Tucson, battery packs are the choice of energy storage device [2,3,14]. The development and implementation of a hydrogen-fuelling infrastructure poses several challenges. Among the most important is the need to produce hydrogen with minimal accompanying CO_2 emissions. Using renewable source and nuclear will prove to be expensive bringing down the economic viability. When fossil fuel

is used to produce hydrogen, it comes with emission of CO_2 in the air. The industry and the government are still working on these issues.

Fuel cell starvation and its prevention

As seen in the reaction shown in Eq. 2, oxygen is one of the two important part of the reaction. When more current is drawn from the fuel cell it means that the reaction must take place at a faster rate. So, the oxygen used in the reaction in the fuel cell must be replenished very quickly [15]. If that does not happen, the partial pressure of oxygen drops at the cathode which in turn causes the stack voltage to drop drastically damaging the membrane as well. This phenomenon is called fuel cell starvation. This will in turn lead to reduce the power response of the fuel cell stack [15]. A standalone fuel cell in a car will suffer from fuel cell starvation during aggressive drive cycles like US06. Apart from the FC's inability to handle sudden variation in power demand, the cooling requirements and water balance of the FC are critical in maintaining the stability and performance of the FC stack [16]. These factors have a direct effect on the lifetime of the FC stack as well. Since this is the only power source in a car, there is no alternative way that power can be controlled. Until now the auto industry uses batteries as the main ESS. So, hybridization of FC vehicles with ESS improves the dynamic behavior of the vehicle, prevents drawing of current from the FC during transient high power demand thus increasing the lifetime of the FC. Batteries have been the most preferred power source until recent times. But recently Ultra-Capacitors (UC) are also being considered by the industry for ESS. Both batteries and UC have their pros and cons. A powertrain configuration having both in their ESS so that they can be used to the best of their capabilities would make a system quite efficient.

But having three power sources in a powertrain and creating a power management strategy can be quite complicated. Thus, creating the power management strategy for this kind of powertrain is the objective of this research.

3. HYBRIDIZATION OF FCHEV AND ARCHITECTURE DEPENDENT POWER MANAGEMENT STRATEGIES

3.1. Powertrain Topologies of FCHEV and Degree of Hybridization (DOH)

Based on the number of power sources, the powertrain topologies can be divided into full power source with UC or Battery and Triple Hybrid power source topologies. Figure 4 shows a pictorial representation of the different kinds of power source topologies.

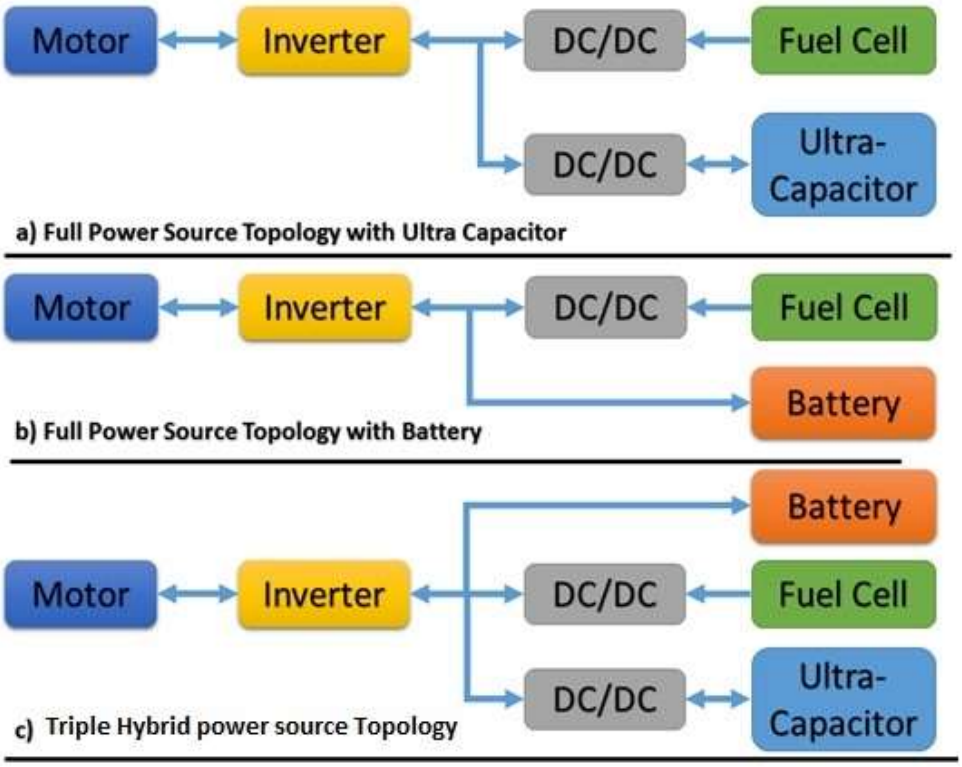

Figure 4 Different Topologies for FCHEV [2]

Hybridization with multiple power sources adds more degree of freedom which increases the complexity of the control strategy but also creates an opportunity for optimizing the control strategy. A new way of defining the degree of hybridization is shown in the Eq. 4 below:

$$DOH = P_{EM}/(P_{EM} + P_{FC}) \quad (4)$$

Where DOH is the degree of hybridization, P_{EM} is the power from electric motor and P_{FC} is the power from the FC. The FC in a FCHEV acts like an engine except the fact that it charges the ESS that in turn provide current to the motor. In special cases where the SOC of the ESS is not sufficient, the FC can also be used to provide power to the wheels. The degree of hybridization is a very important criterion used to determine the size of power components in the powertrain like the FC, batteries and UC. Relying more on the ESS power will make the DOH higher. Similarly relying more on the FC generated power will reduce the DOH.

3.2. FCHEV Power Management Strategies

Control Strategy regulates the energy in such a way that power demand is satisfied consistently and the battery is sufficiently charged at all time and the overall system efficiency is maintained optimal [17]. In any FC vehicle powertrain configurations, the energy exchanges from the FC to ESS operates in three modes [17]:

- Charge mode - The FC supplies energy to the ESS and the load
- Discharge mode - The FC and storage devices supply energy to the load
- Recovery mode - The energy is supplied by recovering power through regenerative braking and stored in the ESS. (BP and/or UC).

The control strategies can be based on different techniques. Experiments have been carried out using control strategies following these different techniques. The details of these control strategies are discussed in the next section.

Based on the type of algorithm and control logic, the power management strategies can be categorized into two types [18]. These are categories are:

- Rule Based.
- Optimization Based.

3.2.1. Rule Based Control Strategy

Rule based strategies are computationally less expensive compared to optimization based strategies. They are a perfect fit for real time problem solving as they are mainly based on a set of rules based on which various decisions like power split, etc. are calculated. Within the rule based category, there are different power management strategies which are discussed in this section.

3.2.1.1. Deterministic/Heuristic Rule Based

This method determines the power split between fuel cell and ESS by analyzing the power flow among different power sources in the powertrain, takes into account the efficiency map of fuel cell. So, the set of governing rules are based on all this information. There are certain conditions that must be satisfied at all time which should be kept in mind while designing the PMS. The conditions are defined as [19]:

- The power demanded by the vehicle is always satisfied.
- The ESS devices always remain within the maximum and minimum limit of healthy operation of the ESS devices.
- Fuel cell power and current is drawn within its allowable limit so it prevents starvation

A flowchart of rule based control strategy is shown in Figure 5 The flowchart shows the process of decision making based on the set of rules and the conditions that must be satisfied at all time**.**

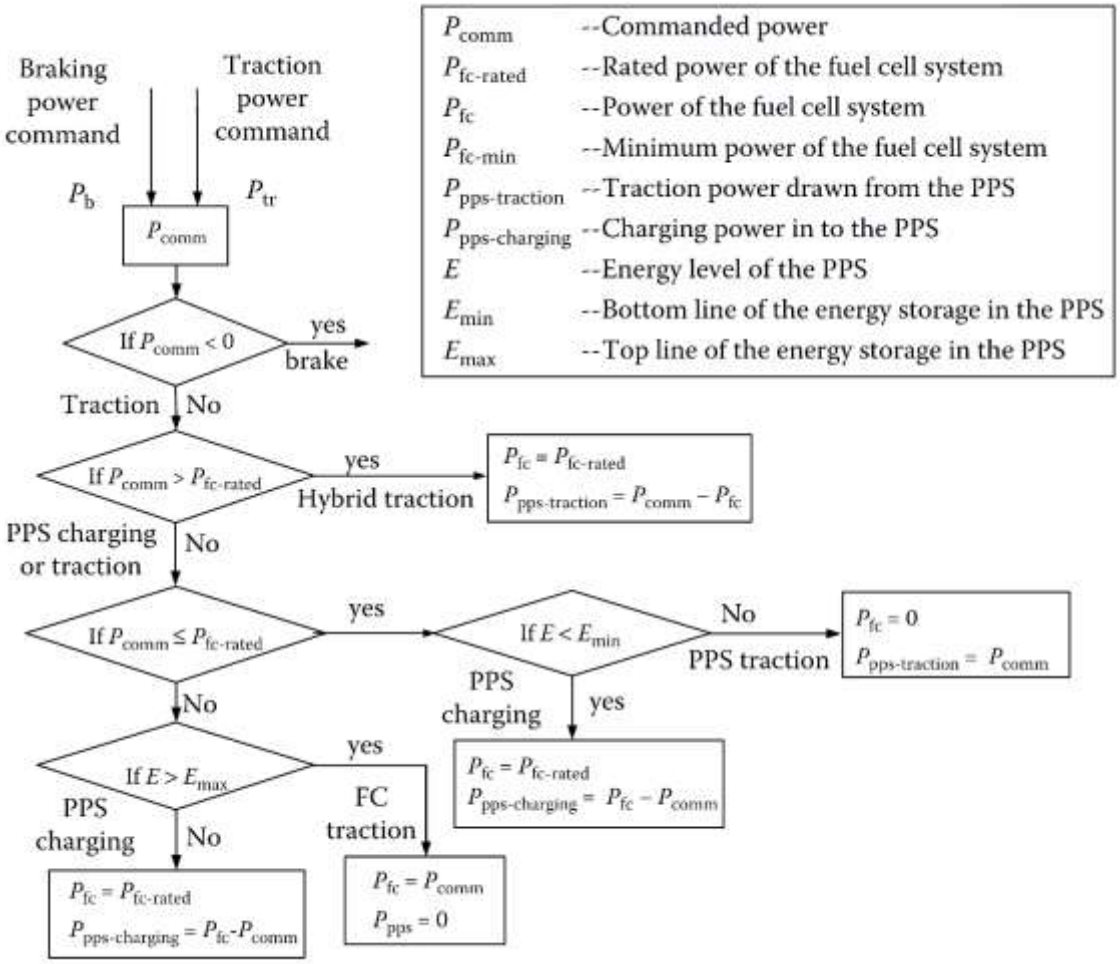

Figure 5 Rule Based FCHEV-EMS Flowchart [19]

As seen in this flow chart, this strategy follows a set of pre-defined rules which govern how the commanded power is satisfied. With the addition of UC into the powertrain, the hybrid traction that is used to provide commanded power needs to be better managed since there

are two source that can provide power. Different power sources must be used to the best of their capabilities. So, a detailed set of rules that take into consideration

3.2.1.2. Power Assist Power Management Strategy.

Power assist is another PMS that falls within the category of rule based category. This method takes into account the SOC of the ESS and the stack voltage and tries to reduce load in the fuel cell by requesting more power out of ESS if the SOC of the ESS is above a certain threshold [20]. To break it down into a set of rules, this strategy can be written as:

- For the SOC of the ESS is above a threshold, the battery provides a greater proportion of power. The remaining power comes from the fuel cell. If the SOC drops below the set threshold value, the fuel cell provides a higher proportion of power.
- For the stack voltage higher than a threshold value, higher proportion of power is drawn from the fuel cell. This power split remains valid until condition 1 becomes true again.

The threshold values for SOC of the ESS and stack voltage depend on the size of the fuel cell stack and the ESS. This strategy shows an improvement of 5-16 % in the fuel economy as reported in [20].

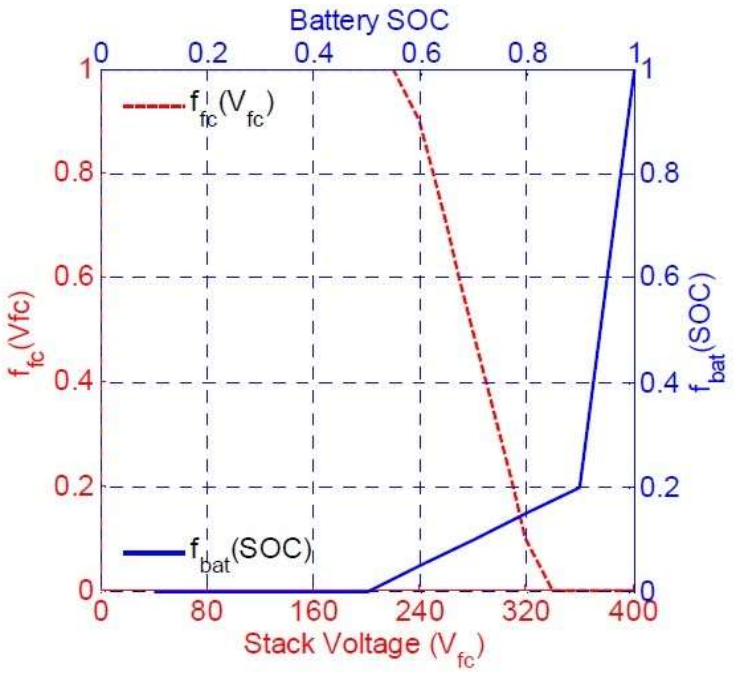

Figure 6 Power Split Factor Assist Control Strategy

3.2.1.3. Fuzzy logic

With the UC becoming more and more a topic of interest, Haroune Aouzellag *et al* in [21] has designed a fuzzy logic based control strategy. The power drawn from the fuel cell dictates the current drawn from the fuel cell which directly translates to the amount of hydrogen that is consumed. Since the aim of the control strategy is to minimize the amount of hydrogen consumption, this control strategy has FC power as a parameter and is used to provide power requested by the vehicle which does not depend on the SOC of ESS components. Simply stating if the ESS components are low on SOC or not capable of providing enough power, the fuel cell supplies the power. The two main variable on which the control strategy is based are SOC and vehicle speed:

- If $47 \leq SOC \leq 75$ and $10 \leq V_V \leq 60$, the UC fulfils the power lack or receives the extra power from braking while the SOC oscillates in this fixed range.
- If $47 \leq SOC \leq 75$ and $V_V > 60$ the vehicle speed is in low level and the power demand is delivered by the UC system.
- If SOC > 75: there is no need to charge the UC because the SOC is in high level of charge. Must decrease the SOC to recover the energy in case of braking.
- If $SOC < 47$ and $10 \leq V_V \leq 60$, in this case, the power demand is assured by the UC system and $P_{FC,ref} = 0.6\ P_{FC,max}$ and $P_{UC} + P_V$.
- If $SOC < 47$ and $V_V > 60$ the UC should be charged until its maximum SOC. In this case $P_{FC,ref} = 0.6\ P_{FC,max} + P_V$.

The algorithm is summarized and presented as shown in Table 4. By controlling the power and hence the current drawn from UC, the DC bus voltage can be maintained within the best operation limits. The FC power is more stable and UC is used more for power compared to FC which enhances the life of the FC. The operation of UC is limited to the upper and lower threshold which enhances cell durability.

Table 4 Fuzzy Logic Algorithm [21]

Fuzzy Logic Energy Management		
Condition	**Power from UC**	**Power from FC**
$47 \leq SOC \leq 75$ and $V_V < 60$	Yes	No
$47 \leq SOC \leq 75$ and $V_V > 60$	Yes	No
SOC > 75	Yes	No
$SOC < 47$ and $10 \leq V_V \leq 60$	Yes	Yes
$SOC < 47$ and $V_V > 60$	No until charged, then Yes	Yes

By controlling the power and hence the current drawn from UC, the DC bus voltage can be maintained within the best operation limits. The FC power is more stable and UC is used more for power compared to FC which enhances the life of the FC. The operation of UC is limited to the upper and lower threshold which enhances cell durability.

3.2.1.4. Load following

In the load following control strategy, the governing function is power demand. The power threshold depending on the battery SOC governs the ON/OFF function of the FC. Whenever the power requirement increases beyond the predefined threshold value the controller turns the FC ON to fulfill the power difference. This strategy facilitates the maximum charge depletion of the BP [22]. While defining the threshold for the FC to provide power, the dynamics and the response time of the particular FC should be taken into account as it's not as fast as an ICE.

In load following strategy, and during the ON state of the FC the power produced is the difference between the power demand and the power provided by the electric motor. The power unit does not produce excess power hence under the load following control strategy; battery recharging does not take place. Figure 7 describes the power split between FC and the ESS [22].

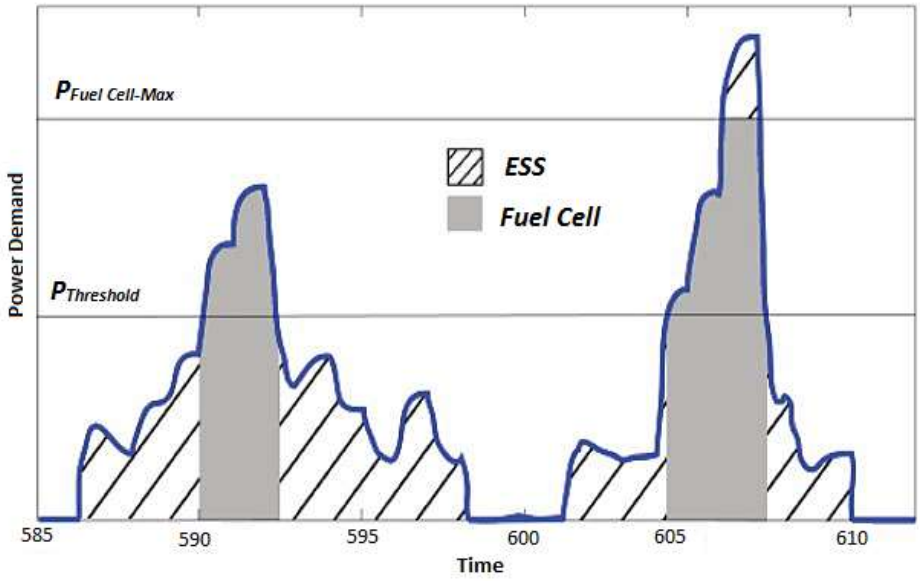

Figure 7 Load Following Control Strategy [22]

Load following control strategy depends solely on the power thresholds set in the strategy. So, load following can restrict the power provided by FC and only be used to provide power when the capacity of the BP isn't enough to supply the power demand of the vehicle. Setting the power thresholds keeping in mind the dynamics of the FC can help reduce fuel consumption.

3.2.1.5. Thermostatic Control Strategy

This strategy falls under the broader category of rule based control strategy and works around rules laid down based on the SOC of the ESS and the power demand from the FC. This strategy as discussed in [23] works by maintaining the SOC of ESS within SOC_{low} and SOC_{high}. This also keeps into account the power drawn from FC and maintains it within the $P_{FC\ min}$ and $P_{FC\ max}$. Figure 8 below shows a pictorial representation of the thermostatic presentation.

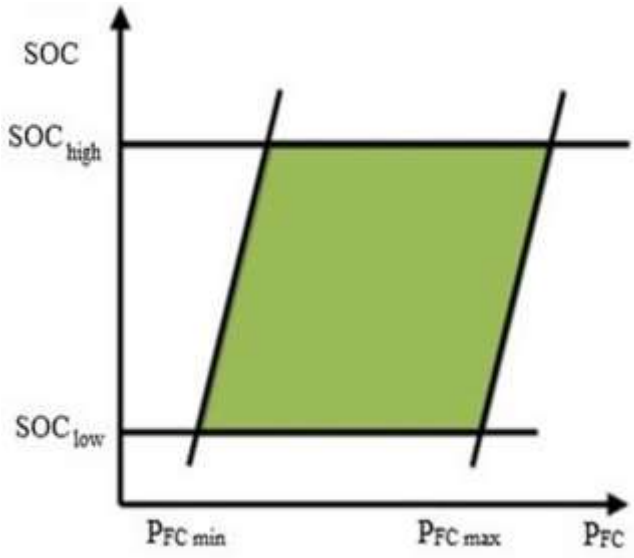

Figure 8 Thermostatic Control Strategy [23]

The thermostatic principle is an easy strategy to implement in real time driving conditions and helps reduce the charge/discharge cycle of the battery by using FC power to drive the vehicle at steady state low power demand. Experimental results in [24] show that thermostatic strategy is more efficient for city driving compared to load following strategy. However, one major drawback of thermostatic control strategy is in the event of SOC of ESS falling below the lower threshold of SOC_{low} and power demand being more than the allowable limit of $P_{FC\,max}$ of the FC.

3.2.2. Optimized Rule Based Control Strategy

Rule based control strategies are real-time implementable but don't necessarily provide the most efficient power split. Optimization based control strategies on the other hand aim at maximizing the efficiency of the power train, simultaneously minimizing the losses [25]. This method calculates the optimal reference torques for power controllers by minimizing

a cost function which represents the hydrogen fuel consumption. A global minimum may be obtained when optimization is performed over fixed drive cycles. Some optimization techniques are computationally heavy and some also require the knowledge of future route to optimize the power management. A driving pattern recognition process can be used to identify the power demand profile ahead of time and can be used to adjust the control strategy accordingly. The following sections talk about this idea.

3.2.2.1. Driver Pattern Recognition

The rule-based control strategy is highly dependent on the driver demand. So, driving pattern recognition gives the ability to operate a vehicle in a multi-mode control algorithm which gives a controller to tune the control strategy on the fly to optimize the power from multiple power sources in a powertrain results in improved fuel economy. Driving pattern recognition algorithm works by identifying certain characteristic parameters of a drive cycle that describe driving pattern including speed, acceleration, deceleration and other parametric driving mission recordings. Recognition of driving pattern is done based on measurement data obtained at certain defining points. Based on this measurement data of the pattern, the process of feature extraction selects feature members. A feature vector is formed consisting of these feature members and is used to identify driving pattern. A feature vector *f* is defined in [26] and is expressed as Eq. 5:

$$f = (k_1 \text{ x } a_1, k_2 \text{ x } a_2, k_3 \text{ x } a_3, \ldots, k_n \text{ x } a_n,)^{\mathrm{T}} \quad (5)$$

Where a_i is a feature member, k_i is a weight factor and n is the dimension of the feature vector. The weight factors depend on the feature parameter. The weight factors corresponding to each feature parameter as listed in Table 5 as defined in [26]:

Table 5 Driving Pattern Feature Parameter [26]

Index Number *(i)*	Feature Parameter *(a)*	Weight Factor *(k)*
1	Average Speed (m/s)	10
2	Positive Average Acceleration ($a>0.1$ m/s^2)	1
3	Low Speed Time (15-30 Km/h)/Total Time (%)	10
4	Mid High Speed Time (70-90 Km/h)/Total Time (%)	100
5	High Speed Time (>90 Km/h)/Total Time (%)	10
6	Extreme Deceleration Time ($a>-2.5$ m/s^2) /Total Time (%)	1000
7	High Deceleration Time ($a<-2$ & $a>-2.5$ m/s^2)/Total Time (%)	1
8	Maximum Cycle Acceleration (m/s^2)	100
9	Maximum Cycle Speed (Km/h)	6
10	Standard Deviation of Cycle Speed (Km/h)	1
11	Mid Deceleration Time ($a<-1$ & $a>-1.5$ m/s^2)/Total Time (%)	1000
12	Mid High Deceleration($a>-2$ & $a<-1.5$ m/s^2)/Total Time (%)	1000
13	Mid Acceleration Time($a>-2$ & $a<2$ m/s^2)/Total Time (%)	1
14	High Acceleration Time($a>2$ & $a<2.5$ m/s^2)/Total Time (%)	1000
15	Extreme Acceleration Time($a>2.5$ m/s^2)/Total Time (%)	1000

After calculating the feature parameters as explained in the table above, the feature vector as explained in Eq 5 is created. Simulation were performed in [26] to identify feature vectors which have the most impact on driving pattern to make the application of DPR real-time implementable. To measure the effectiveness of DPR, Feng, L *et al.* in [26] conducted simulation on a Prius. Four standard drive cycles, SC03, UDDS, US06 and HWFET were used for this simulation. An output value identified the driving cycle by assigning them numbers 1,2,3,4 to the drive cycles SC03, UDDS, US06 HWFET

respectively and assigning 0 to any unrecognized drive cycle. Figure 9 shows the effectiveness of the simulation for the driving pattern recognition.

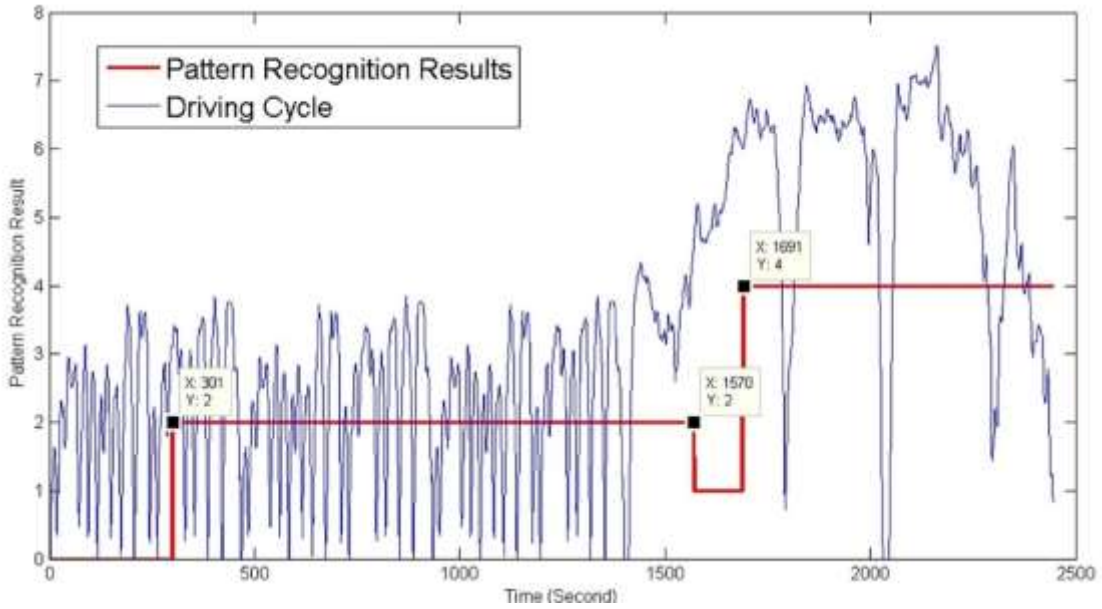

Figure 9 Driving Pattern Recognition [26]

Once the driving cycle is identified, the controller parameters can be modified to improve the fuel economy. Constant cruising on the highway has a medium range power demand and the FC can be used to provide power with utmost efficiency. For city driving, ESS can be used to provide power owing to the slow dynamics of a FC. For aggressive driving, the control strategy can be designed in a way to optimally use ESS and FC in the view of their strengths and limitations.

3.2.2.2. Equivalent Consumption Minimization Strategy

Equivalent Consumption Minimization Strategy (ECMS) is an instantaneous optimization strategy which does not depend on the information of future route or driving cycle information. With active constraints and an appropriate equivalence factor (EF)

denoted as *s*, ECMS can generate near optimal solution. In a FCHEV, the power comes from the ESS and the FC. So, the energy consumed by the battery is consumed as future hydrogen consumption and thus an equivalent total hydrogen consumption shown in Eq. 6 is formulated in [27] as:

$$\dot{m}_{eqv} = \dot{m}_{H_2} + \dot{m}_{equi.H_2.by.ESS} = \dot{m}_{H_2} + \frac{s}{LHV_{H_2}} \tag{6}$$

Where $m_{equi.H2.by.ESS}$ is the equivalent hydrogen consumption rate from the ESS, LHV which is the lower heating value of the H_2 and P_{ebt} which is the electric battery power flow. The equivalent hydrogen consumption from the ESS which depends on the EF is then computed to obtain an optimal power split ratio between the ESS and the FC system.

In ECMS, the SOC of the battery is defined as a state constraint and the objective of this strategy is to compute an optimal EF such that SOC of the ESS remains within the bounds so that the state constraints are inactive. In case of state constraints becoming active, i.e. the SOC of the battery reaching lower or upper bound, the ECMS solution is not optimal at that point. Adding a penalty function to the EF can make the ECMS adapt and avoid the state constraints from becoming active. This penalty function is activated as soon as the constraints become active adjusting the EF to prevent discharge in case of low SOC making FC solely responsible for proving power and prevent charging in case of maximum SOC by using conventional braking instead of regenerative braking. Eq. 7 is the equation with penalty function is expressed in [27] as:

$$s(t) = s + f_p(t) \quad \text{where, } f_p(t) = \begin{cases} Kp(x_{max} - x) & x > x_{max} \\ 0 & x_{min} < x < x_{max} \\ K_p(x - x_{min}) & x < x_{min} \end{cases} \tag{7}$$

Here K_p is the penalty function, $K_p\ (x_{max} - x)$ is the penalty for SOC exceeding upper bound and $K_p\ (x\text{-}x_{min})$ is the penalty for SOC falling below lower bound. This penalty function and the entire strategy can also be based of FC power for which the EF will adjust itself to keep the FC power provided to keep its operation in the optimal efficiency region. For a FCHEV going uphill or downhill, the EF will change because of the road grade at which point the current value of EF will no longer be valid. So the EF has to be recomputed so that the power split is optimum. The most efficient technique to optimize the EF is Dynamic Programming (DP). Since the ECMS is a computationally heavy strategy, using the driving pattern recognition allows it to have an approximate value of the EF closes to the optimal value at the beginning of driving.

3.2.2.3. Maximum Power Point Tracking Energy Management Strategy

There are control strategies that work by maximizing the efficiency of the FC and switch to the maximum power when the power demand is too high [28]. The efficiency curves indicate that the FC system has a unique maximum power point, which is determined by the FC operation conditions. For given operating conditions, the Mean Power Point Tracking (MPPT) control strategy discussed in [29] focusses on determining the maximum power that can be delivered to the wheels from FC. The maximum efficiency and maximum power point are defined as fixed points in control strategy. In reality, these maximum points vary based on the operating conditions of FC stack such as, but not limited to, temperature, pressure, etc. [30]. The maximum power point tracking is used to avoid these drawbacks. The objective of this strategy is to give the FC stack a current reference corresponding to the Maximum Power Point (MPP) [31]. A differential equation shown in

Eq. 8 determines the change of FC power with respect to change of FC current which is used in the algorithm. The Perturbation & Observation method which is perturbing a point and observing the behavior of the system is used. The value of I_{fc}, which is FC current is perturbed to see in which direction the variation goes in order to find the MPP. The point where the differential equation is zero is the MPP [31].

$$\frac{dP_{fc}}{dI_{fc}} = \frac{dV_{fc}}{dI_{fc}(I_{fc},P_{H2},P_{O2},T_{fc})} * I_{fc} = 0 \quad (8)$$

Where P_{fc} is the power from the FC, V_{fc} is the voltage of FC, T_{fc} is the temperature of FC, P_{H2} is the pressure of hydrogen, P_{O2} is the pressure of oxygen.

This strategy provides maximum power to reduce charge/discharge cycles of the BP. This strategy is best suited for low speed vehicles in which FC is used as range extender. The MPP optimization methodology has difficulties to track the maximum efficiency points of FC stack due to the challenge of accurately modeling the highly coupled electrochemical and thermos-fluid behavior of within the FC stack. This drawback is taken into account by the Maximum Efficiency Point Tracking methodology which is discussed in the next section.

3.2.2.4. Maximum Efficiency Point Tracking Energy Management Strategy

The efficiency of a FC is largely dependent on various conditions like temperature, pressure, fuel flow, etc. So, with different values of its operating conditions it's possible to find an operating point that gives maximum efficiency of the FC. The Maximum Efficiency Point Tracking (MEPT) strategy aims to find this most efficient FC operating point. The efficiency of FC is based on how much power a FC stack produces vs how much power in

terms of the amount of fuel is supplied to the stack. Using this definition, Eq. 9 which is the equation of the efficiency of FC stack as defined in [32] can be formulated as:

$$\eta = \frac{P_{fuel}}{P_{net}} \tag{9}$$

Where P_{net} is the net power produced by the FC stack and P_{fuel} is the power supplied in terms of amount of fuel. Eq. 10 defines the power contained in the hydrogen supplied to the stack as defined in [32]:

$$P_{fuel} = \frac{Hn_{cells}}{2F} I_{st} \tag{10}$$

Where H is the low heating value of the hydrogen supplied, n_{cells} is the number of cells, F is the Faraday constant and I_{st} is the stack current. Combining the equations 1 and 2, efficiency as a function of current is expressed in Eq. 11 as:

$$\eta(I_{st}) = \frac{2FP_{net}}{Hn_{cells}I_{st}} \tag{11}$$

The maximum efficiency point of the FC is the point where the point where the FC stack operates at maximum efficiency for a given fuel flow rate. The fuel flow rate is defined as the fuel being supplied to the stack vs maximum allowable fuel that can be supplied to the stack expressed in percentage. Figure 10 shows the relation between the fuel flow and efficiency for given FC.

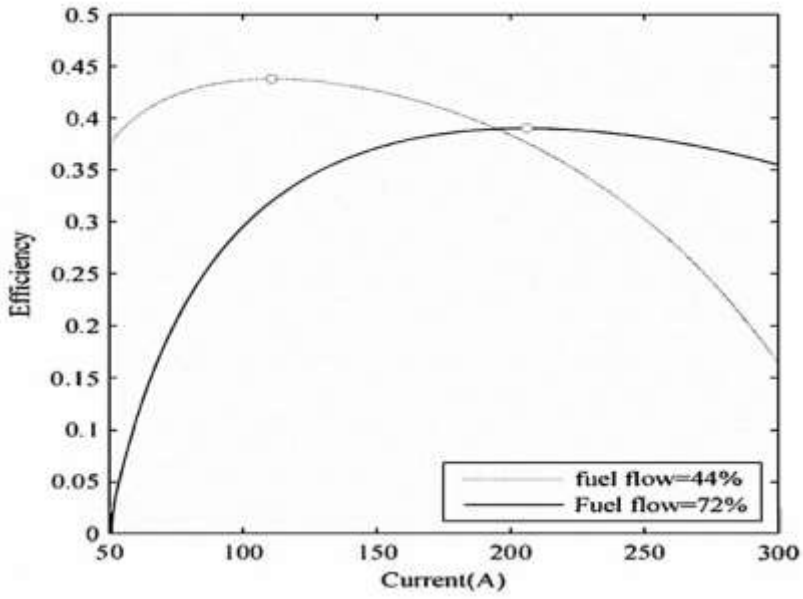

Figure 10 Fuel Flow Vs Efficiency Curve for FC [32]

This control algorithm maximizes the efficiency by regulating the stack current which acts as the control input to the controller in response to the disturbance input provided as fuel flow. The FC stack current is an important factor in calculating the efficiency based on equation above. Since the MEP depends on the operating conditions, the controller reads the stack information and the power produced by the stack and makes an estimate of the efficiency and search for MEPs.

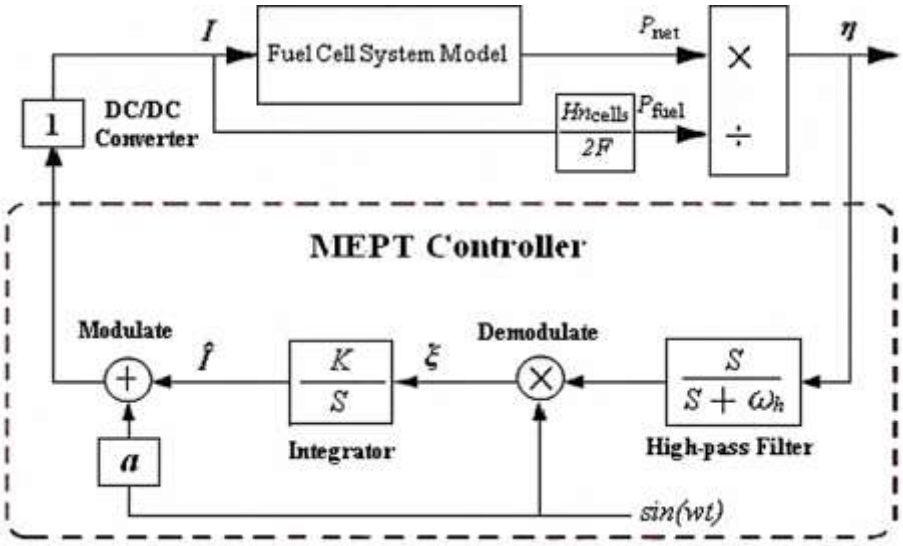

Figure 11 Maximum Efficiency Point Tracking Control Strategy [32]

A small perturbation sinusoidal signal is fed into the MEPT controller shown in Figure 11 into the estimated optimal current thus modulating the current. This disturbance causes a change in the system efficiency. The FC system is just a static map for high frequency perturbations. The efficiency value is passed through a high pass filter and demodulated to remove any static values present in the signal. The maximum efficiency is then calculated through gradient method of optimization.

4. PEAK POWER SHAVING IN FCHEV WITH INTEGRATED UC ENERGY MANAGEMENT STRATEGY

The concept of hybridization was created when it was identified that at low engine RPM, the torque of ICE is low and that the electric motor on the other can be provide full torque at low RPM. This concept can be used to increase the efficiency of the standalone ICE vehicles by hybridizing it with the electric motor and ESS. The ESS can be used to harvest the braking energy as regenerative power which would otherwise just be wasted as heat. The basic idea behind designing the algorithm is to use each power in its optimum and make the best out of all. With this idea in mind, the entire power demand of the vehicle during the US06 drive cycle was categorized into low, medium and high power demand. A deeper look into the characteristics of three power sources dictates what power source to use at what instance.

Fuel cells have slow current dynamics and have a high efficiency in the mid region of it entire range of power operation [33]. Due it's slow dynamics, at times of high power demands a standalone fuel cell might not be able to provide enough power. Using an ESS along with a standalone fuel cell can help in overcoming the drawbacks of the slow dynamics of fuel cell. ESS can be used to take most of high power load. It provides an additional advantage of recovering the regenerative energy during braking.

All these benefits of having an additional power source in the powertrain of a vehicle have it quite beneficial for automakers from an environmental point of view. But with this arrives the need of developing an efficient power management strategy to make the best of

this hybridized powertrain. In this research, with a third power source, it becomes even more crucial to have an efficient PMS.

4.1. UC Versus Battery Dynamics

In modern urban driving conditions, there are many start/stop scenarios like stopping at a traffic light or at stop signs along with rapid accelerations and braking on urban and highway driving condition. A drive cycle like US06 which is a very aggressive drive cycle incorporates all these conditions. While driving with conditions like this, the UC becomes an ideal power source to be used to provide quick energy and capture regenerative energy while braking. UC have a very fast charge-discharge transient response, typically in the range of microseconds as shown Figure 12. Batteries on the other hand have a slow charge/discharge profile. So, the UC is capable of harvesting a lot of regenerative energy quickly and efficiently.

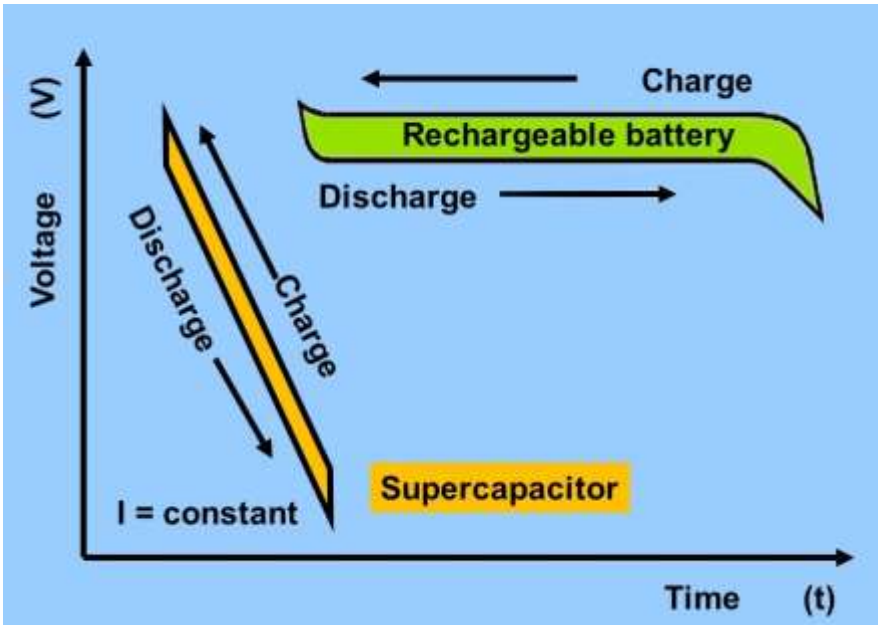

Figure 12 Charge/Discharge Profile Comparison [34]

The basic mechanism for storing energy in UC is fundamentally different from batteries. Batteries have a chemical reaction happening in them through which they conduct electricity. UCs on the other hand have two terminals and an insulator that separates them. The Figure 13 below shows the structure of an UC.

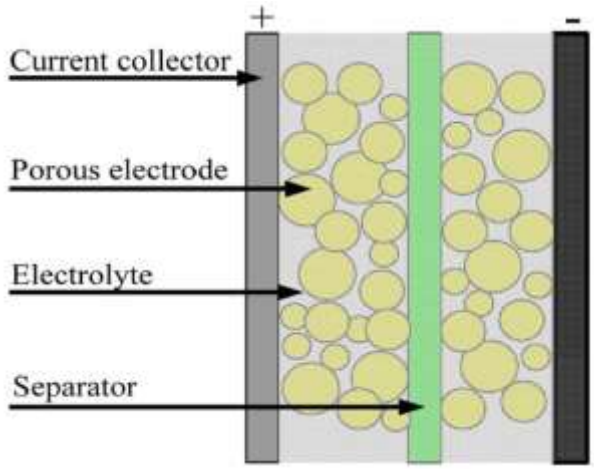

Figure 13 Ultra-Capacitor Cell Structure [35]

The Figure 13 shows the insulator compartmentalizing the positive and the negative terminals with the electrolyte. The positive terminal attracts the negative ions from the electrolyte and positive terminal and attracts the negative ions. So, the terminals store charge on the terminals. UC have much higher power density as compared to battery because of the terminals storing charge. The fact that they store charge on terminals and that UC have a low internal resistance makes them capable of providing current in large transient power demands.

Batteries have high energy density but low power density. Batteries produce current based on a chemical reaction happens inside the battery which produces electrons and provide electricity. Lithium ion batteries are the mist suitable choice for vehicles compared to other batteries due to its higher energy density [38]. Lithium-ion batteries move ions

between anode and cathode creating flow of electricity. When current is being drawn from the battery, ions are produced in the lithium in the anode which travels to cathode. The reverse reaction happens when the battery is being charged. Since the ions produced are because of a chemical reaction, a batteries capability to handle a sudden surge of current request is limited.

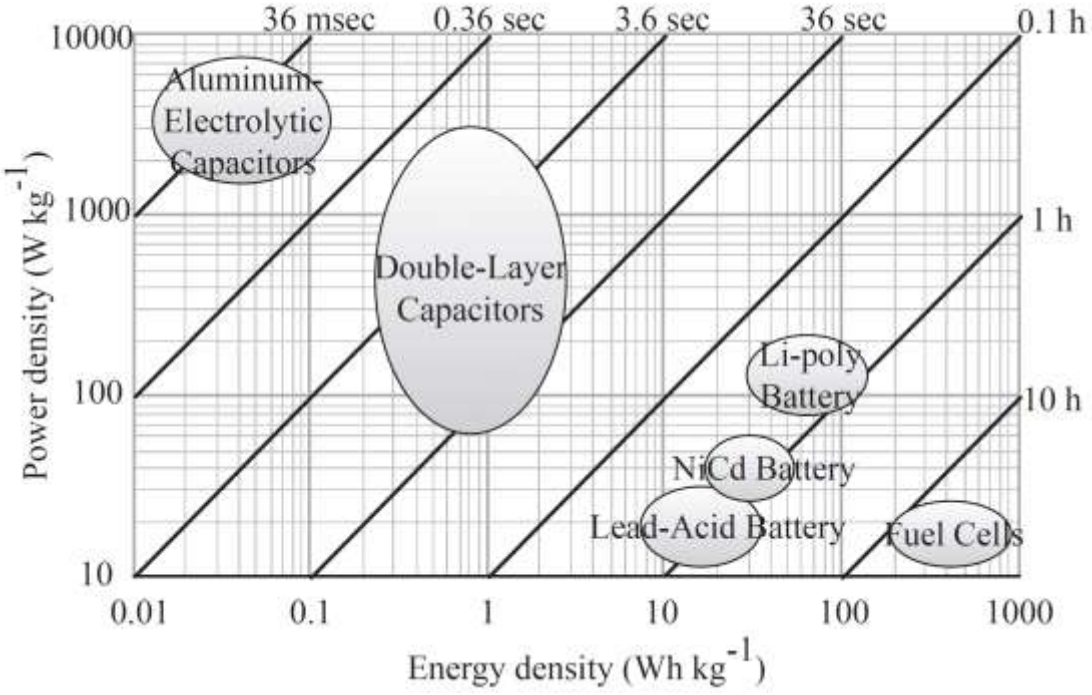

Figure 14 Energy Density vs Power Density of Energy Storage Devices [37]

To analyze the benefits of adding an UC to the powertrain, [37] used an all-electric vehicle PSAT model based on the platform of 2003 Honda Accord. Simulations were ran for the UDDS drive cycle with and without the UC in the powertrain. Without the assistance of UC at peak power demands, the battery would have to provide power up to 60 kW. After the addition of UC in the powertrain, due to the properties of the UC discussed in the previous paragraphs, the majority peak power demands can be drawn from the UC.

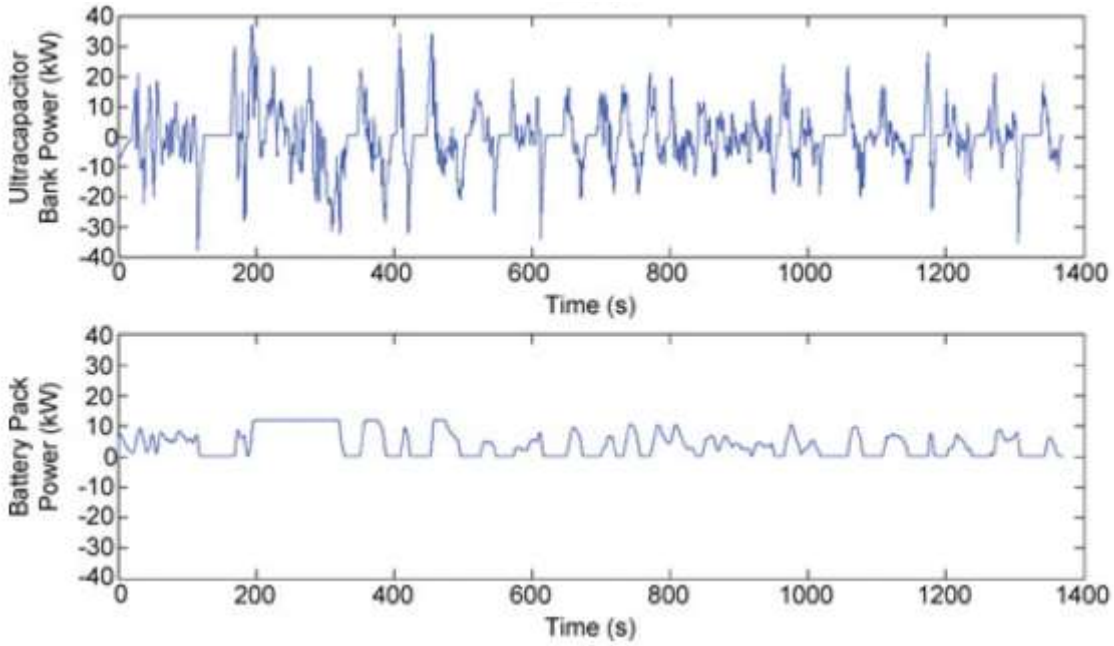

Figure 15 Effect of Adding UC to ESS on Battery Power Profile [37]

Figure 15 shows the effect of adding the UC on the power profile of the battery. The important thing to note here is that there are no spikes in the power profile of the battery. This is an important aspect of the combined UC/battery ESS that it increases the power limits of the ESS and use the higher power limits of UC for peak power and recover the maximum amount of energy during breaking. The ESS of HEVs and AEVs are subjected to frequent charge/discharge cycles and hence need regulation. If a sudden surge of power is drawn from the battery it reduces the life and health of battery. Thus, a properly regulated power management can protect the battery while utilizing the UC to still satisfy power demand. In spite of benefits of the UC, in current scenario UC can only be used as assistant or secondary ESS. Batteries still remains the preferred choice of primary ESS due to the fact that batteries have much higher energy density compared to UC. For longer range of

driving ESS should have high energy density to increase the electric range of cars. So combining both of them in the powertrain can help overcome each other's limitations.

4.2. Fuel Cell Efficiency Characteristics

A fuel cell operates best in the mid region of its entire operating region. This can be seen in Figure 16 which is a plot of efficiency and power.

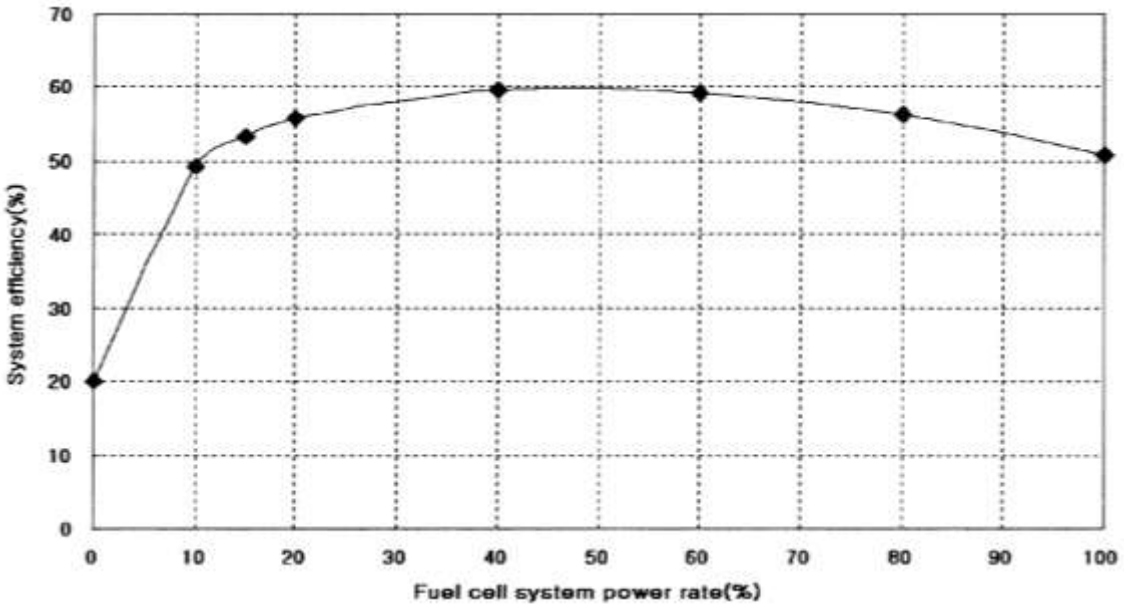

Figure 16 Fuel Cell System Efficiency Versus Power Demand [33]

When the load is low, there are activation losses in the fuel cell. At mid region, the fuel cell has high efficiency because it just has ohmic losses like any electrical circuit [38]. For operations at high power regions, the efficiency decreases as the current increases. [33].

4.3. Optimization of Fuel Cell Based on Polarization Curve

Maximizing the power while trying to keep the hydrogen consumption minimum was also a part of the objective. To achieve that, the fuel cell polarization curve shown in Figure

17 was studied to understand how that can be achieved. The figure shows different regions of losses and the voltage losses. To optimize the operation of fuel cell, understanding these losses is important. The losses can be categorized mainly into 3 type [38].

- Activation Losses

This loss is essentially the loss that occurs in the beginning of the fuel cell operations at low temperature. There is an overall voltage loss that occurs in the beginning when the fuel cell is trying to complete the reaction in which hydrogen is split into electrons and protons. which travel across the electrolyte towards the cathode to produce electron.

- Ohmic Loss

Ohmic losses are the losses that occur due to the resistance in the system just like any other electrical or electronic device. The voltage loss occurring here are governed by the simple equation shown below where *I* is the current and r is the resistance of the system.

$$v = Ir \tag{8}$$

The value of *r* dependents on the conductivities of the electrodes.

- Concentration losses

This loss occurs when the hydrogen is being consumed at a very fast rate which cause the pressure to drop. As a result, the entire reaction slows down causing a loss in the voltage.

With the understanding of all the losses of the fuel cell, the region with maximum power has to be chosen. Power is a product of current and voltage. As seen in the figure, as the current density increases the voltage drops. So to obtain maximum power from fuel cell it's advisable to operate the fuel cell in the region of ohmic losses indicated in the Figure 17.

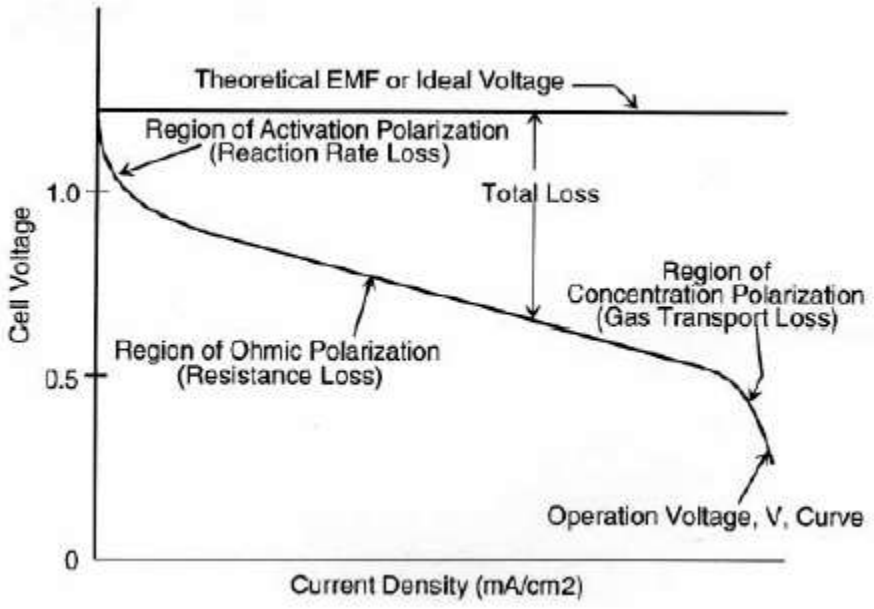

Figure 17 Fuel Cell Polarization Curve [39]

4.4. Power Shaving with UC and Application of Driving Pattern Recognition.

As explained in section 3.2.2.1., a feature vector for a particular drive cycle is created based on the characteristics of the drive cycle and the feature parameter as listed in Table 5. A MATLAB code that does that analysis is ran and the resultant feature vector is generated. The feature vector for US06 drive cycle is shown in Figure 18.

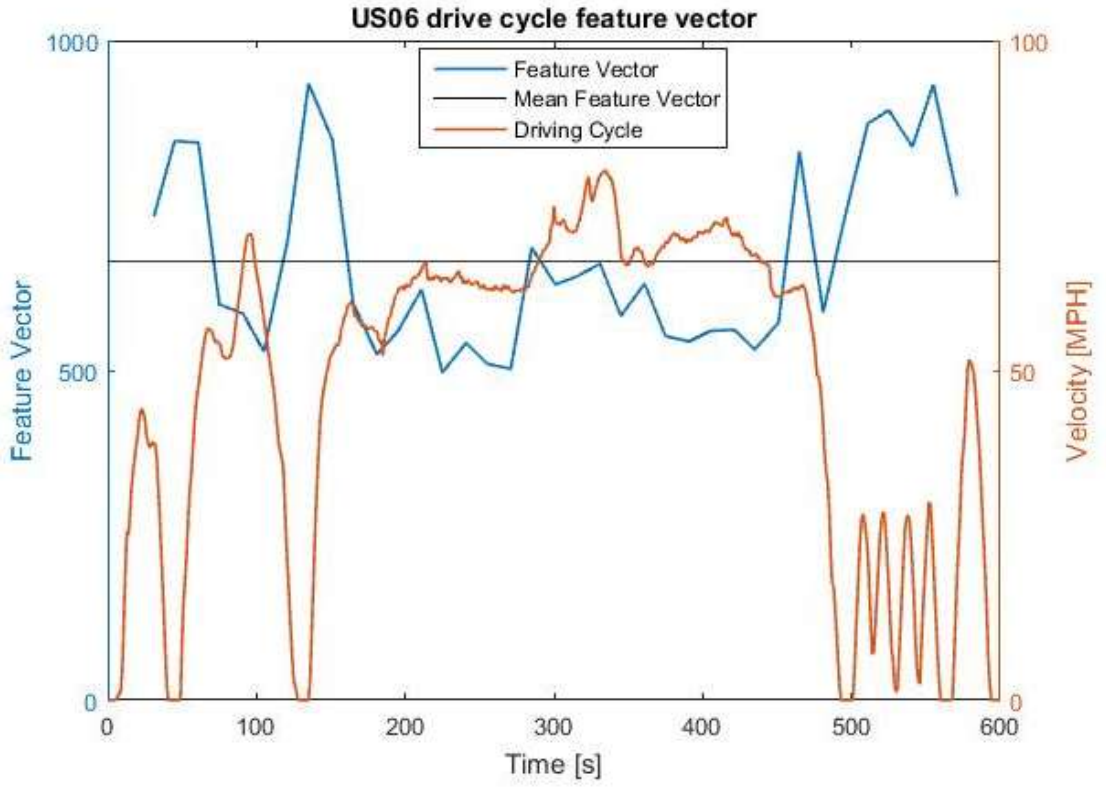

Figure 18 US06 Driving Pattern Feature Vector

The driving pattern recognition feature vector for urban drive cycle FUDS is shown in the Figure 19. The important thing to observe in the two feature vector figures is that the feature vector for US06 in general has higher values as compared to the feature vector of FUDS drive cycle with the highest value in US06 being 934 versus the highest value in US06 being 666.

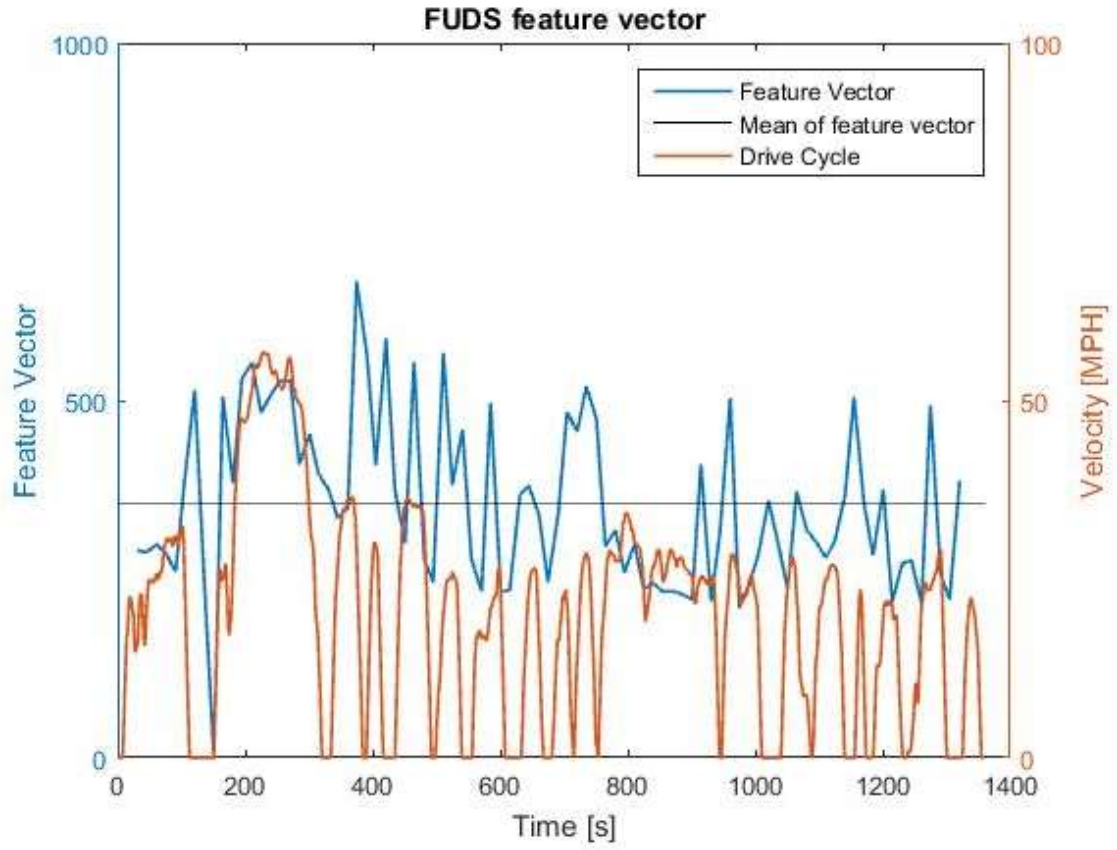

Figure 19 FUDS Driving Pattern Feature Vector

With the information about the drive cycle available as the feature vector, the controller should be made to change the control strategy according to the dynamics of the identified drive cycle. To do this a Driving Pattern constant is calculated which is the mean of the feature vector for the drive cycle. This mean is calculated at the end of the driving pattern recognition program. Since the values in the aggressive US06 drive cycle feature vector is higher, the mean will be higher than the urban FUDS drive cycle. Figure 20 shows the application of driving pattern recognition in the form of a flowchart.

For the US06 drive cycle, the minimum threshold for the SOC for both battery pack and UC is kept lower as compared to FUDS drive cycle. This allows a higher depth of

discharge during the US06 drive cycle since this a much more aggressive drive cycle and the maximum power demand and instantaneous power demands are higher as compared to the FUDS drive cycle. The FUDS drive cycle being a city drive cycle is less aggressive but had more start stop conditions which uses more of the hybrid ESS. So, to use the fuel cell in its efficient region and to keep a good reserve of SOC, the minimum threshold for SOC of battery pack and UC is kept higher.

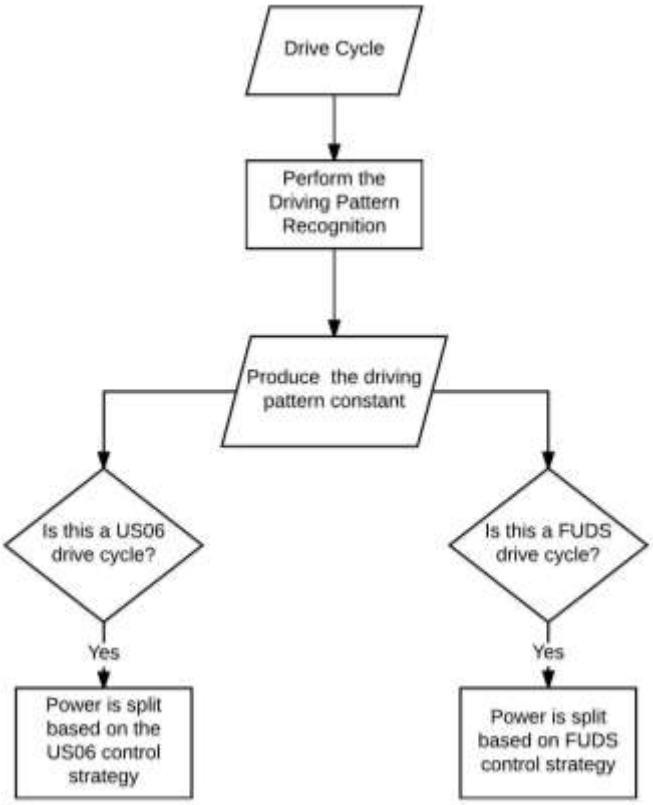

Figure 20 Driving Pattern Recognition Application

Thus, after calculating the Driving Pattern constant, this value goes into the Simulink model and switches the control strategy between the control strategy of aggressive drive cycle (US06) and urban city drive cycle (FUDS). Inside the Simulink model as shown in

Figure 21, the Driving Pattern constant based on its value activates the respective control strategy for that drive cycle.

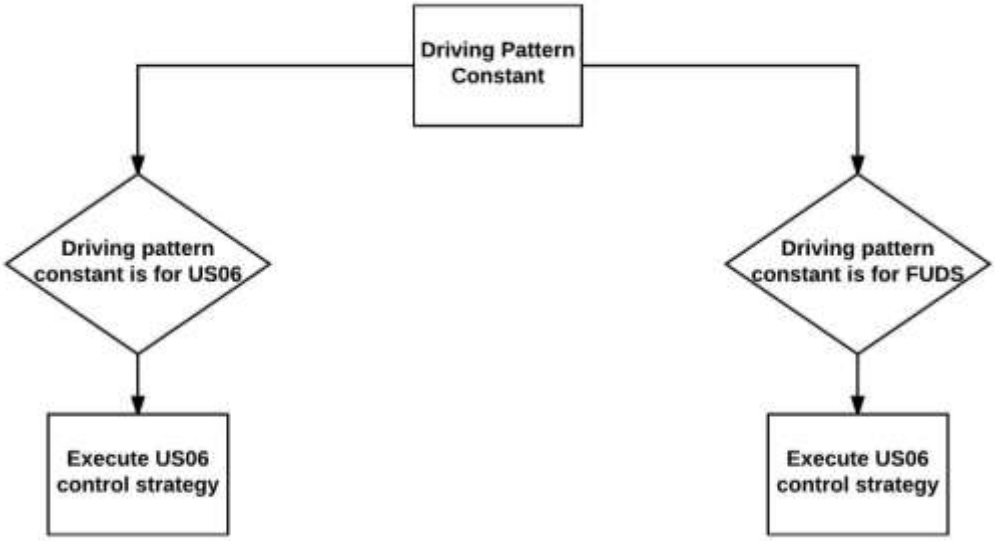

Figure 21 Control Strategy Switching

For the US06 drive cycle, the minimum threshold for the SOC for both battery pack and UC is kept lower as compared to FUDS drive cycle. This allows a higher depth of discharge during the US06 drive cycle since this a much more aggressive drive cycle and the maximum power demand and instantaneous power demands are higher as compared to the FUDS drive cycle. The FUDS drive cycle being a city drive cycle is less aggressive but had more start stop conditions which uses more of the hybrid ESS. So, to use the fuel cell in its efficient region and to keep a good reserve of SOC, the minimum threshold for SOC of battery pack and UC is kept higher.

4.4.1. Control Strategy for Aggressive Drive Cycle US06.

Three power sources present complexity in developing a PMS to use all three power sources efficiently. So, for the ease of implementation a strategy based on fuzzy logic presented in [40]. Fuzzy logic control strategy works on simple “if then” conditional logic. Different scenarios that can occur while driving are taken into consideration and conditions are defined with the respective action. So, if a certain scenario occurs, then the defined action is taken in the strategy. Typical input variables to the strategy are power demand and SOC of battery and SOC of UC. These inputs are processed and based on the constraints imposed in the model, decisions are taken. As discussed in the previous section, each power component in the powertrain has its limitations and advantages. So, this PMS is designed to make use of the advantages and overcome one components limitations with other components advantage. Thus, this PMS aims at shaving peak power from batteries and redirecting it to the UC along with high power demands.

The battery specification allows 110 Amperes maximum discharge current drawn from the battery. This comes out to be 9 kW of power to be drawn from the battery. For the fuel cell of 85 kW of power, the power range for it was chosen to be 35 kW to 55 kW as an initial value based on the curve shown in Figure 17. The remaining high power demands and excess load on the battery was all transferred to the UC and that’s how power shaving for batteries is achieved. Thus, characteristics of batteries, fuel cell and UC were analyzed. With the limitations of batteries power and current, peak power was shaved with assistance of UC. The losses occurring in the fuel cell based on polarization curve is used to optimization fuel cell operation range. UC are used for all the transient demands. A PMS

is developed with all these criteria and a flowchart in Figure 22 gives the outline of the distribution and flow of power.

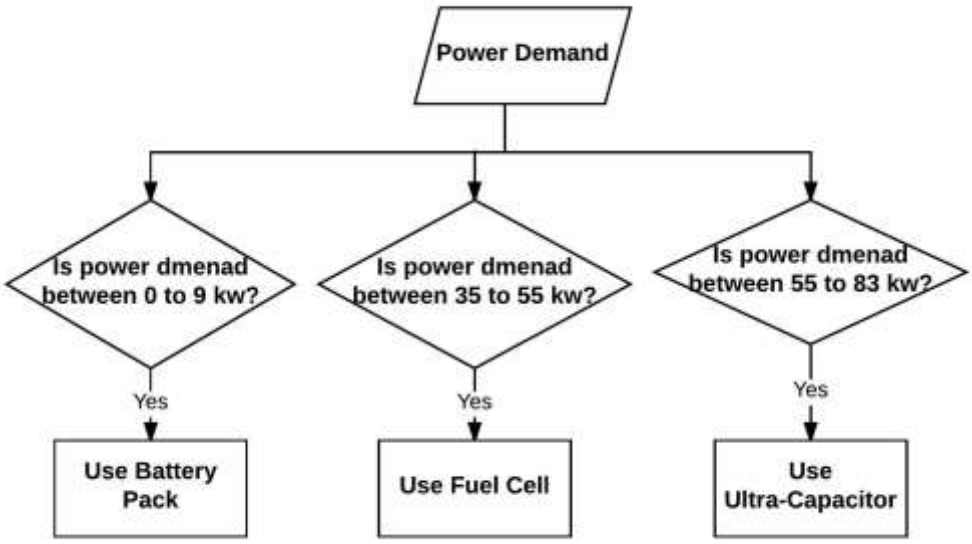

Figure 22 Power Split Strategy for Aggressive Drive Cycle US06.

After all the signals are processed, at the end of this algorithm, the values of power to be drawn from all three components are calculated that is then passed on to the ESS block and the fuel cell system block. This section of the PMS just processes positive power. The negative power is just passed through to the regen power management block which is discussed in the next section.

4.4.2. Control Strategy for Urban City Drive Cycle FUDS

The FUDS drive cycle is an urban city drive cycle with lots of stop and go situations and accelerating from stops. Thus, the control strategy for this cycle should reduce dependency on fuel cell as much as possible since the fuel cell responds very slowly to

change in power demand. The reliance on power demanded by the ESS components i.e. battery and UC is thus increased since UC can be used for high power demands and then the battery can supply power once the vehicle is in motion.

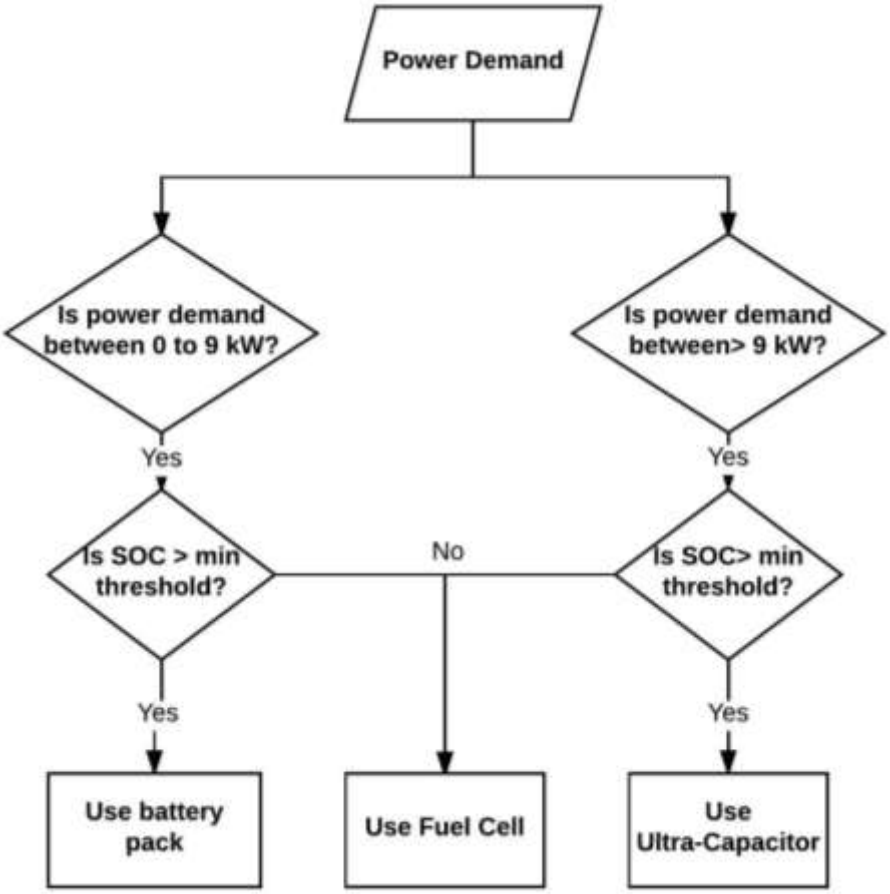

Figure 23 Power Split Strategy for Federal Urban Drive Cycle (FUDS)

The flowchart shown in Figure 23 shows the working of the control strategy. As explained above, the ESS provides most of the power until they hit the minimum SOC threshold. At that point, the fuel cell kicks in and fulfills the power demand. Since the battery can provide up to 110 A of current, the power drawn from the battery is limited to 9kW. The high-power demands are drawn from UC. As the vehicle start moving from zero velocity, the

UC provides power. As the car is in motion, it's power demand decreases and the battery can provide power since the power requirement is low at that point. This makes the fuel cell stack to work as an auxiliary power unit which helps in reducing the amount of hydrogen consumed.

The limitations and advantages of the components that have been discussed in section 4.4.1. are applicable to this control strategy as well and the power distribution for FUDS drive cycle also is designed keeping in mind the limitations and making use of the advantages.

4.5. Dynamic SOC Based Regenerative Energy Management

How to improve the ways to harvest the regenerative braking energy is still an issue that is being investigated by many researchers. There is a lot research on managing the positive power demand for all vehicles. But there are few papers when it comes to managing the regenerative power although there is lot of scope to harvest this energy. There is even less investigation in control strategy for regenerative power with multiple source in the ESS or what can be called a Hybrid ESS since there is both UC and battery pack in the ESS. Since there are two devices that can harvest the regenerative power during braking. So just like the PMS for the positive torque request, a power management for regenerative power.

In drive cycles with frequent stop and go, every time the driver hits the brake, the kinetic energy of the car can drive the motor shaft essentially turning it into a generator. When going downhill on a road can cars going at very high speeds have, again there is

kinetic energy that can produce large amount of regenerative energy. Although there is a huge amount of power that can be generated when the motor turns into a generator when braking at high speeds, usually there is a limit to the amount of current that can be pushed into the battery. UCs have a much higher limit of acceptable charging current. In the absence of UC, the excess current above the acceptable charge current of the battery, would have to be discharged as heat through a resistor. So, it is important to characteristics of UC to the maximum which in turn will help protect the battery from excess charge current also enhancing the efficiency of the electric system at the same time. With the UC in the ESS, almost all the regenerative current can be utilized based on the SOC of the components. With this idea in mind, a dynamic SOC based regenerative control strategy was developed which is discussed in the following section.

To efficiently manage the regenerative power, it is essential to direct the major portion of regenerative power to charge the component which has a lower SOC compared to the other. So, a comparison between the SOC of two components is made to assign them a priority based on which one has a lower SOC. Then a regen weight ranging from 0 to 1 is assigned to each component based on a look up table which decides the value of weight to be assigned. The weight is multiplied to the regenerative power and the resultant value is then redirected to the component. The remaining regenerative power after the amount supplied to the component with lower SOC is redirected to the other component. This way it's always ensured that the component with lower SOC get charged first and since the remaining power is given to the other component there is least wastage of power.

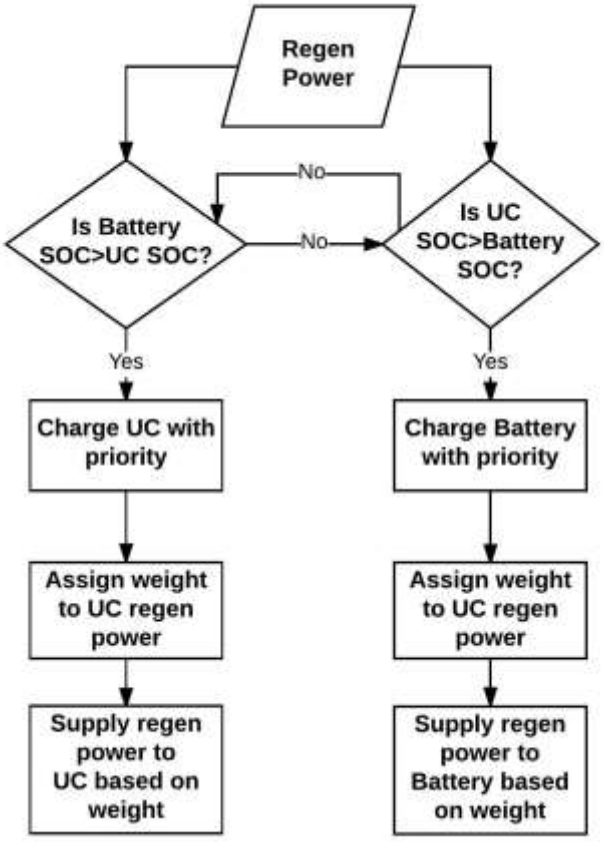

Figure 24 SOC Based Regen Energy Management Flowchart

5. MODELLING APPROACH AND SIMULATION

The software used to develop the model is MATLAB/Simulink developed by MathWorks. Inc. Simulink which is a part of the package is the tool used for modelling the vehicle along with its components and for developing the PMS strategy. Simulink is a tool which provides libraries with different functions associated with different kinds of libraries. These libraries provide blocks that are used to create a block diagram for modelling and simulating systems. All the systems in this FCHEV model have been modelled using these library blocks.

The initial model of FCHEV upon which this model was developed contained a battery and fuel cells. It had a basic PMS which worked based on power thresholds as the main criteria for distributing power among the components keeping in check the lower limit of battery SOC. The new model contains an UC in the ESS system and a redesigned PMS which is discussed in the later part of this chapter.

The top level of the model consists of three main blocks. They are:

1) Driver block
2) Electric Powertrain
3) Vehicle model

All these blocks collectively represent the entire FCHEV model. Figure 25 shows the top-level structure of the model.

5.1. The Driver Block

The driver block takes the input from the MATLAB workspace. The drive cycles are loaded from an initialization file. These drive cycles are predefined drive cycles by US Environmental Protection Agency (EPA). These drive cycles are tables with velocities over an interval of time. These are typical drive cycles used for vehicle and fuel emission testing. Figure 26 shows the internal structure of the driver block. The data for the drive cycles determines the desired velocity at different point of time.

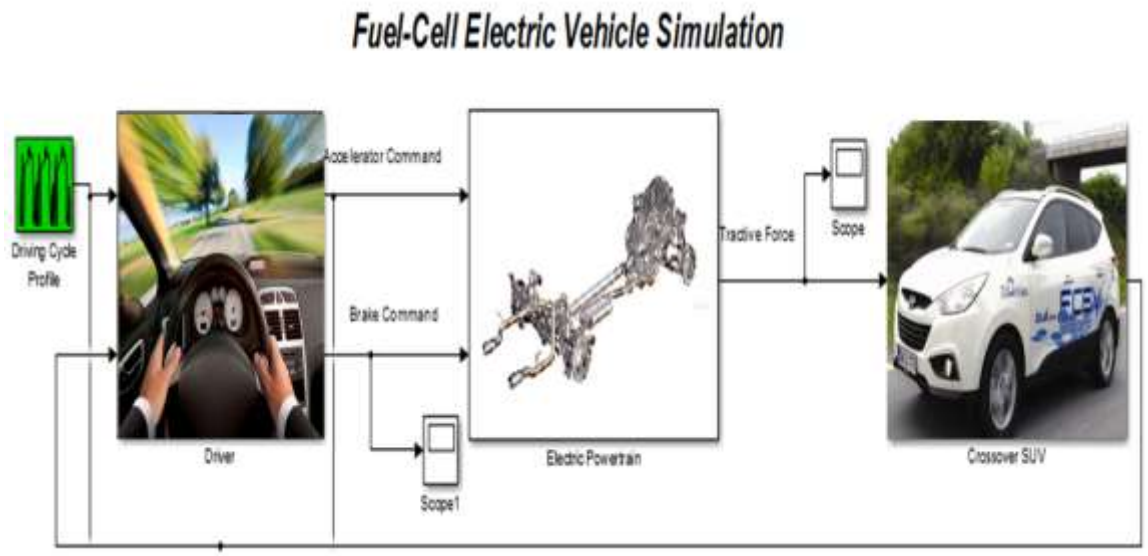

Figure 25 FCHEV Model Top Level

This model is a closed loop system. So, the actual velocity that the vehicle has is fed back into this block and an error value is calculated. A PID controller calculates the acceleration and brake command based on the correction from the PID. A gain of negative one is multiplied by the brake command. Two switches that determine if the value of the output of the PID is positive or negative. Positive value is defined as acceleration command and negative value is defined as brake command. These acceleration and brake values are fed into the powertrain block shown in Figure 25.

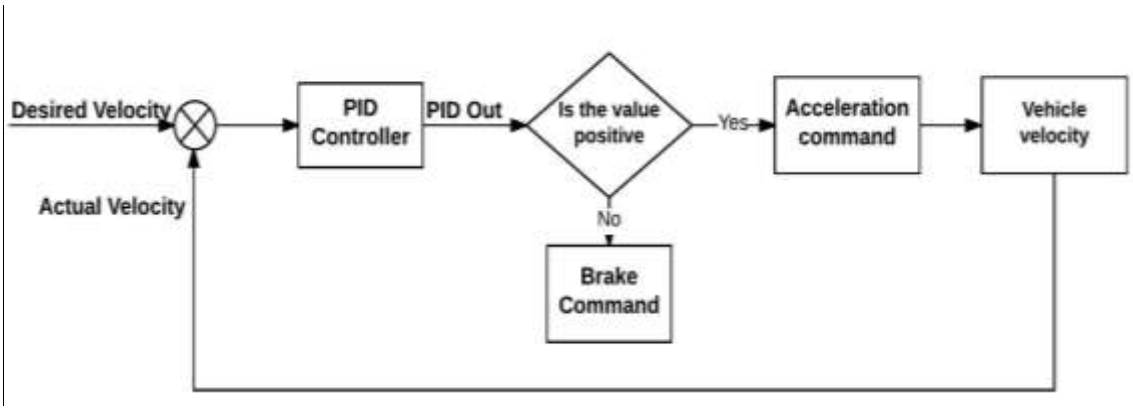

Figure 26 Driver Subsystem

5.2. The Electric Powertrain Block

The powertrain block consists of many subsystem blocks that collectively model the entire powertrain. The major subsystems inside the powertrain block are listed below:

1. Fuel Cell System
2. Energy Storage System
3. Controller

A block diagram shown in Figure 27 shows the flow of commands and signals between model and the controller where the torque split between components happen.

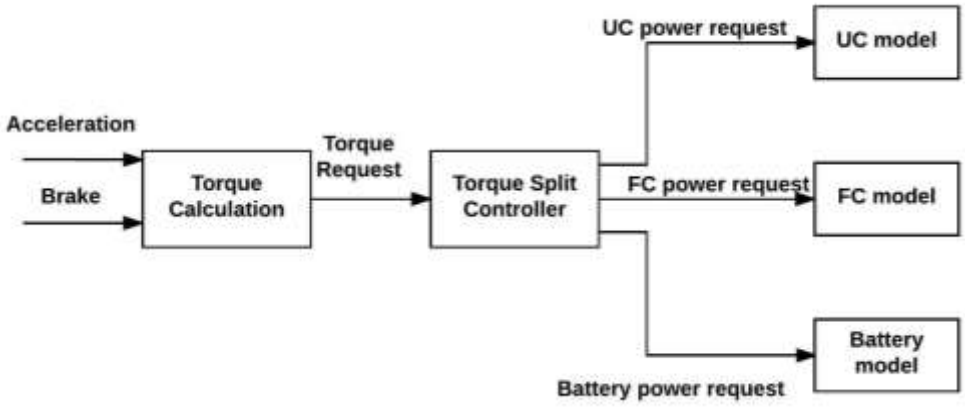

Figure 27 Powertrain Block Signal Flow

5.2.1. Fuel Cell System

The fuel cell subsystem takes in the power requested from the fuel cell stack out the total power requested by the vehicle. This power request is fed into a power control block as shown in Figure 28. This block contains a map which outputs current based of the power demand. This current request is sent to the fuel cell system where the fuel cell is modelled.

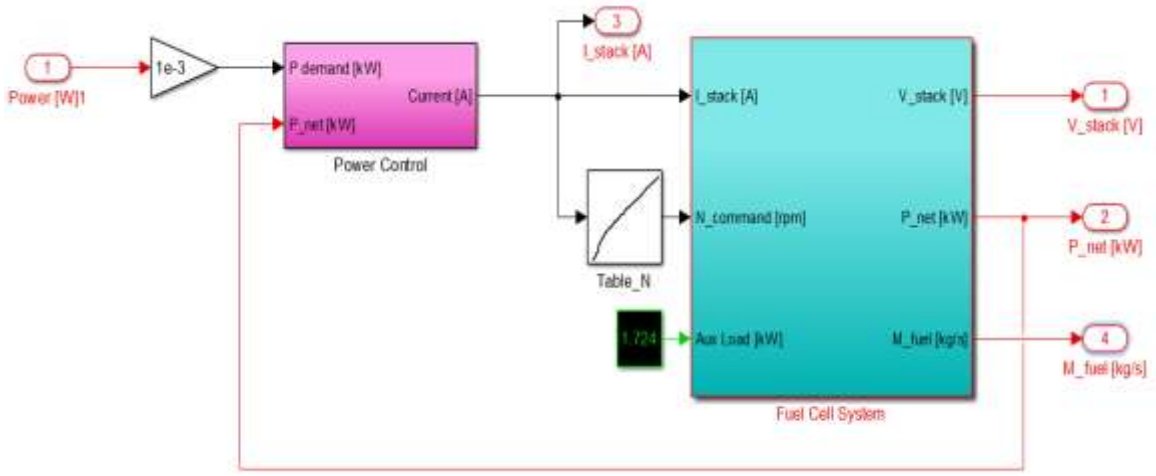

Figure 28 Fuel Cell Subsystem

The fuel cell system needs a few parameters as input which it receives from the initialization files. These parameters are the specifications of the fuel cell. These specifications are listed in the Table 6 below.

Table 6 Fuel Cell Parameters

Parameter	Description	Value
Area.FC	Cell Area [cm^2]	420
N_FC	Number of stack cells	380
H_2_FC	Hydrogen Utilization Factor	0.9

Lhv_FC	Lower Heating Value of Fuel [kJ/kg]	11300

A fuel cell polarization curve is a 2-D table which takes in cathode pressure and current density as the input. To calculate the current density, the current is divided by the area of the stack. The cathode pressure and current density when fed to the 2-D fuel cell polarization curve give the stack voltage as the output. This value when multiplied by the number of cells give the stack voltage. The voltage when multiplied by current gives power delivered by the fuel cell. The Figure 29 below shows this above described system.

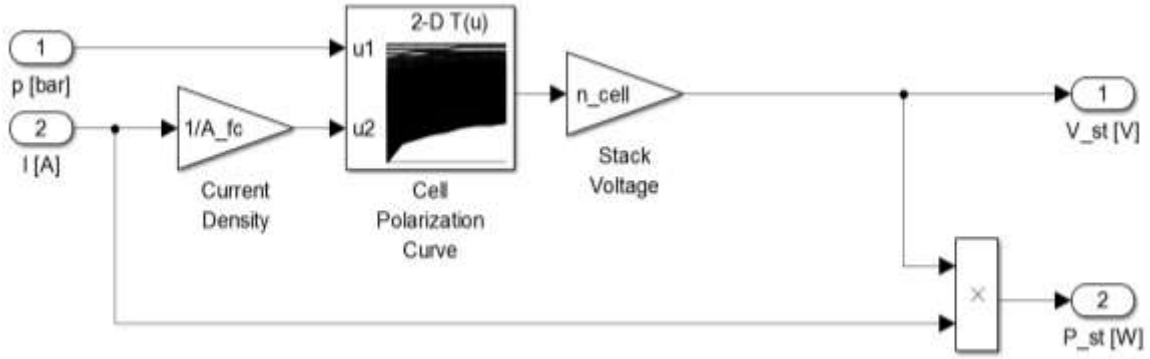

Figure 29 Stack Voltage and Power

This value of power from stack is then fed back into the power controller block which is shown in Figure 30. The power control block takes in the power demand and compares it with the actual stack power. The internal structure of this block shown in Figure 30 shows that it contains a power vs current map. The demanded power is fed into this map to get the value of corresponding current. A feedback block which contains a PID takes in the power demand and the power generated in the fuel cell and creates a correction value for the stack current.

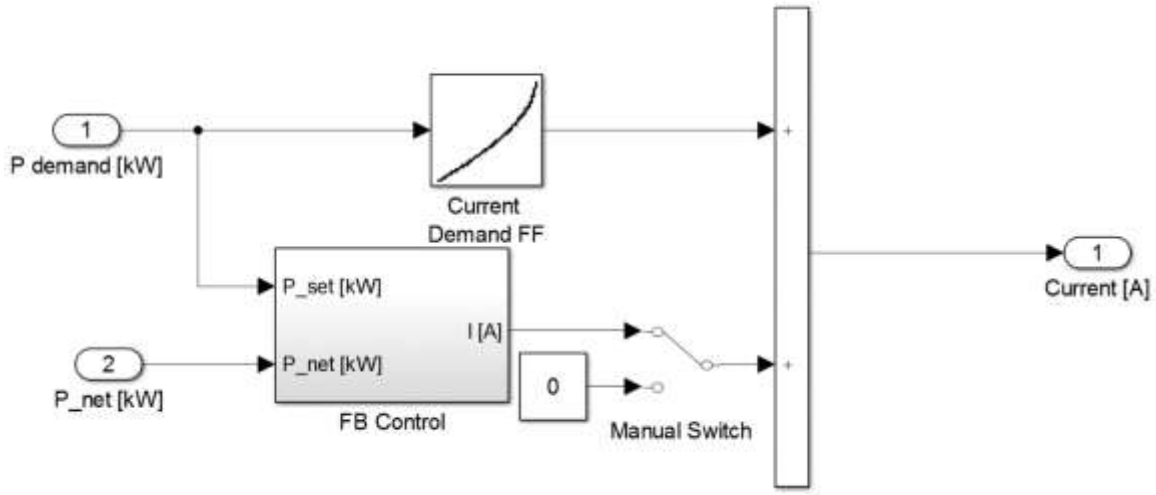

Figure 30 Fuel Cell Power Control

5.2.2. Battery Subsystem

The battery subsystem consists of battery model. It consists of smaller subsystems that contains equations to calculate current, open circuit voltage and SOC based of the power being pulled out of the component. A top level view of the subsystem is shown in Figure 31.

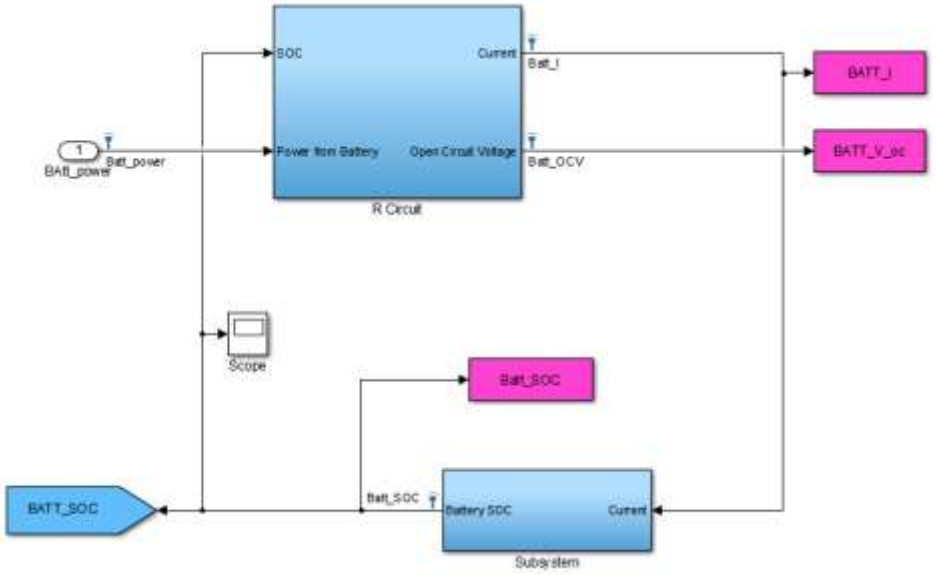

Figure 31 Battery Model

The input to the R circuit SOC and Battery power request based on the power split controller are the inputs to the block. Inside the block is a map which contains data for SOC vs Open Circuit Voltage. So, based on the SOC, the open circuit voltage per cell is calculated which is then multiplied by the number of cells in series to obtain the open circuit voltage of the battery pack.

The power requested from the battery is used to calculate the battery current. The initialization file loads maps for SOC vs Resistance during charging and discharging. A switch which checks if the power value is negative or positive. The output of this switch is multiplied by the number of cells to get the total resistance of the battery pack.

Following the basic electrical equations, we can get the current from the battery pack. The basic equation for power can be given as [41], where R is resistance and I is current

$$P = R * I^2 \tag{9}$$

Using Eq. 10, we can get current from this as:

$$I = \sqrt{\frac{P}{R}} \tag{10}$$

Figure 32 shows the block diagram for current calculation explained in the above section.

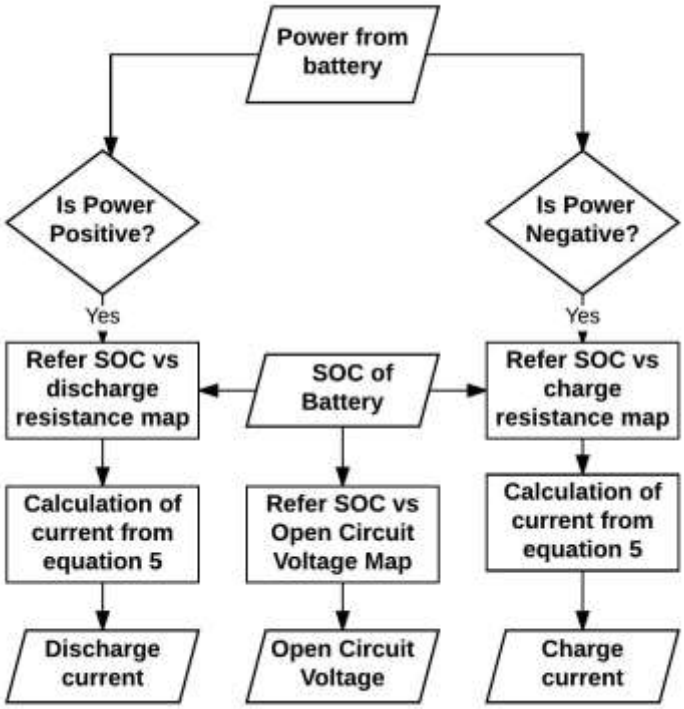

Figure 32 Battery Circuit Model

5.2.3. Ultra-Capacitor Subsystem

The major criteria for selecting the ultra-capacitor was the charge/discharge-power. For an aggressive drive cycle like US06, the maximum instantaneous power can go up to 83 kW. The most renowned maker of ultra-capacitor in the market is Maxwell. There are various modules of Maxwell capacitor for different types of application. The one that is recommended by Maxwell for automotive applications are 48V modules. The BMOD0165 module was selected for this application. It can provide 91 kW power for impedance matching and 100 A RMS current [42]. The current calculation block gives the UC current and open circuit voltage. The current is then fed into the SOC calculation block which

calculates the SOC based on the amount of current drawn and pushed back into the UC. The Figure 33 below gives an overview of the top level of UC equations.

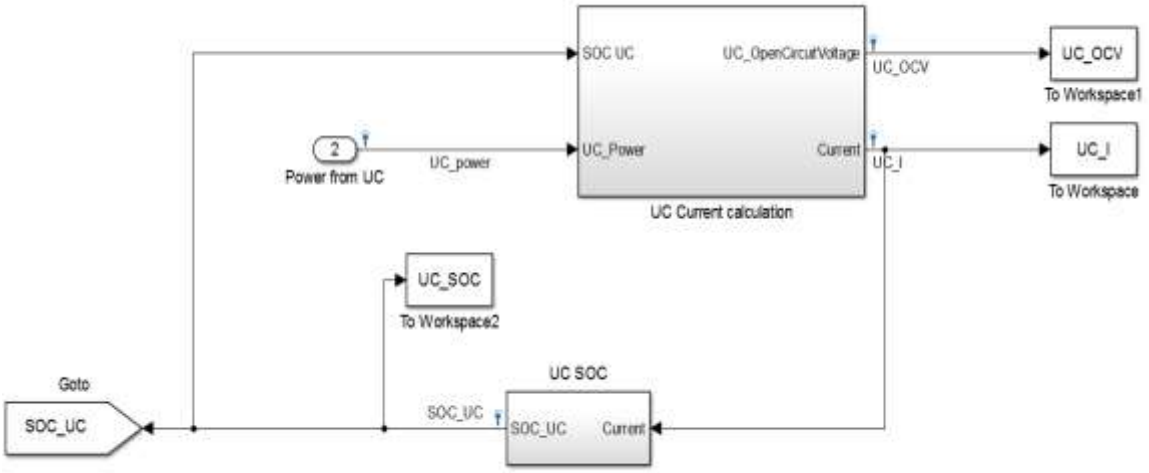

Figure 33 Ultra-Capacitor Model

These two blocks shown in the Figure 33 contains equations that give the outputs mentioned above. The current equation derived in [43] is a function of SOC, lumped resistance of the system mainly consisting of the internal resistance of UC and connecting cables. The Eq. 11 of current from a capacitor is:

$$\mathrm{I}=\frac{\mathrm{SOC}*\mathrm{Vmax}-\sqrt{SOC*Vmax^2-4*R*PUC*\eta}}{2*R} \tag{11}$$

In the above equation *R* is the lumped resistance, *Vmax* is the maximum voltage of the UC and η is the efficiency during the charge/discharge cycle. The value of charge/discharge efficiency was taken as 90% based on the research shown in [44].

The State of Charge (SOC) equation is modelled as shown in the Eq. 12 below [45]:

$$\mathrm{SOC}=\int(I*\eta)/Qdt \tag{12}$$

Where, η is the coulomb efficiency of the capacitor, Q is the electric quantity and I is the current drawn from UC.

The Q in the above equation is given by the following Eq. 13:

$$Q = C * OCV \tag{13}$$

Where, C is the capacitance of the Ultra Capacitor, OCV is the Ultra Capacitor Open circuit voltage.

The open circuit voltage modelled is defined by Eq. 14 shown below:

$$\text{OCV} = \int \left(\frac{I}{C}\right) dt \tag{14}$$

Where, I is the current requested from the Ultra Capacitor, C is the capacitance of the UC.

5.2.4. Electric Motor Subsystem

This system consists of two parts. One determines the torque requested out of the motor based on the drive cycle and the other determines the speed of the motor in rad/s. The vehicle model block determines the velocity of the vehicle. The vehicle velocity is divided by the radius of the tire to get the rotational speed of the vehicle. This speed when multiplied by the transmission ratio gives the rotational speed of the motor. This motor speed is fed as inputs to torque maps to determine maximum and minimum torque limits based on which the output torque of motor is determined. The requested torque is also fed to an efficiency map and then on to a switch which determines if the power drawn is positive or negative. The product of rotational speed of the motor and torque is then divided by the efficiency to determine the power. Figure 34 shows the block diagram of the motor torque subsystem.

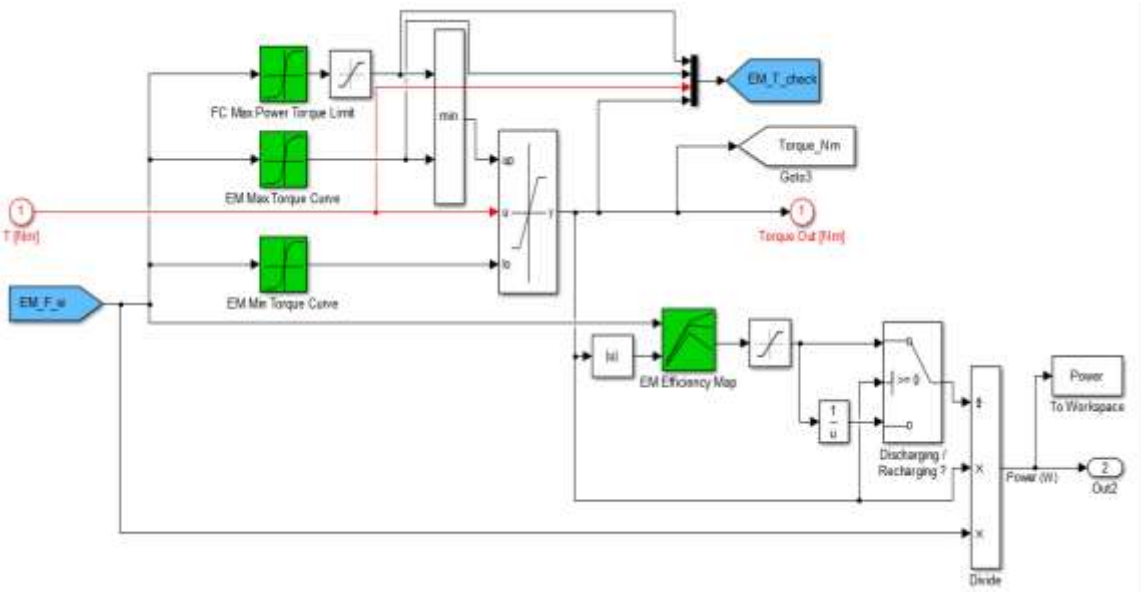

Figure 34 Motor Torque Subsystem

5.2.5. Controller Block

The electric powertrain block takes in the acceleration and brake commands from the driver block which goes into a controller block inside the powertrain block. In the controller block it gets multiplied by the maximum torque the motor can provide to determine the torque to be requested from the model. This makes the torque request a function of acceleration request by the driver. The same method is used to determine the negative command. Figure 35 shows the flowchart for the working of controller block. Two additional switches seen in the figure determine if both components in the ESS are above the above the maximum SOC limit. In that case no regen power goes into the ESS since they are already above their maximum limit.

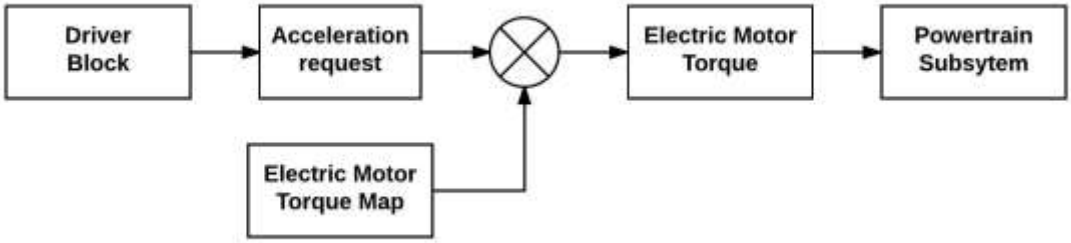

Figure 35 Controller Block

5.3. Vehicle Dynamics

The electric powertrain block after all the signal processing generates a tractive force which is fed into the vehicle model block. The tractive force propels the vehicle forward overcoming the resistances it faces. The typical resistances a vehicle faces are rolling resistance, aerodynamic drag and grade resistance. Figure 36 shows the forces that act on a car while driving on the road.

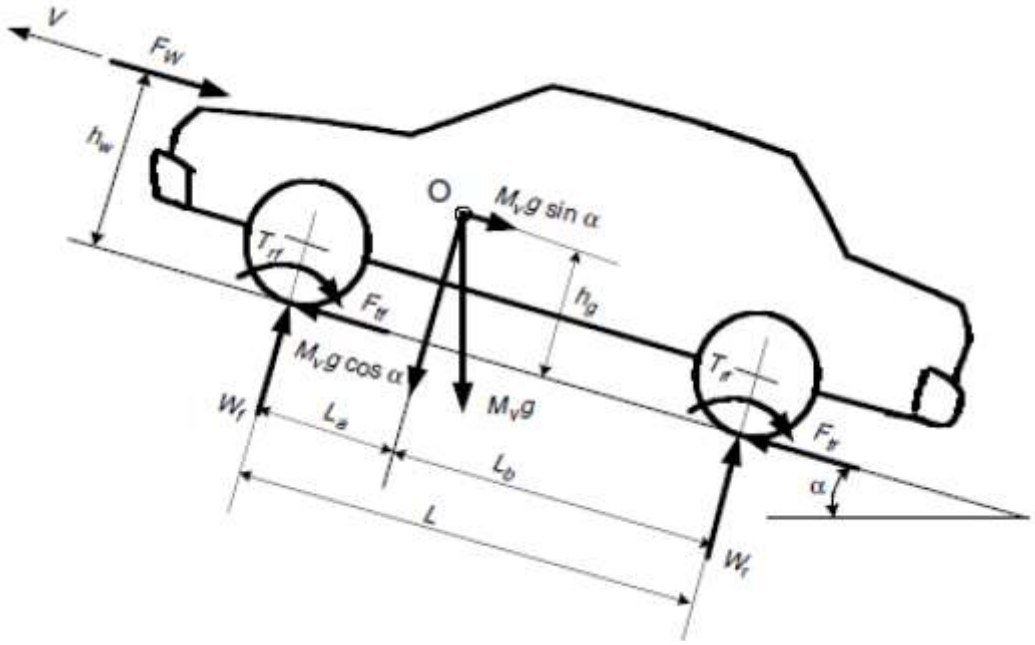

Figure 36 Forces Acting on a Car [46]

5.3.1. Rolling Resistance**:**

Rolling resistance is the friction or the force resisting the motion of a circular that's rolling on a surface. For modern radial tires, there is a deflection in the part of the tire which is in contact with the road surface. This causes the normal force to shift as shown in the Figure 37. As a result, the normal force is higher in the front part of the tire in contact with the ground. This shift in the normal force causes a moment about the center of rotation which acts in the opposite direction which is shown as M_f in the Figure 37 thus resisting the motion of the wheel.

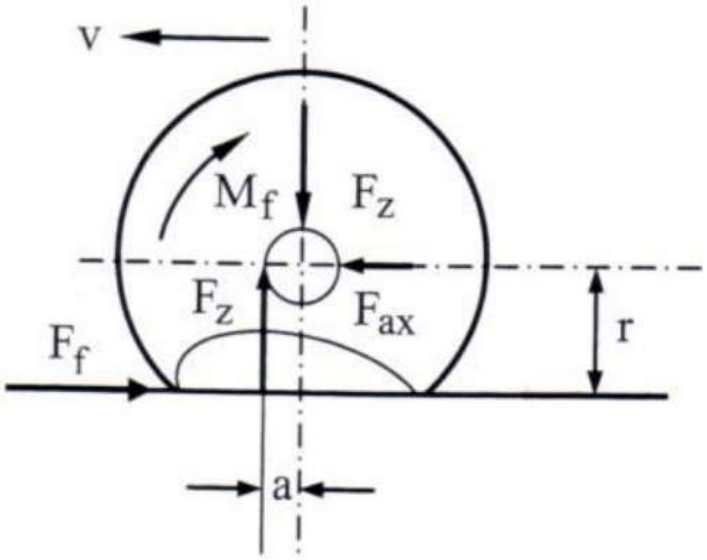

Figure 37 Tire Normal Force Distribution [47]

In the Figure 37, the distance of shift in the normal force is a and F_Z denotes the normal force. Based on this, the opposing moment comes out as Eq. 15:

$$M_f = F_Z * \mathrm{a} \tag{15}$$

To overcome this resistance, the force needed to be applied to the center of the wheel comes out to be [46]

$$F_{CW} = \frac{F_Z * a}{r_d} = P * \mu \quad (16)$$

In the Eq. 16, r_d is the effective rolling radius of the tire and μ is the rolling resistance coefficient. The above force is only when the vehicle is on a straight road. When going on a slope a cos component of the force is needed to propel the vehicle forward. So, the Eq. 17 for a vehicle on a road with slope α turns out to be [46]

$$F_P = P * \mu * \cos(\alpha) \quad (17)$$

For a vehicle running on dry asphalt, an approximate assumption for the value of coefficient friction was made to be 0.015. Also since *P* is the normal force, the acceleration causing that force is gravity at 9.8 m/s^2. So, the Eq. 17 can be rewritten with *M* being the mass of the vehicle as shown in Eq. 18:

$$F_P = M * g * \mu * \cos(\alpha) \quad (18)$$

5.3.2. Aerodynamic Drag

A vehicle driving on the road faces resistance from the surrounding air specially the air in the front. This resistance is directly proportional to the speed of the vehicle is called aerodynamic drag. Along with the velocity of the vehicle, the amount of aerodynamic drag a vehicle faces also depends on the front shape of the vehicle or the frontal area as its referred. The vehicle when moving forward, leaves behind an area of low air pressure. As the rule of physics, air flows from high pressure area to low pressure area thus increasing the aerodynamic resistance. Considering all the factors, the equation for the aerodynamic drag can be defined as [46]:

$$F_A = \frac{1}{2} * \delta * A_f * C_d * V^2 \quad (19)$$

In Eq. 19, the δ is the density of the surrounding air, C_d is the drag coefficient, A_f is the frontal area of the vehicle and V is the velocity of the vehicle. The value of C_d depends on the aerodynamic shape of the vehicle.

5.3.3. Grade Resistance

When a car is going uphill, it experiences an additional resistance component which is due to the grade of the road and it's called the grade resistance. But when going downhill, it helps in the motion of the vehicle. The Eq. 20 defines the amount of grade resistance or assistance depends on the mass of the vehicle denoted as M and is defined in [46] as:

$$F_g = M * g * \sin(\alpha) \quad (20)$$

Table 7 shown below shows an assumption of the variables for the model of the vehicle based on a general model of the car running on zero grade.

Table 7 Vehicle Parameters [46]

Parameter	Value
Tire Radius, r_d	0.3305 m
Vehicle Mass, M	1913.8 kg
Gravitational Acceleration	9.8 m/s^2
Air Density, δ	1.29
Frontal Area, A_f	2.82 m^2
Aerodynamic Drag Coefficient, C_d	0.416

So, to calculate the total force that propels the vehicle forward is all the resistive force subtracted by the generated tractive force. To further simplify it, we can write it in the form of an equation as Eq. 21:

$$Total\ Force = Tractive\ force - \ Rolling\ resistance - Aerodynamic\ drag - grade\ resistance \quad (21)$$

With this deduction, the Eq. 22 for this force after substituting all the values comes out to be:

$$m_{eff} * acc = Ftr - Mg\mu\cos(\alpha) - \frac{1}{2}\delta A_f C_d V^2 - Mg\sin(\alpha) \quad (22)$$

As the effect of rotating components in the vehicle, the mass of vehicle is taken as m_{eff}. Based on the above equation, the equation for tractive force comes out to be:

$$F_{tr} = m_{eff} acc + Mg\mu\cos(\alpha) + \frac{1}{2}\delta A_f C_d V^2 + Mg\sin(\alpha) \quad (23)$$

The equations discussed in the section above are modelled in Simulink inside the vehicle model block as shown in Figure 38. Integration of acceleration gives velocity which is fed back into the driver block to be compared with the demanded speed to create the acceleration signal with corrections.

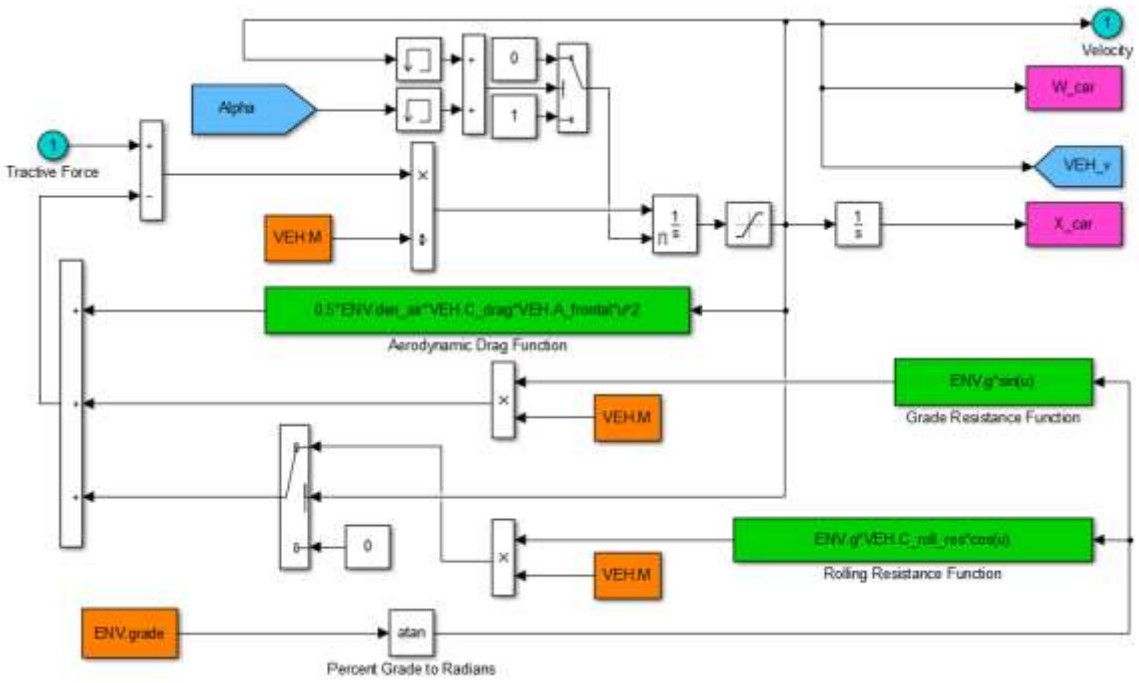

Figure 38 Vehicle Dynamics Model

6. RESULTS AND DISCUSSION

6.1. Simulation Results for US06 Drive Cycle

Upon successful development of complete UC-FCHEV, the output from the model (power, tractive effort, torque at wheels, power drawn from UC, FC, BP, etc) were compared to an in-production vehicle. The model proves to be realistic and results are within reasonable margined. Thereafter, the PMS was tested on simulations using Simulink and running Model in Loop (MiL) simulations. The DPR algorithm implementation activates the PMS for US06 drive cycle which is designed to be an aggressive drive schedule. The power demand profile of the US06 drive cycle is shown in Figure 39. As seen in this figure, the power demand has great variations caused by four stops followed by sharp acceleration of ~ 3.8 m/s^2. This make the power demand very high since sharp acceleration from a standstill requires more power in order to overcome the huge road load during initial vehicle motion due to significantly high resistive rolling and inertial forces.

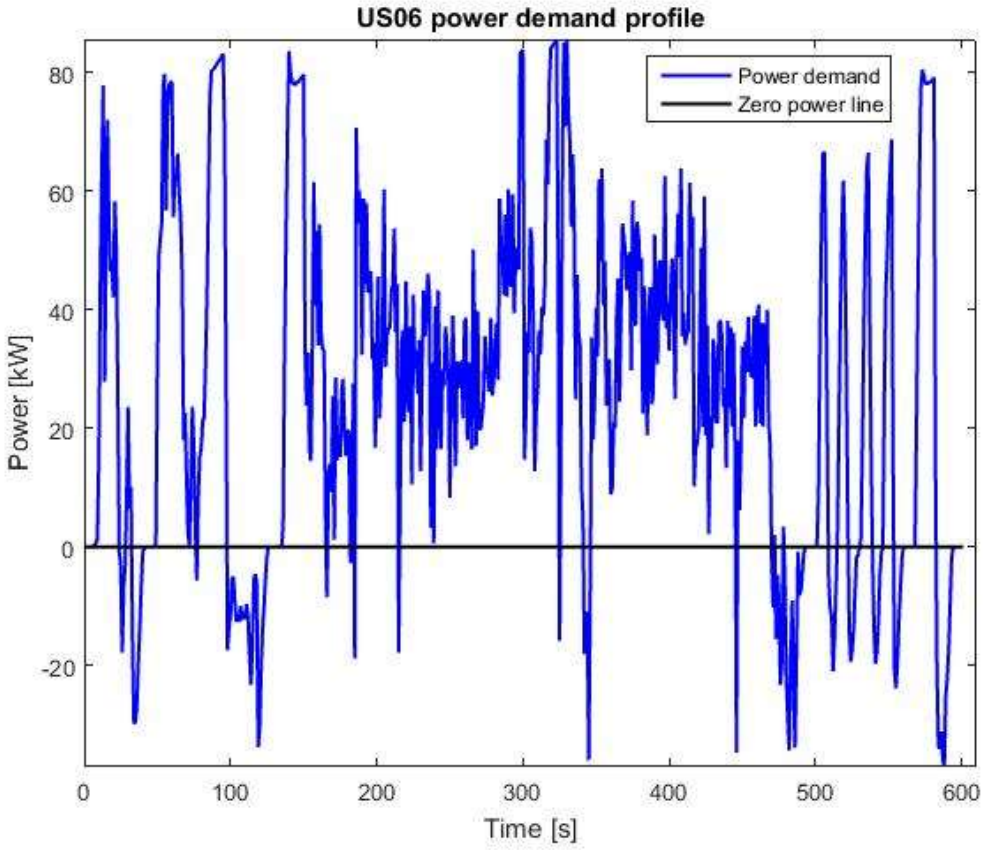

Figure 39 The Overall Power Demand as Dictated by US06 Drive Schedule

To assess the effectiveness of designed PMS, the most important parameter to look at is the current because the torques produced by the motor is directly related to the current and the SOC of the ESS components are also dependent on the current drawn from it. The comparison between the old FCHEV model with just the battery as the ESS is also done to see the effect of adding UC into the ESS. An initial comparison of the old model with just adding the UC to the ESS is discussed first. Then the effect of optimization is discussed with the UC added and how it improves the whole system.

Figure 40 shows the comparison between the fuel cell polarization curves before and after the UC being added to the powertrain. In the old configuration, the operating points

of the fuel cell are along the curve which is not advisable [30]. In the initial part when the activation losses are too high, the current density is too low. Also in the right side of the curve there are concentration losses which are high in the configuration without the UC. In comparison, the operating points seen in the FCHEV with UC, the operating points are more concentrated in the activation losses but closer to the center but operates within a limit and is not spread throughout the region. The results from the initial phase are discussed next in this section.

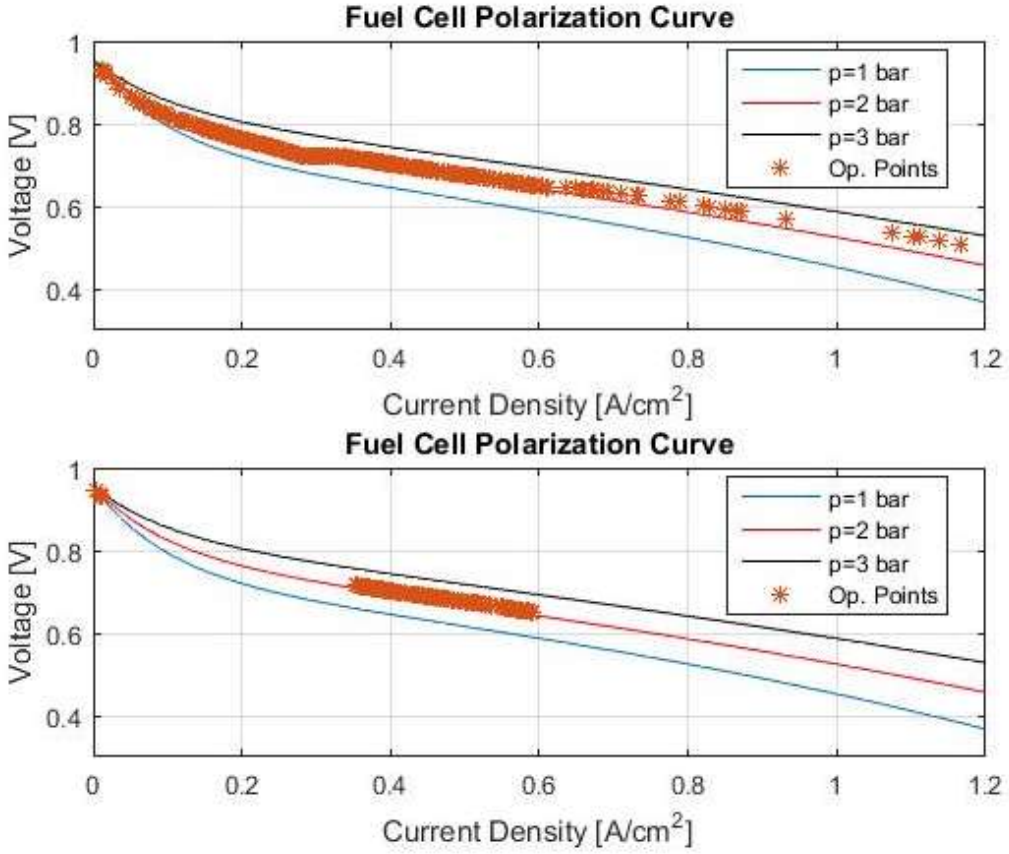

Figure 40 Fuel Cell Polarization Curve with and without UC

The fuel cell in the FCHEV configuration without the UC was the only power source once the battery is depleted. So, it would cause more power to be drawn from the fuel cell. With the UC added, the operation of fuel cell is limited to certain regions of power demand in the entire drive cycle. The difference can be seen in the Figure 41. The maximum value of current being drawn from the fuel cell comes down from 550 A to 125 A. The current without the fuel cell would often be in the range of 200 to 300 A but that's changed by the UC with current mostly staying in the 80 A to 120 A range.

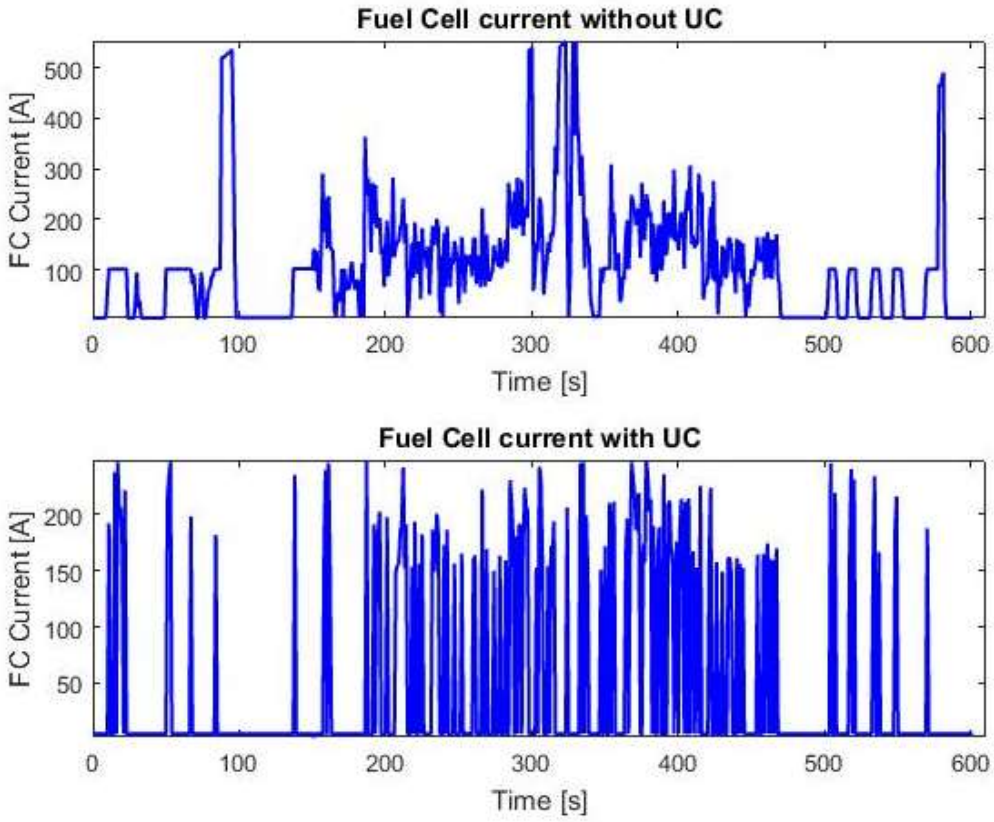

Figure 41 Fuel Cell Electrical Current Comparison

Figure 42 shows the comparison of the power drawn from the fuel cell with and without the UC. The PMS with the UC added in the ESS is also different. The effect of

both a new PMS and the UC is that the fuel cell operates in a certain region instead of being used almost all over the drive cycle. The maximum amount of power drawn is also reduced to 55 kW. In the old configuration in which the maximum power drawn from the fuel cell goes to around 80kW. The maximum capacity of fuel cell is 85kW and operating a fuel cell in such higher power region is not efficient as shown in Figure 16. This is considered in the new configuration.

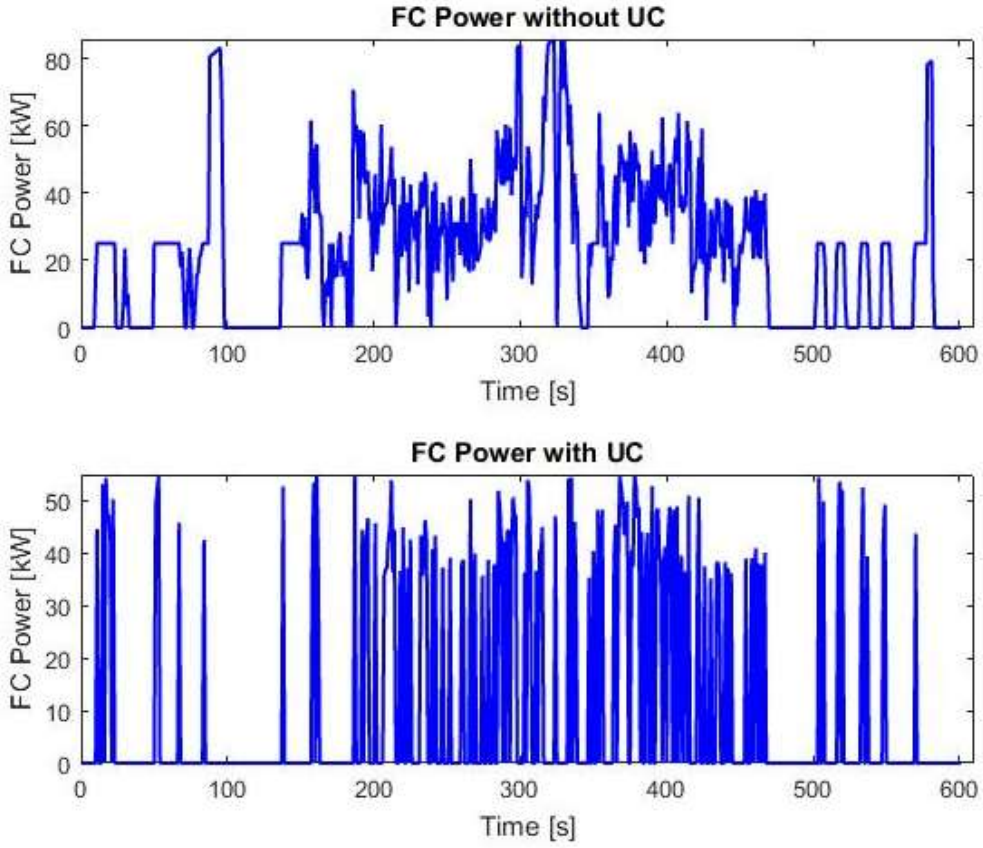

Figure 42 Fuel Cell Power Comparison

Figure 43 shows the battery current profile and the effect of adding UC to the ESS. Without the UC, the battery current goes high close to almost 300 A. Also, the instances at which the current is drawn from the battery is less frequent. But with the UC in the ESS and the

new PMS, a maximum utilization of the battery is done while considering its limits and dynamics.

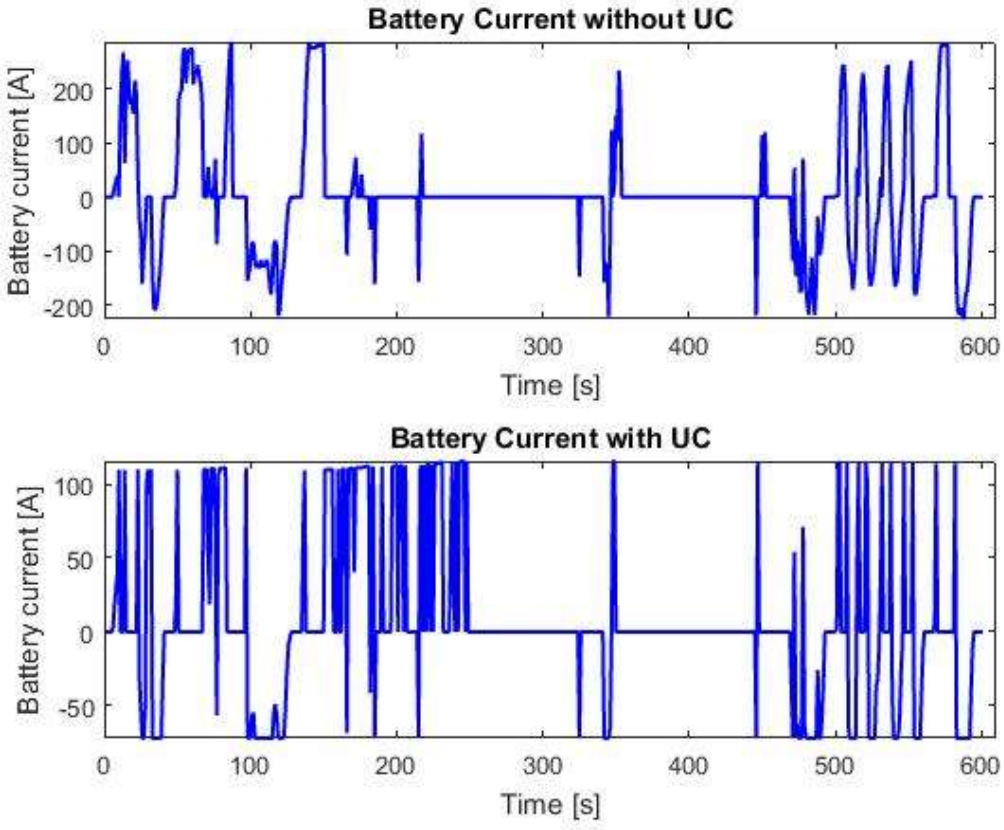

Figure 43 Battery Current Comparison

Figure 44 shows the difference in the SOC of the battery. As seen in the figure, the SOC of the battery hits it lowest allowable SOC level and stays there for quite some time which makes battery redundant until its SOC goes up again. With the UC added, the OSC of the battery doesn't go so low which makes the whole operation improve the lifetime of the battery. The peak currents without the UC close to 300 A whereas with UC its limited to 120 A. This happens because the current is saturated so it stays in its allowable current

limit. This shows that adding an UC brings down the discharge current of the battery reducing power being drawn from it and makes its operation safe.

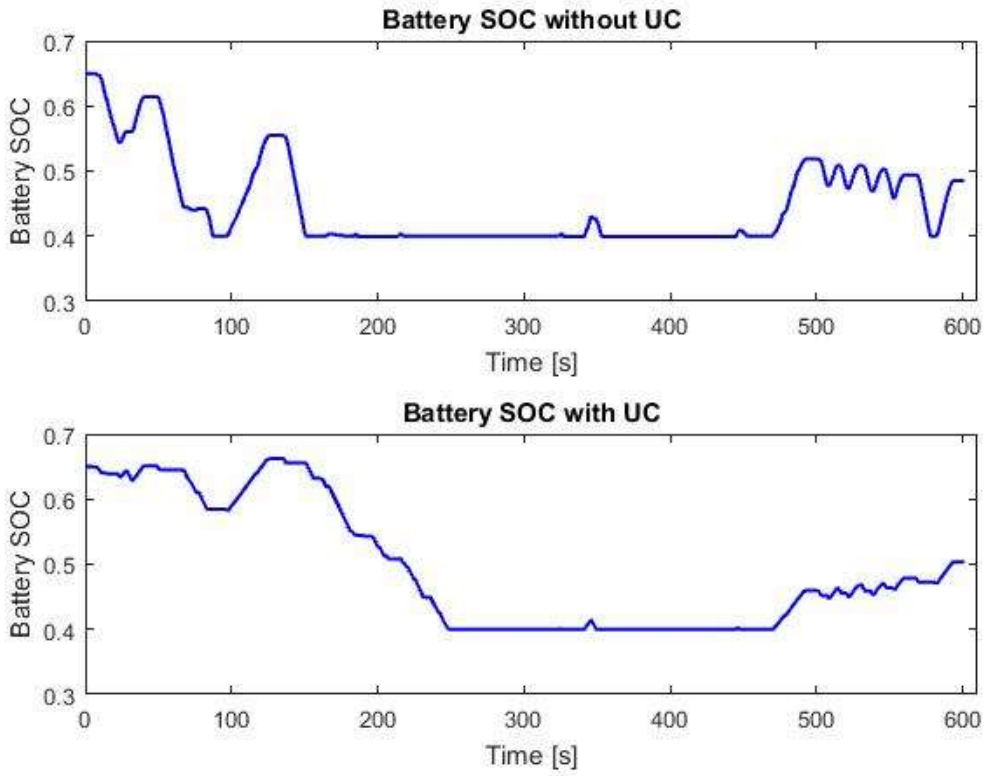

Figure 44 Battery SOC Comparison

On the other hand, adding UCs, resulted in eliminating peak power demand from battery packs. As illustrated in Figure 45 , the difference in the power consumed by the battery a difference of 48 kW. Since batteries are a good power source for sustained power demand, the operation of battery was limited to 9 kW which also keeps the current drawn from under its maximum limit of 120 A. Thus, it's used for more instance, reducing the power drawn from the fuel cell and taking more of the low energy power which it is designed to handle.

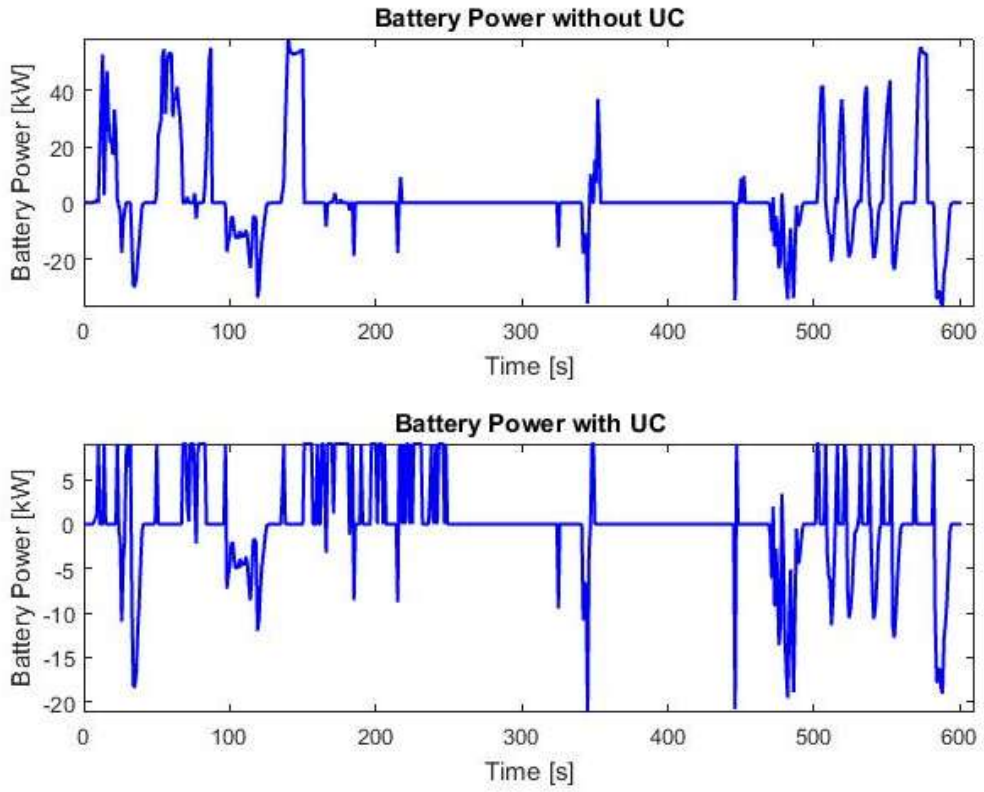

Figure 45 Battery Power Comparison

As seen in the polarization curve in Figure 40, the operating points indicated in the figure operate in the region of activation loss with very low current density. The fuel cell is advised to be operated in the high current density region due to concentration losses. So, the range of power operation that would put the operating points in the mid region which is the ohmic loss region. So, after that modification is done, the lower and upper limit of the have higher values than before. This increases the overall current being drawn from the fuel cell and this the amount of hydrogen being used, but it operates at a higher efficiency than before.

Figure 46 shows comparison between the optimized and pre-optimized results. This optimization is done based on the fuel cell polarization curve which is based on the chemistry behind the working of the fuel cell. Based on the drive cycle input, we can see the how different components react to the PMS. In the beginning of the drive cycle since the power demand high as the vehicle moves from standstill, the UC assists the battery and when the battery reaches its maximum limit, fuel cell kicks in. In all the stop and go situations, the power demand goes high to low as the speed of the vehicle increases. During this change of power demand, the UC assists and does current shaving to prevent excess load on battery and quickly fulfill the rapidly increasing power demand of the vehicle. In plot II of the subplot, the current drawn from fuel cell increase than before because the power drawn from the fuel cell is increased to operate it in its higher efficiency region.

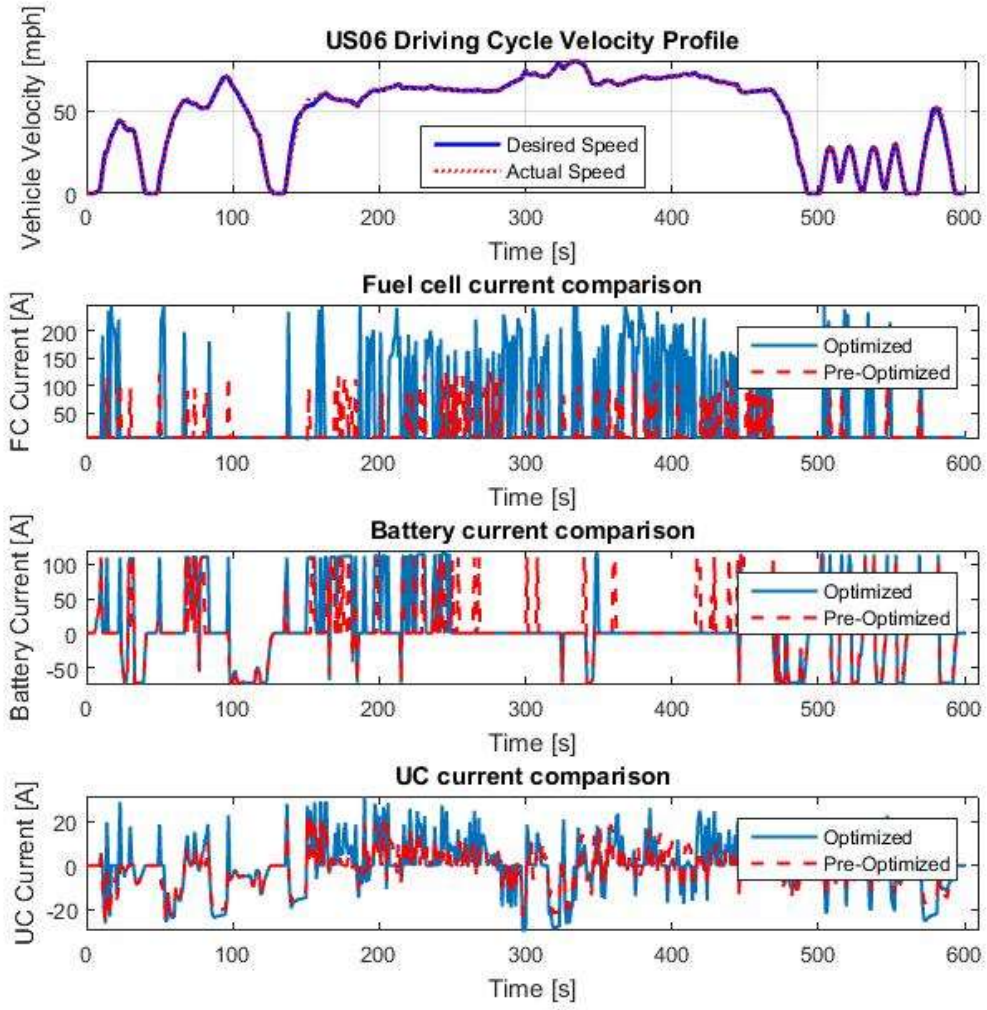

Figure 46 Current Comparison of FC, Battery and UC Under Optimal EMS

Figure 47 shows improvement in the hydrogen consumption. In the old configuration without the UC, the hydrogen consumption for one US06 drive cycle run was 0.2925 kg as seen in Figure 47. With the UC added, the hydrogen consumption comes down to 0.1277 kg.

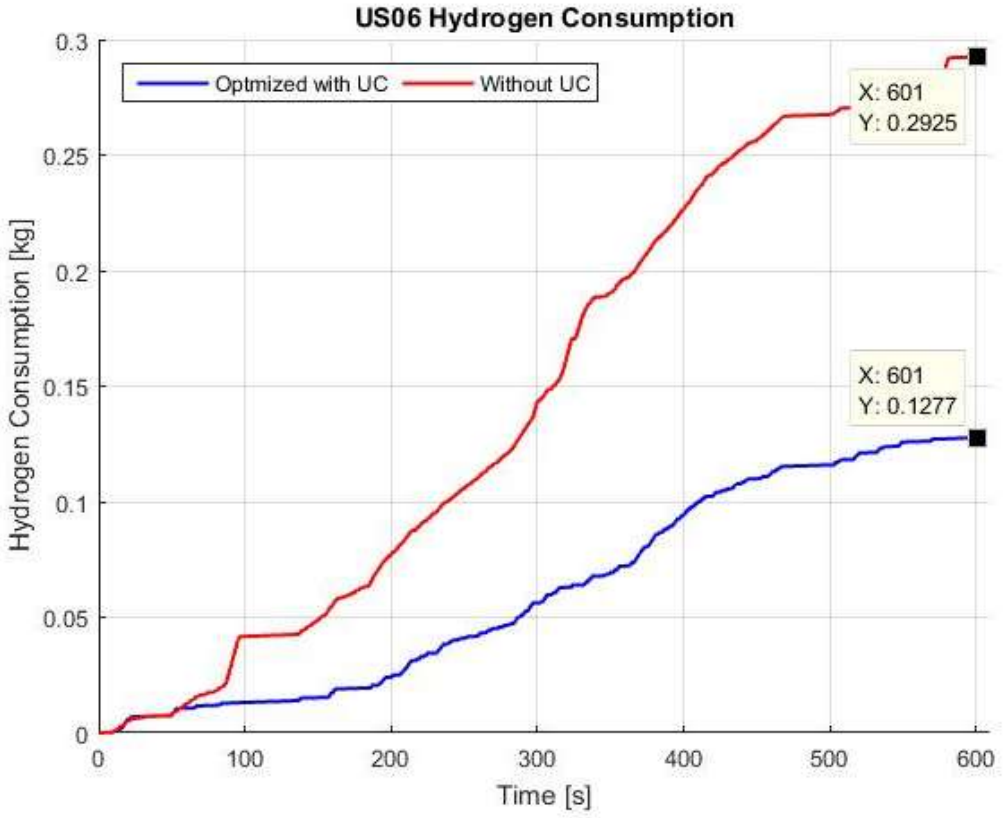

Figure 47 Fuel Consumption Comparison US06

Figure 48 shows the polarization curve with the optimized power operation range. As seen in the figure, the operating points shown lie in the region of ohmic loss which as discussed is the best region for the fuel cell to operate.

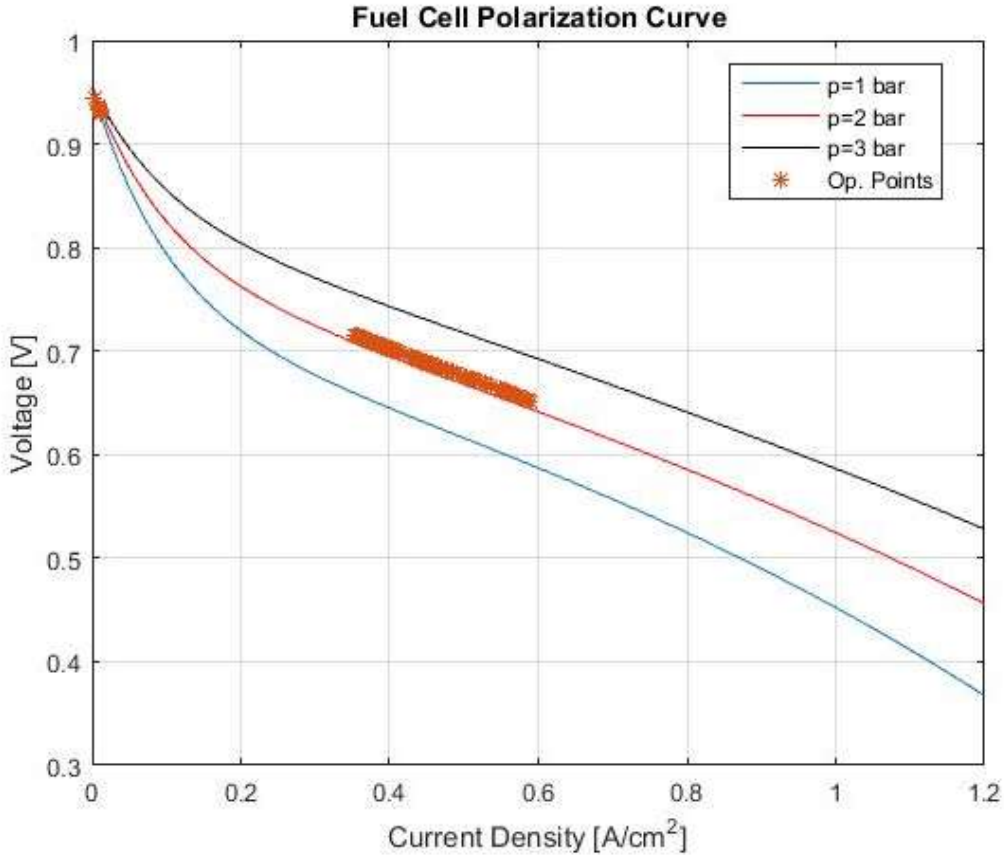

Figure 48 Fuel Cell Optimized Polarization Curve

6.2. Simulation Results for Federal Urban Drive Cycle

The FUDS drive cycle is an urban city drive cycle which is involves significant number of frequent stop and go compared to the US06 and hence needs a different PMS compared to the US06. The power demand profile shown in Figure 49 has 18 stop and go situations with accelerations leading up to 35 mph. So, using the less amount of power from the fuel cell is the best option because of its slow dynamics. Hence the same kind of PMS will not be most efficient for FUDS.

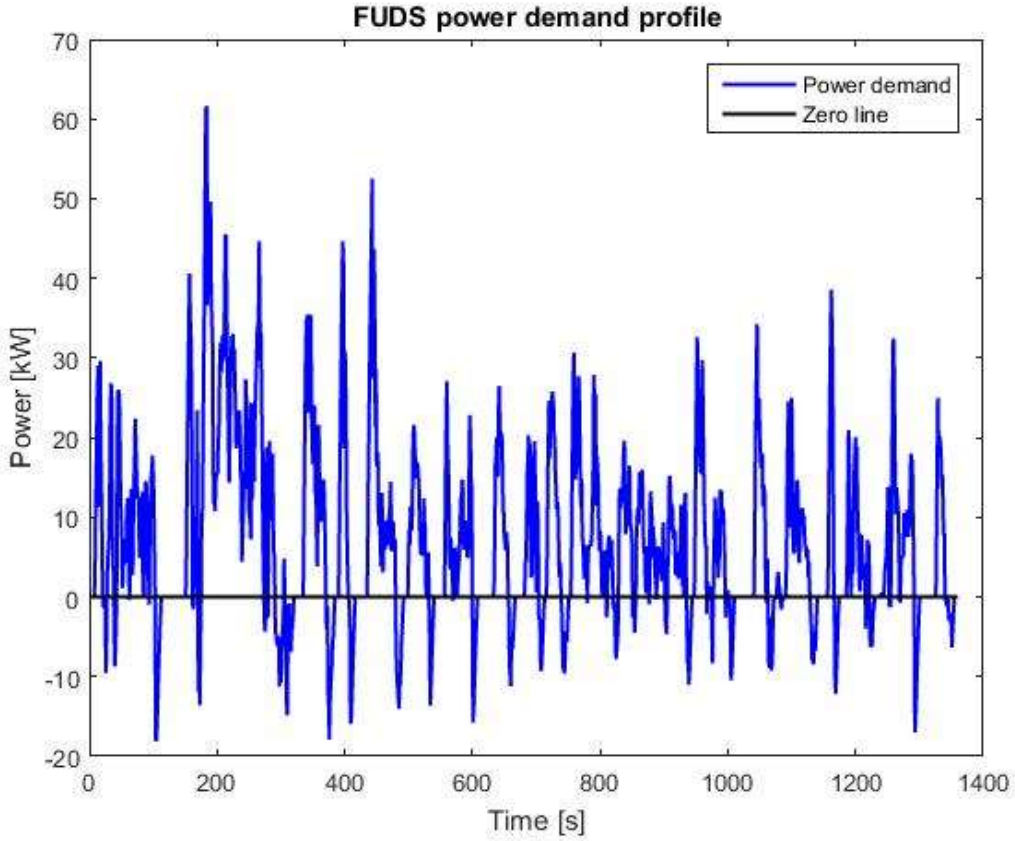

Figure 49 Power Demand of Federal Urban City Drive cycle (FUDS)

The PMS for the FUDS drive cycle uses more power from battery pack and the UC and the fuel cell just supplies power when the SOC of the components falls below the lower threshold. To look at the effectiveness of the PMS for FUDS and to analyze the pattern of current and power drawn from all three power sources and are discussed in the sections that follow.

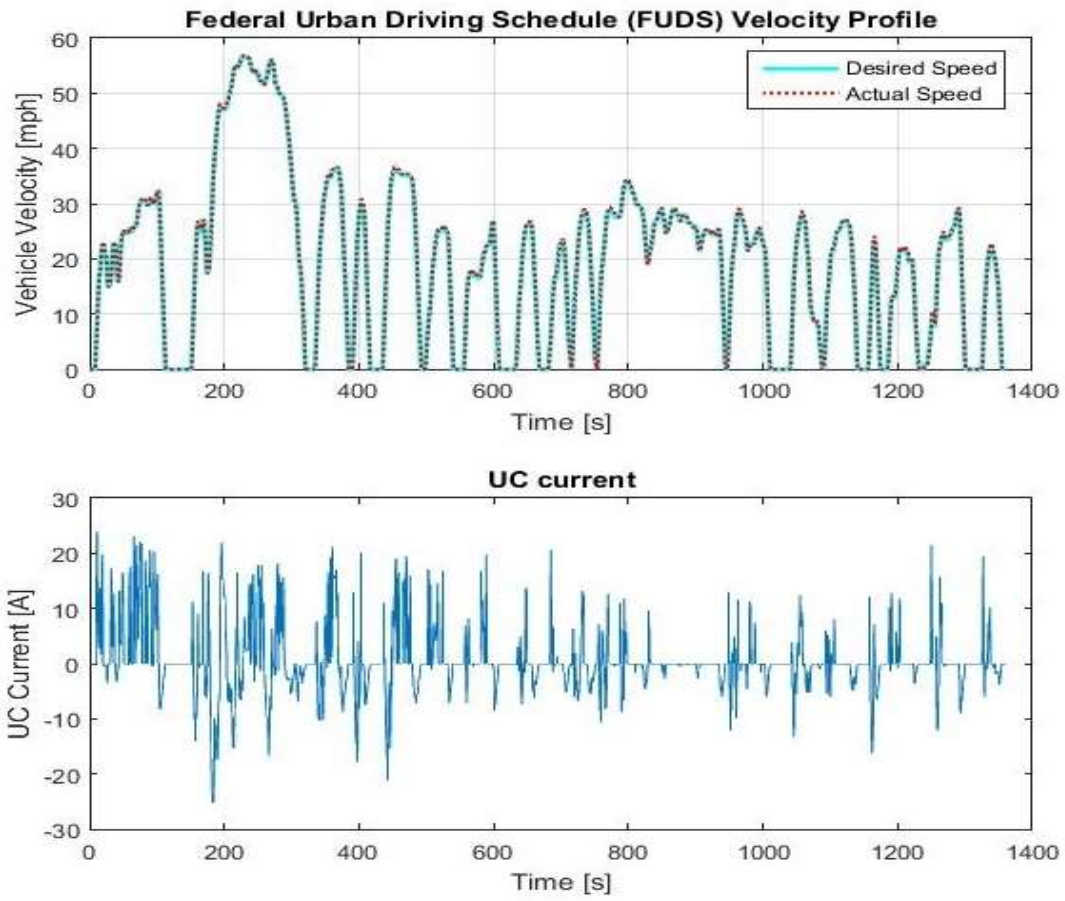

Figure 50 Ultra-Capacitor's Current Profile Under FUDS

As explained earlier, Initial Vehicle Motion (IVM) requires high power demand. Therefore, the torque supplied by the electric motor directly translates the amount of current being pulled by the UC. Figure 50 shows how the UC assists in the stop and go situations that pose high transient current demand and thus handling most of the high-power demand situations. Once the vehicle is in motion, its power demand goes down and once it's in the range which the battery can handle the vehicle can draw current from the battery.

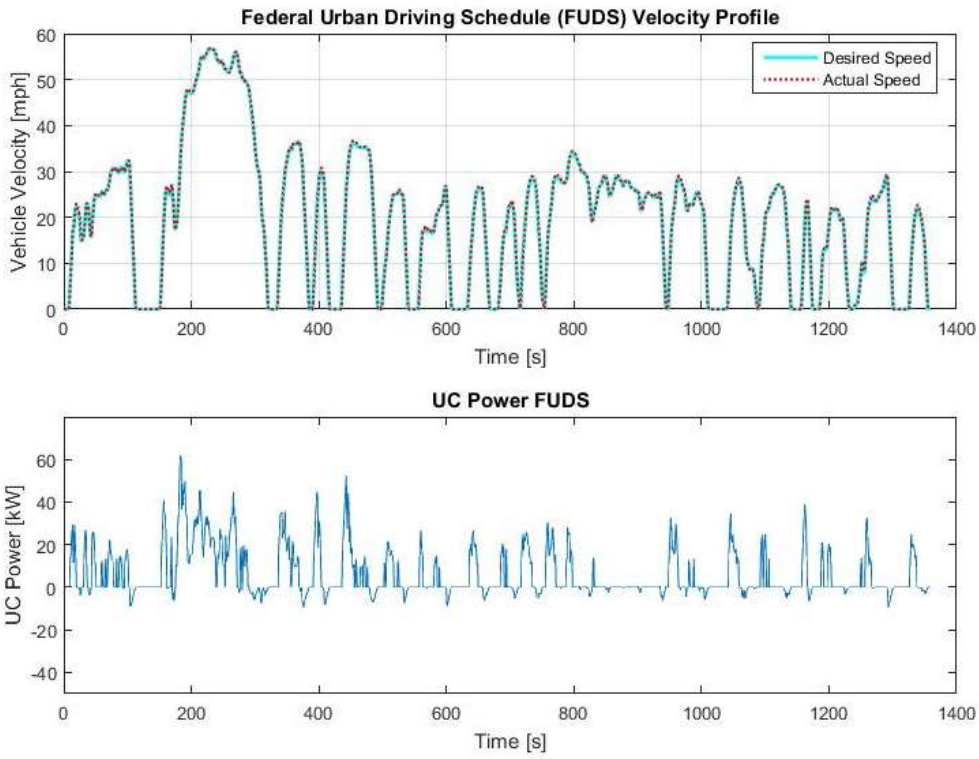

Figure 51 UC Power Profile for Urban Drive Cycle (FUDS)

Since the FUDS cycle uses current from the UC because of its frequent start and stop nature, the power drawn from it also has a lot of peaks since UC assists in peak power demands and then the control strategy allows the battery to provide power once the power demand falls in the region in which battery can provide power without running into the problem of overcurrent which result in increased temperature and ultimately damaging the battery.

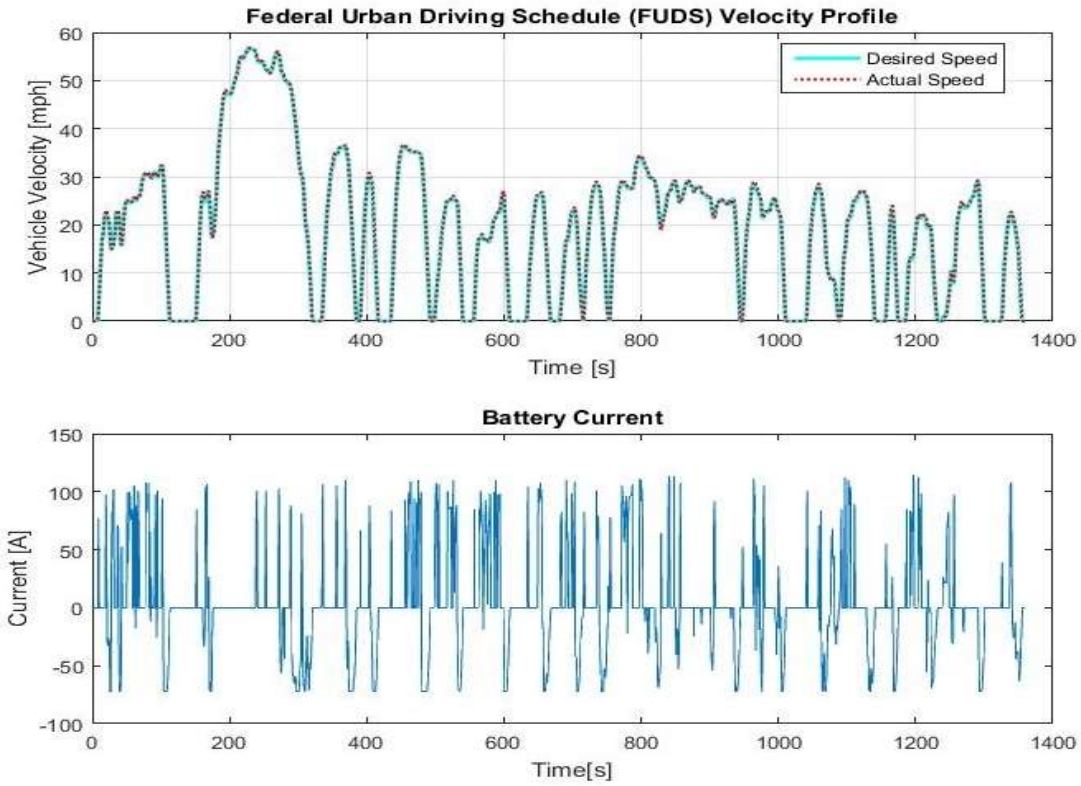

Figure 52 Battery Current Profile for Urban Drive Cycle (FUDS)

Figure 52 shows the current drawn from the battery and as seen in the figure that this control strategy relies a lot on battery power as its used frequently and to the maximum amount of current that can be provided by the battery. Since there are lot of stop and go situations, more current is drawn from ESS. The speeds and acceleration in this profile are not too high as compared to the US06 drive cycle and so the power demand is also not as high. Thus, it's appropriate to use ESS components for most part of the drive cycle. After UC provides initial assistance, battery can take over and provide a most of the power.

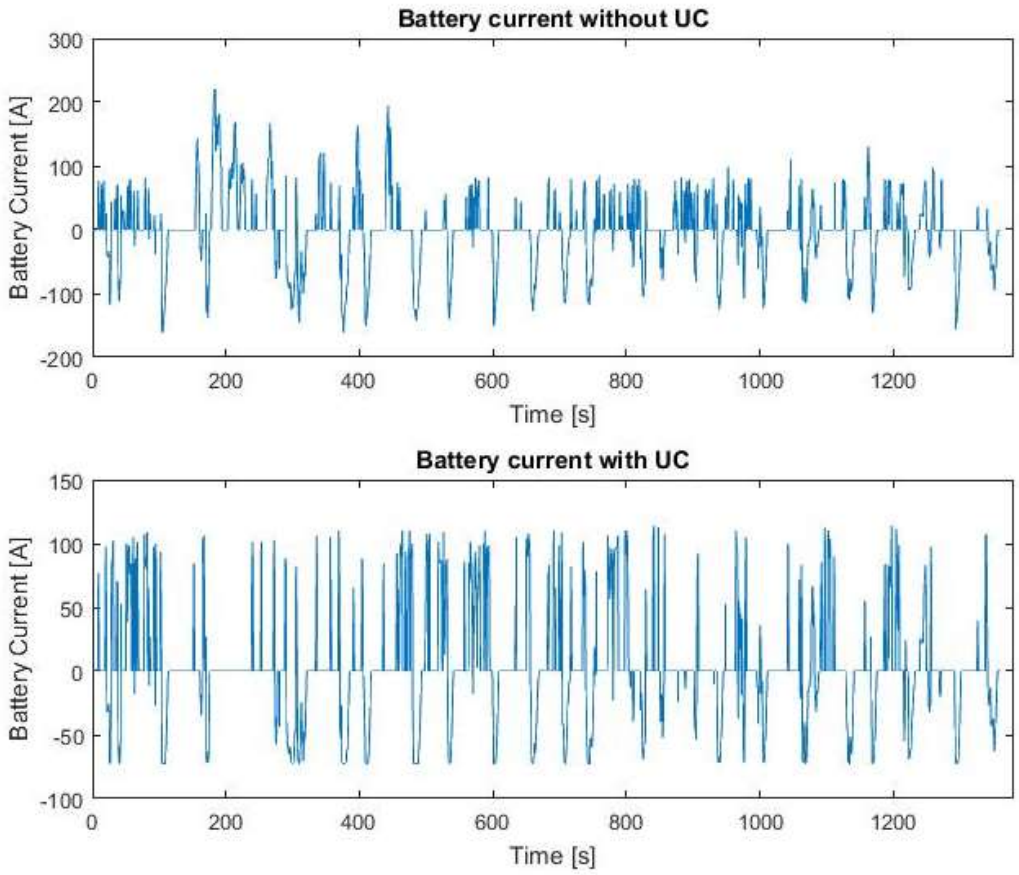

Figure 53 Battery Current Comparison Profile for Urban Drive Cycle (FUDS)

Analyzing the Figure 53 , it can be seen that even earlier the dependance on battery current was high, but adding an UC has two benefits. First it reduces the maximum and the average current drawn from the battery. This helps in maintaining the SOC and reduces the number of charge discharge cycle improving the state of health of the battery. Secondly there are instances that when the current from battery is zero which wasn't the case with previous logic. This again reduces the power drawn from the battery while improving the performance of the car since UC can handle that higher current demand much better.

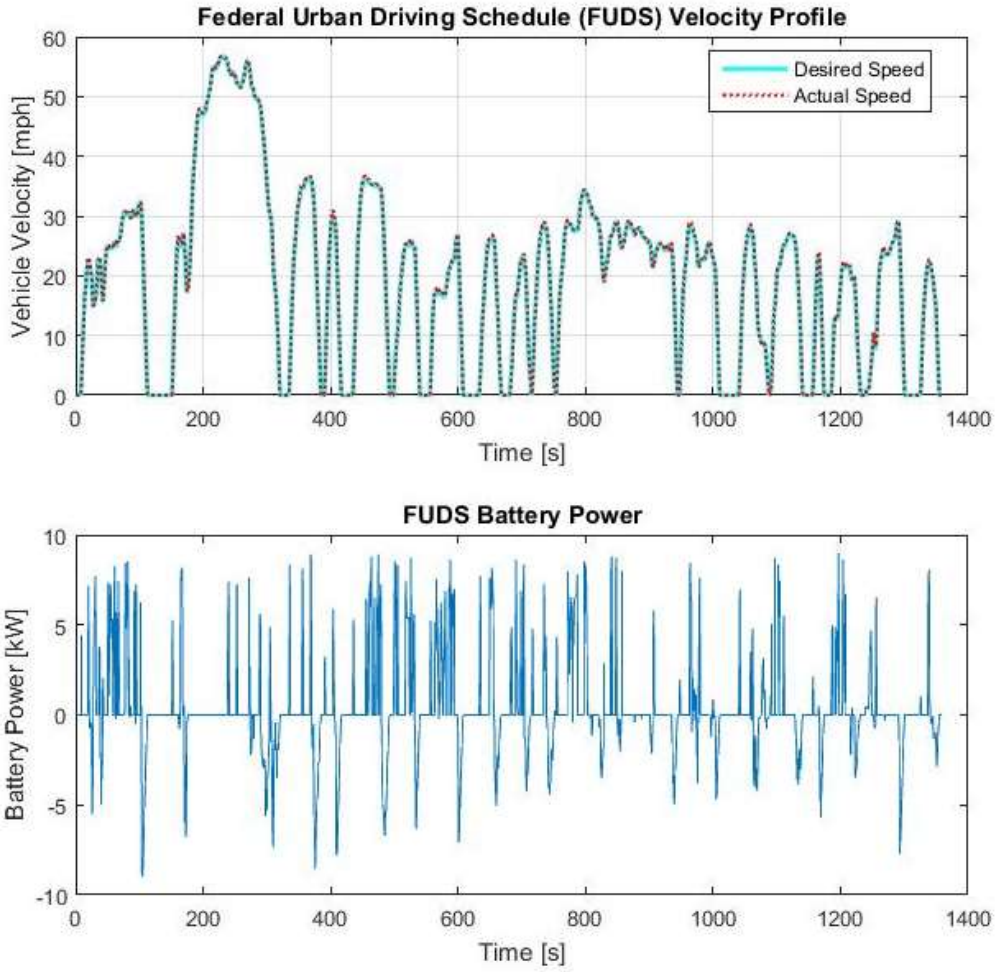

Figure 54 Battery Power Urban Drive Cycle (FUDS)

As seen in the Figure 54, this control strategy relies heavily on battery power. So, there are a lot of instances in which the battery is depleted. Because of this reason, the battery is also capable of accepting a lot of regenerative power as well. For a drive cycle like this which is not aggressive, battery is an ideal source of power.

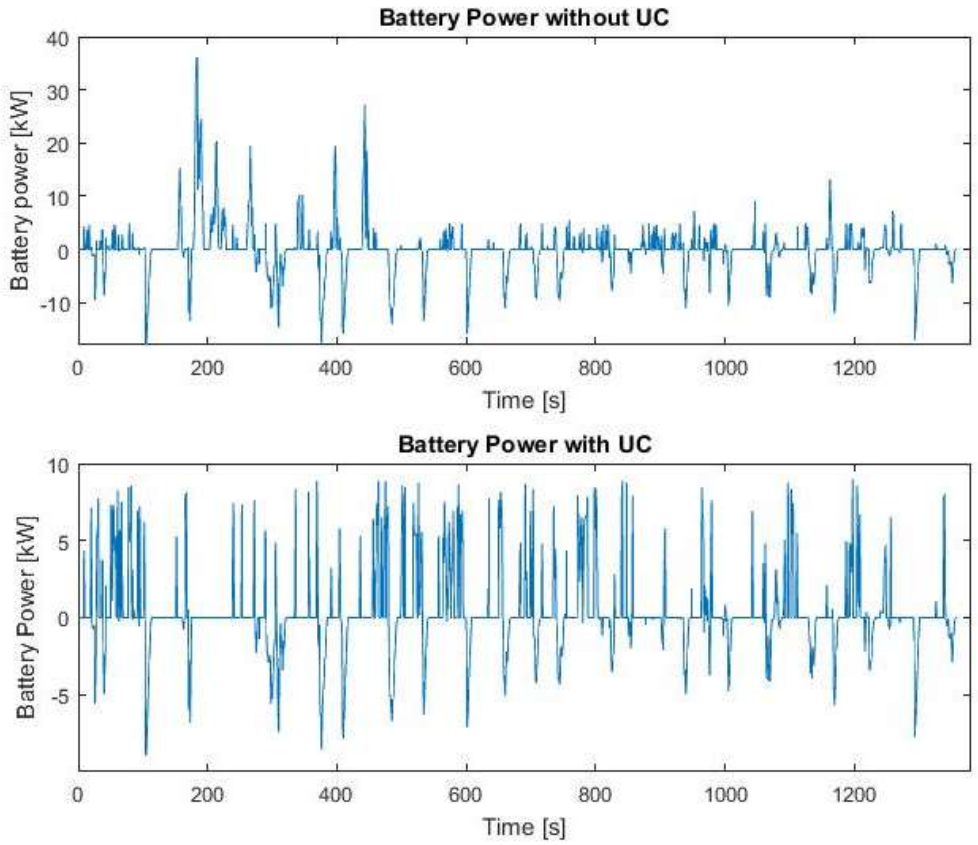

Figure 55 Battery Power Comparison for Urban Drive Cycle (FUDS)

Without the UC, its clearly visible that there are many spikes that occur on the power demand profile of battery as seen in Figure 55. Also, there are several peaks on the power demand profile. So, adding the UC levels out the power demand from the battery using it for low power high energy kind of situations which its suitable for. The high-power peaks seen in the figure are redirected to UC in the control strategy thus making this strategy more efficient.

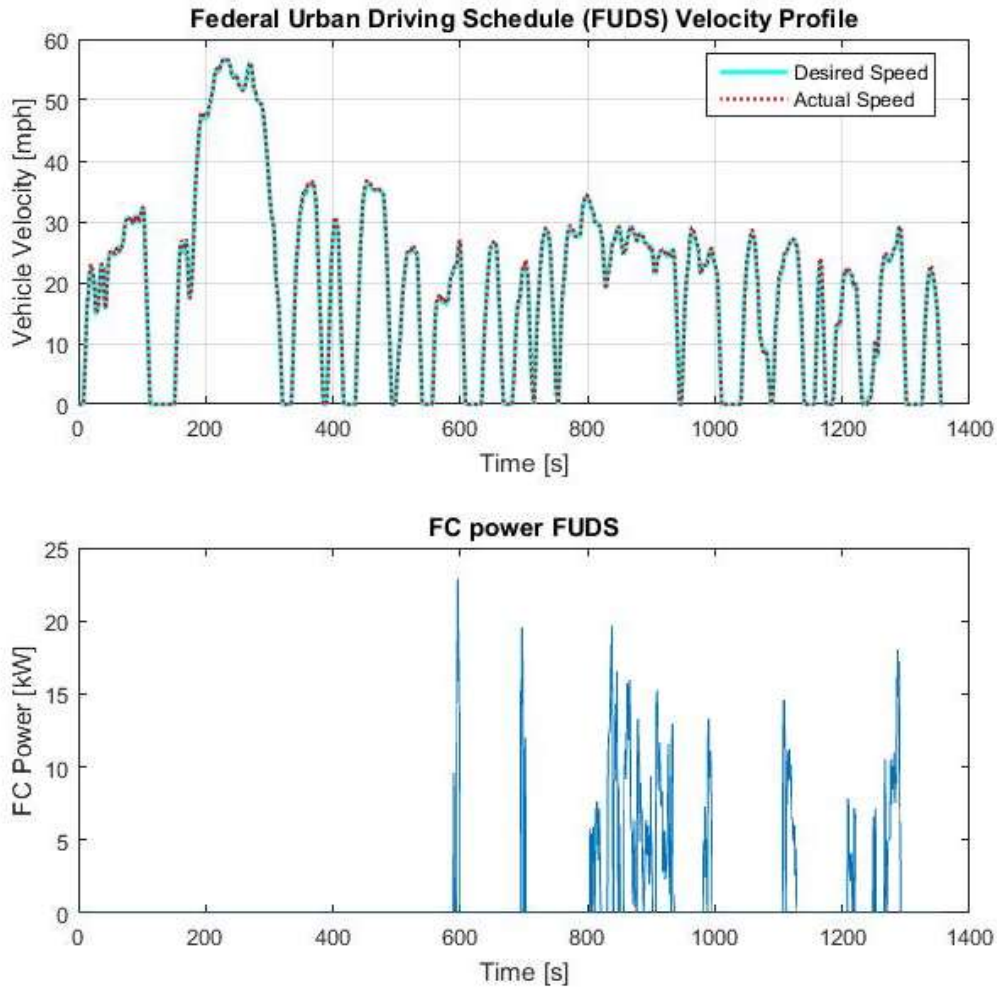

Figure 56 FC Power Profile Urban Drive Cycle (FUDS)

In accordance with the current profile shown in Figure 56, one can see that the power drawn from the fuel cell is zero until about 600 seconds when the ESS components go below the threshold SOC. This type of control strategy makes the fuel cell work like an auxiliary power unit that is used more like a range extender on electric vehicles. Also, the power consumed from the FC comes down to a maximum of 22.8 kW which is way less than the power drawn from FC during the US06 cycle as shown in Figure 42. This comparison

demonstrates the motive behind designing a separate control strategy to achieve maximum fuel savings while satisfying the power demand of the vehicle.

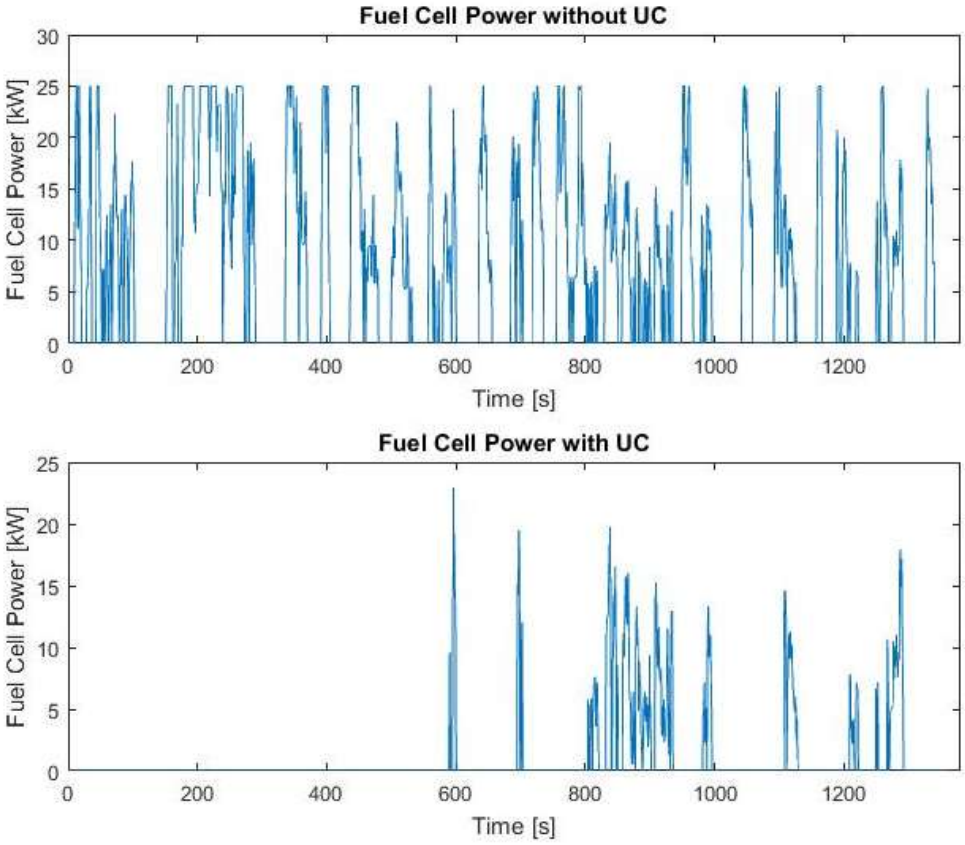

Figure 57 Fuel Cell Power Comparison for Urban Drive Cycle (FUDS)

With UC in the powertrain as an additional source that can handle high power demand, there is a flexibility to use FC as a secondary power source when the SOC of either of the components goes below the minimum threshold. In this case if the single component of the hybrid ESS is not capable of handling the power demand, the FC can provide power to satisfy power demand. So, this makes FC just a backup power source bringing down the hydrogen consumption.

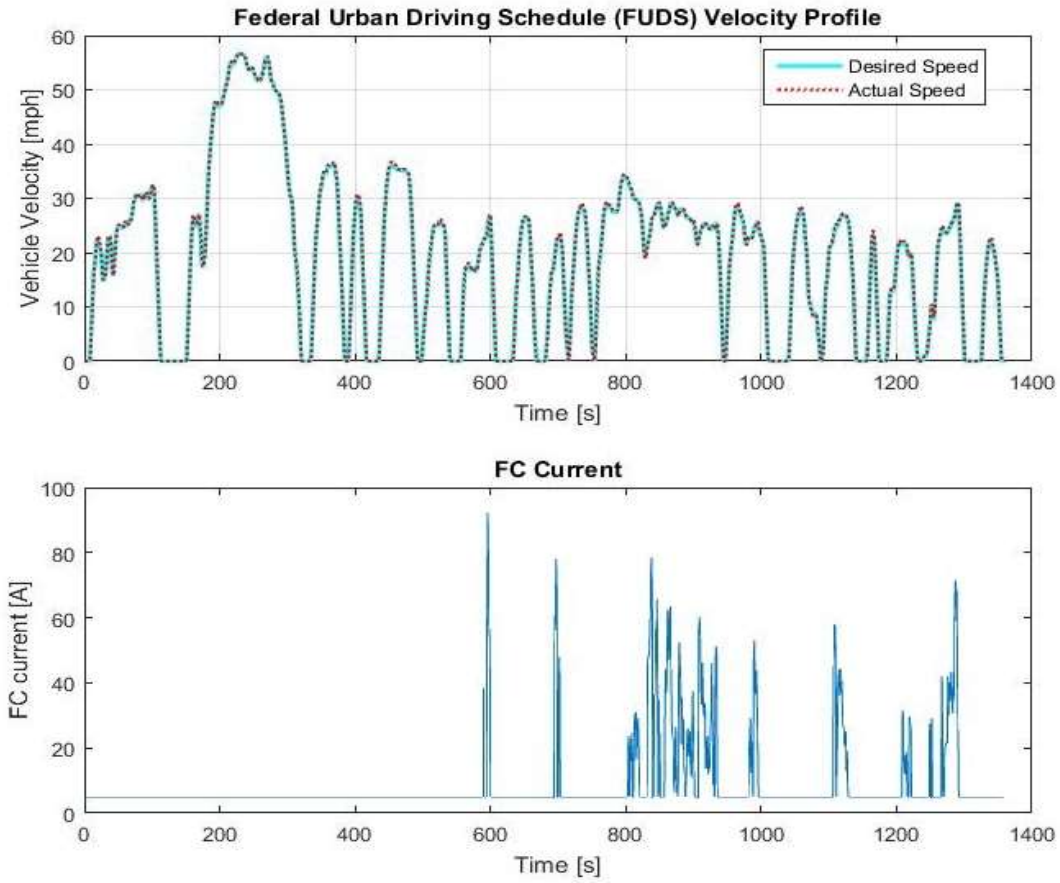

Figure 58 FC Current Profile for Urban Drive Cycle (FUDS)

With increasing the reliance on ESS, the possibility of them hitting the lower threshold is higher. So, in that case, the fuel cell must handle the power demand. Figure 58 shows the current profile of the fuel cell. As observed in this figure, there are very few instances when the fuel cell is used in the drive cycle and thus it can be considered to just be a backup power source in this control strategy as battery pack and UC can provide the power unless there SOC drops below the threshold. Hence it reduces the hydrogen consumption in the entire drive cycle.

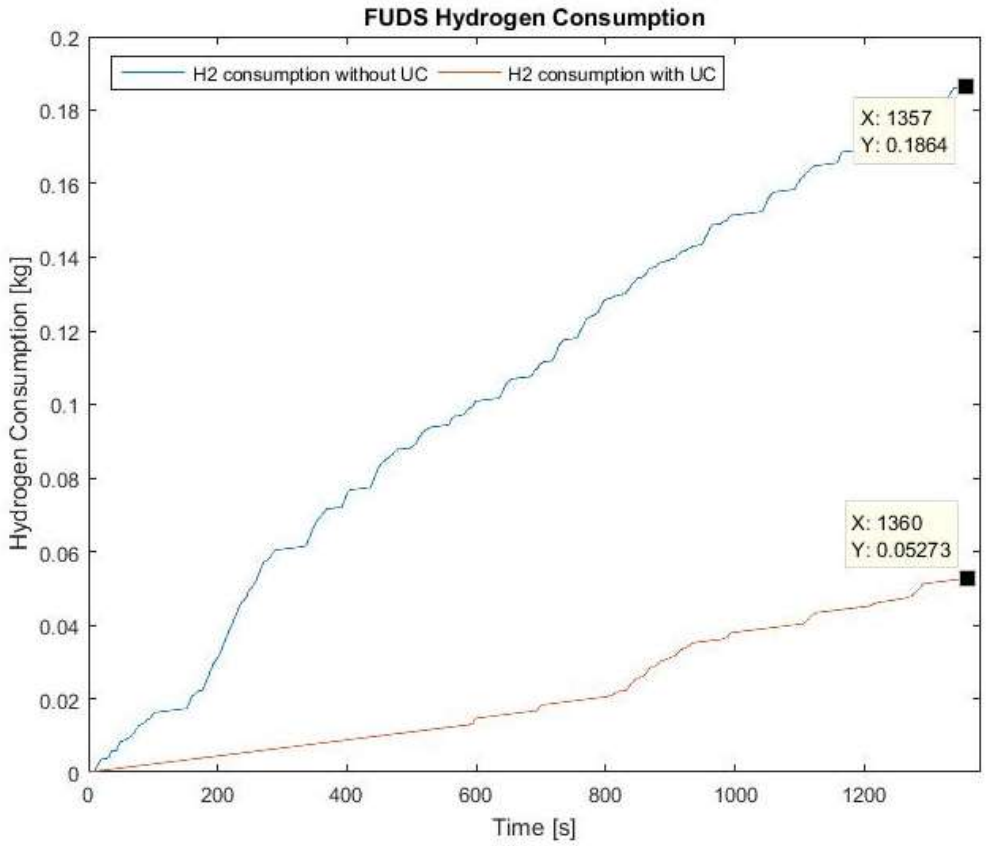

Figure 59 Hydrogen Consumption Improvement

Figure 59 shows the reduction in the amount of hydrogen consumption in the FUDS drive cycle because of adding the UC to the powertrain and the effect of the improved control strategy that reduces reliance on FC and increasing the degree of hybridization. The amount of hydrogen consumption comes down from 0.18 kg in one drive cycle to 0.05 kg which is a significant improvement.

7. CONCLUSION & FUTURE SCOPE OF WORK

This research investigates the effect and advantages of adding an UC into the ESS of FCHEV. A power management strategy that utilizes each component in its most optimum operating points. A deeper look into the characteristics and property of fuel cell taken and based on the knowledge of all the losses provided by efficiency maps that occur inside the fuel cell stack, an optimum range of power operation was determined which focusses on drawing as much power as possible while trying to keep the hydrogen consumption minimum. Simulations were based on US06 drive cycle and results were generated. First a comparison was done between the configuration with and without the UC. Then analysis was done with the fuel cell operating in its optimum range. An analysis is presented based on the velocity profile about how each component behaves at different times.

Addition of UC shows that the use of battery is reduced at many instances preventing it from going to the minimum SOC level as would happen earlier without SOC. This can help in maintaining the health of the battery as its charge/discharge cycles are reduced, thus increase its calendar life. Since the UC is designed for more cyclic charge/discharge loading, it can be depleted by satisfying high power demands. Inclusion of UC in the powertrain, allows the fuel cell to relax during good part of the drive cycle. Without UC the fuel cell would have to be used to supply power to the wheels in case the battery is depleted or is not capable of providing power on its own. This would happen at times at the cost of operating fuel cell in low efficiency region. The UC gives the flexibility to keep the operation of fuel cell in the best efficiency region providing a backup for power in case of low SOC of the battery or even assisting it at times. The inclusion of UC to FCHEV

results in reduction of hydrogen consumption in aggressive US06 drive cycle from 0.29 kg per drive cycle to 0.12 kg. The maximum charge/discharge battery current was reduced from 286 amperes to 110 amperes in the aggressive city drive cycle. Results for the urban drive cycle FUDS show a reduction in fuel consumption from 0.18 kg to 0.05 kg in one drive cycle. This reduction in current increases the life of the battery since its protected from overcurrent and thus does not get hot. The SOC profile of the battery also shows that the battery is not discharged to its minimum threshold which increase the health of the battery that depends on number of charge/discharge cycles.

The current from the FC determines the speed of the reaction and since the reactions are exothermic in nature, higher current creates a thermal management issue [16]. So many power management strategies try to operate FC in the region of ohmic losses where the reaction is within it's allowable limit. Simulation results in [48] shows the power drawn from the FC based on a maximum efficiency optimization algorithm. It can be seen from the Figure 60 that the optimized efficiency algorithm switches the power being drawn from the battery and the FC.

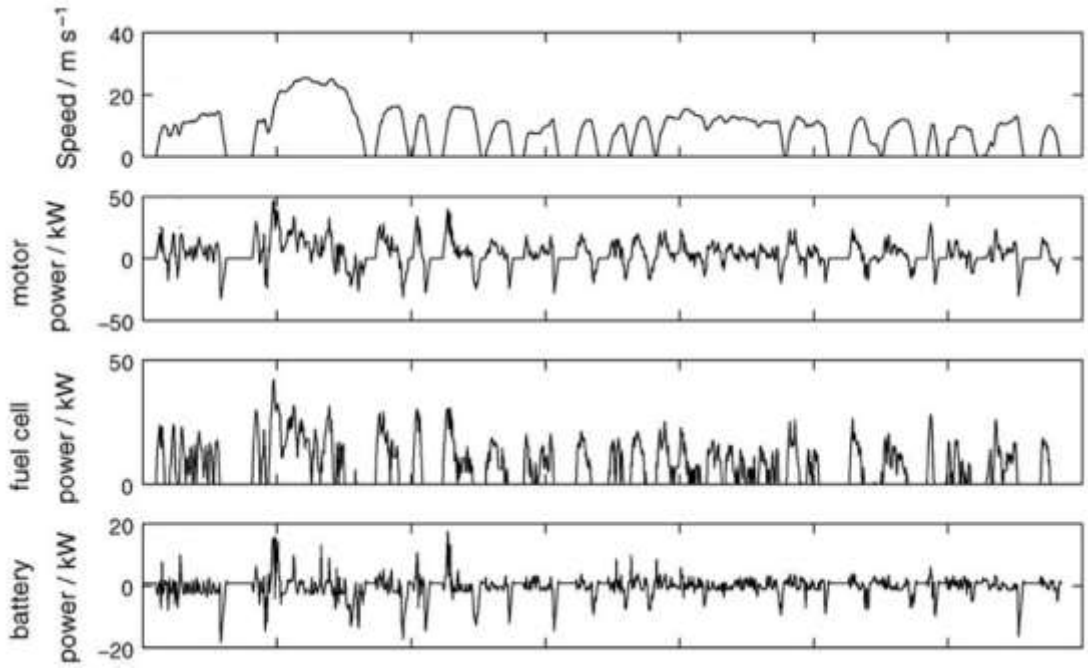

Figure 60 Power distribution based on maximum efficiency optimization [48]

Thus if at a certain region of power demand, the battery is a better alternative, then the optimized algorithm restricts power being drawn from the FC. Based on this type of energy management, the FC current and power results shown in the figures 41-42 and figure 56 are justified since the operating points are in the region of ohmic losses as seen in figure 17. This reduces the thermal management issues too and puts the FC in its region of maximum efficiency shown in figures16.

The results prove an increase in the overall efficiency of the system and increase improvement in the performance of the vehicle and optimal utilization of powertrain components.

7.1. Future Scope of Work

The newly proposed architecture-dependent FCHEV optimal EMS allows the integration of future traffic and road terrain information using connected power train

methodology to improve the overall efficiency of FCHEV fleet. The integration of UCs to the system will allow fleet of FCHEV to adapt most optimum speed to manage the flow of the FCHEV within traffic in urban areas. This represent one of the critical building blocks of the next generation of cyber infrastructure. This creative architecture-driven solution results in an adoption of real-time implementable EMS that are computationally less expensive which are more appropriate for current in production vehicle.

An effort was made to optimize the fuel cell operating range using Response Surface Method. This method was chosen to optimize the operation was response surface method because of reduced time and computational effort in it [49]. Since the main objective here was to find the optimum operating range, the values of the upper and the lower limit of fuel cell operation range was varied over a selection of random points. These random points were created using a latin hypercube function in MATLAB. These values of lower and upper limit of fuel cell operation range were plugged into the Simulink model. Simulations were run for each of these values and the hydrogen consumption value was noted. With these values, a response surface was created using the Curve Fitting Toolbox of MATLAB. After the response surface was obtained, a curve fitting was done to obtain the equation of the curve.

The equation of the curve was essentially the hydrogen consumption. This equation was then ran through a command called fmincon in MATLAB. Due to lack of fuel cell efficiency map which is usually provided by the manufacturers of the fuel cell, the model could not be well formulated and constrained. This can be the future scope of this project. If the efficiency map is made available, the problem formulation can be redefined if

necessary and with proper constraints, a mathematical optimum of the system can be obtained.

REFERENCES

[1] S.F. Tie, C.W. Tan, A review of energy sources and energy management system in electric vehicles, *Renewable and Sustainable Energy Reviews, 20*, 2013, pp.82-102.

[2] Xu, Nan, et al. "Investigation of Topologies and Control Strategies of Fuel Cell Vehicles." *In2015 International Conference on Advances in Mechanical Engineering and Industrial Informatics. Atlantis Press*. 2015.

[3] Ettihir, K., et al. "MPPT control strategy on PEM fuel cell low speed vehicle." *2012 IEEE Vehicle Power and Propulsion Conference*. IEEE, 2012.

[4] Hydrogen Fueling Stations Locations, Alternative Fuels Data Center, US Department of Energy, http://www.afdc.energy.gov/fuels/hydrogen_locations.html

[5] Spendelow, J., Marcinkoski, J., "Fuel Cell System Cost – 2013." *DOE Fuel Cell Technologies Office Record*, 2014.

[6] Offer GJ, Contestabile M, Howey DA, Clague R, Brandon NP. Techno-economic and behavioural analysis of battery electric, hydrogen fuel cell and hybrid vehicles in a future sustainable road transport system in the UK. Energy Policy. 2011 Apr 30;39(4):1939-50.

[7] IEA energy technology essentials: Fuel Cells, 2007.

[8] IEA energy technology essentials: Hydrogen Production & Distribution, 2007

[9] Mekhilef, S., R. Saidur, and A. Safari. "Comparative study of different fuel cell technologies." *Renewable and Sustainable Energy Reviews* 16.1 (2012): 981-989.

[10] Liu, Z. Y., et al. "Characterization of carbon corrosion-induced structural damage of PEM fuel cell cathode electrodes caused by local fuel starvation." *Journal of The Electrochemical Society* 155.10 (2008): B979-B984.

[11] Yousfi-Steiner, N., et al. "A review on polymer electrolyte membrane fuel cell catalyst degradation and starvation issues: Causes, consequences and diagnostic for mitigation." *Journal of Power Sources* 194.1 (2009): 130-145.

[12] Mehta, Viral, and Joyce Smith Cooper. "Review and analysis of PEM fuel cell design and manufacturing." *Journal of Power Sources* 114.1 (2003): 32-53.

[13] Shao, Yuyan, et al. "Proton exchange membrane fuel cell from low temperature to high temperature: material challenges." *Journal of Power Sources* 167.2 (2007): 235-242.

[14] Farnsworth, Jared, et al. *Development of a Vehicle Model for FCHV Control and Functional Specification Development within a Software-in-the-Loop Simulation Environment*. No. 2010-01-0939. SAE Technical Paper, 2010

[15] Vahidi, Ardalan, Anna Stefanopoulou, and Huei Peng. "Model predictive control for starvation prevention in a hybrid fuel cell system." *American Control Conference, 2004. Proceedings of the 2004*. Vol. 1. IEEE, 2004.

[16] Cao TF, Lin H, Chen L, He YL, Tao WQ. Numerical investigation of the coupled water and thermal management in PEM fuel cell. Appl Energ. 2013 Dec 31; 112:1115-25.

[17] Zandi M, Payman A, Martin JP, Pierfederici S, Davat B, Meibody-Tabar F. Energy management of a fuel cell/supercapacitor/battery power source for electric vehicular applications. IEEE transactions on vehicular technology. 2011 Feb;60(2):433-43.

[18] Wirasingha, Sanjaka G., and Ali Emadi. "Classification and review of control strategies for plug-in hybrid electric vehicles." IEEE Transactions on vehicular technology 60.1 (2011): 111-122.

[19] Mehrdad, Ehsani, Gao Yimin, and Emadi Ali. "Modern electric, hybrid electric, and fuel cell vehicles." (2010).

[20] D.E Smith, H. Lohse-Busch, D.K. Irick, A preliminary investigation into the Mitigation of plug-in hybrid electric vehicle tailpipe emissions through supervisory control methods, *SAE International Journal of Engines, 3*(1), 2010, pp.996-1011.

[21] Aouzellag H, Ghedamsi K, Aouzellag D. Energy management and fault tolerant control strategies for fuel cell/ultra-capacitor hybrid electric vehicles to enhance autonomy, efficiency and life time of the fuel cell system. Int J of Hydrogen Energy. 2015 Jun 15;40(22):7204-13.

[22] Rousseau A, Moawad A. Impact of Control Strategies on Fuel Efficient Efficiency Of Different PHEVs Using Real World Driving Conditions. 2010.

[23] Sid MN, Nounou K, Becherif M, Marouani K, Alloui H. Energy management and optimal control strategies of fuel cell/supercapacitors hybrid vehicle. In Electrical Machines (ICEM), 2014 International Conference on 2014 Sep 2 (pp. 2293-2298). IEEE.

[24] Govind Goyal, *Master's Thesis*, Arizona State University, Mesa-Arizona, USA, June 2014.

[25] K.C. Bayindir, M.A. Gözüküçük, A. Teke, A comprehensive overview of hybrid electric vehicle: Powertrain configurations, powertrain control techniques and electronic control units, *Energy Conversion and Management*, 52(2), 2011, pp.1305-1313.

[26] Feng L, Liu W, Chen B. Driving Pattern Recognition for Adaptive Hybrid Vehicle Control. SAE Int J of Altern Powertrains. 2012 Apr 16;1(2012-01-0742):169-79.

[27] Han J, Park Y, Kum D. Optimal adaptation of equivalent factor of equivalent consumption minimization strategy for fuel cell hybrid electric vehicles under active state inequality constraints. J of Power Sources. 2014 Dec 1;267: 491-502.

[28] Ettihir K, Boulon L, Agbossou K, Kelouwani S, Hammoudi M. Design of an energy management strategy for PEM Fuel Cell Vehicles. In Industrial Electronics (ISIE), 2012 IEEE Int Symposium on 2012 May 28 (pp. 1714-1719). IEEE.

[29] Ettihir K, Boulon L, Agbossou K. Energy management strategy for a fuel cell hybrid vehicle based on maximum efficiency and maximum power identification. IET Electrical Systems in Transportation. 2016 Jul 27;6(4):261-8.

[30] Moçotéguy P, Ludwig B, Steiner NY. Application of current steps and design of experiments methodology to the detection of water management faults in a proton exchange membrane fuel cell stack. J of Power Sources. 2016 Jan 30; 303:126-36.

[31] Ettihir K, Boulon L, Agbossou K, Kelouwani S. MPPT control strategy on PEM fuel cell low speed vehicle. In 2012 IEEE Vehicle Power and Propulsion Conference 2012 Oct 9 (pp. 926-931). IEEE.

[32] Lu J, Zahedi A. Maximum efficiency point tracking control for fuel cell power systems. In Power System Technology (POWERCON), 2010 Int Conference on 2010 Oct 24 (pp. 1-6). IEEE.

[33] Jeong, Kwi Seong, and Byeong Soo Oh. "Fuel economy and life-cycle cost analysis of a fuel cell hybrid vehicle." *Journal of Power Sources* 105.1 (2002): 58-65.

[34] Pedelecs Electric Bike Company,
http://www.pedelecs.co.uk/forum/threads/supercapacitors-battery.20595/

[35] Gonder, Jeff, et al. "Hybrid Vehicle Comparison Testing Using Ultracapacitor vs. Battery Energy Storage." (2010).

[36] Lu, Languang, et al. "A review on the key issues for lithium-ion battery management in electric vehicles." *Journal of power sources* 226 (2013): 272-288.

[37] Cao J, Emadi A. A new battery/ultracapacitor hybrid energy storage system for electric, hybrid, and plug-in hybrid electric vehicles. IEEE Transactions on power electronics. 2012 Jan;27(1):122-32.

[38] Rayment, Chris, and Scott Sherwin. "Introduction to fuel cell technology. "*Department of Aerospace and Mechanical Engineering, University of Notre Dame, Notre Dame, IN* 46556 (2003): 11-12.

[39] Huang, Xinhong, Zhihao Zhang, and Jin Jiang. "Fuel cell technology for distributed generation: an overview." *2006 IEEE International Symposium on Industrial Electronics*. Vol. 2. IEEE, 2006.

[40] Li, Qi, et al. "Energy management strategy for fuel cell/battery/ultracapacitor hybrid vehicle based on fuzzy logic." *International Journal of Electrical Power & Energy Systems* 43.1 (2012): 514-525.

[41] K. Rajashekara, Fuel Cell Technology for Vehicles (2000) 179–187.

[42] Maxwell Ultra-Capacitors
http://www.maxwell.com/images/documents/hq_48v_ds10162013.pdf

[43] Vahidi, Ardalan, and Wesley Greenwell. "A decentralized model predictive control approach to power management of a fuel cell-ultracapacitor hybrid."*2007 American Control Conference*. IEEE, 2007.

[44] Burke, Andrew. "Ultracapacitors: why, how, and where is the technology. "*Journal of power sources* 91.1 (2000): 37-50.

[45] Y. Fuyuan, L. Languang, Y. Yuping, Y. He, Characterization, Analysis and Modeling of an Ultracapacitor, *EVS-25 Shenzhen, China*,Vol 4,pp 258-269, 2010.

[46] Jazar, Reza N. 2014. *Vehicle dynamics: theory and application*. http://dx.doi.org/10.1007/978-1-4614-8544-5.

[47] E. Versonnen, Rolling Resistance, http://www.ip-zev.gr/files/teaching/T1-1_Rolling%20Resistance.pdf

[48] Li CY, Liu GP. “Optimal fuzzy power control and management of fuel cell/battery hybrid vehicles”. *Journal of power sources*. 2009 Jul 15;192(2):525-33.

[49] Xuan, Dongji, et al. "Optimal operating points of PEM fuel cell model with RSM." *Journal of Mechanical Science and Technology* 23.3 (2009): 717-728.

APPENDIX A
ELECTRIC MOTOR, BATTERY AND ULTRA-CAPACITOR SPECIFICATIONS

- Electric Motor Specifications
    - Power Output: 80kW
    - Horsepower: 107.28
- Battery Specifications
    - Lithium Ion Battery
    - Output (Volts): 274 V
    - Power Capacity: 30kW
    - Battery Capacity: 110 Ah
- Ultra-Capacitor Specifications
    - Output (Volt): 48 V
    - Power Capacity: 91.8 kW
    - Current Capacity: 100 A